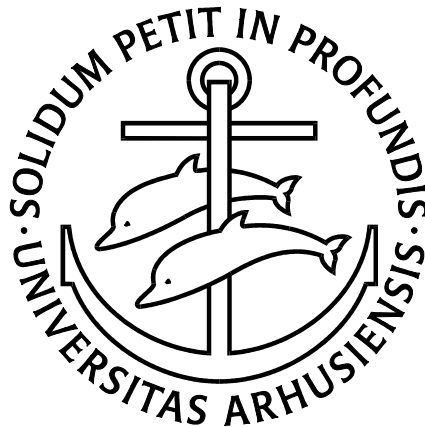


Osteoclastic Bone Resorption in Chronic Osteomyelitis

PhD thesis

Kirill Gromov



Faculty of Health Sciences

University of Aarhus

Denmark

2009

2

From

Orthopaedic Research Laboratory

Department of Orthopaedics

Aarhus University Hospital

Aarhus

Denmark

Osteoclastic Bone Resorption in Chronic Osteomyelitis

PhD thesis

Kirill Gromov



Faculty of Health Sciences

University of Aarhus

Denmark

2009

Table of Contents

PhD and Doctoral Theses from the Orthopaedic Research Group	5
List of Papers	10
Supervisors	11
Preface and acknowledgements	12
Abstract in Danish.....	13
Abstract	15
List of abbreviations:	17
1 Introduction	18
2 Osteomyelitis background: etiology, causes and treatment.....	20
2.1 Pathology.....	21
2.2 Diagnosis	23
2.3 Treatment.....	24
2.3.1 Prophylaxis.....	24
2.3.2 Medical	25
2.3.3 Surgical.....	25
2.4 Emergence of methicillin-resistant <i>S. aureus</i>.....	25
2.5 Multidrug resistant <i>Acinetobacter</i> in warfare	26
2.6 Bisphosphonates.....	27
2.7 Osteonecrosis of the jaw (ONJ).....	29
2.8 Animal models of osteomyelitis.....	31
2.8.1 Bacterial species and inoculation	31
2.8.2 Inoculation routes and infection promoters	32
2.8.3 Animals.....	33
3 Problems and main goals of the study.....	36
3.1 Animal models.	36
3.2 Osteomyelitis and use of bisphosphonates.....	36
3.3 Multi-drug resistant <i>Acinetobacter</i> species	37
4 Materials and methods	37
4.1 strains, pathogenic challenge and surgical procedure	37
4.2 Histology	40
4.3 DNA purification and <i>nuc/b-actin</i> RTQ-PCR	40
4.4 <i>In vivo</i> bioluminescent imaging	42
4.5 Drug treatments	44
4.6 Antibiotic prophylaxis	45
5 Results	47
5.1 Study I.....	47
5.2 Study 2	47
5.3 Study 3	48

6 Discussion	49
6.1 Model	49
6.2 Anti-catabolic treatment	51
6.3 Prophylactic antibiotic treatment.....	52
7 Concluding remarks and future perspectives.....	54
References	55
Paper I.....	Appendix I
Paper II.....	Appendix II
Paper III.....	Appendix III

PhD and Doctoral Theses from the Orthopaedic Research Group
www.orthoresearch.dk,

University Hospital of Aarhus, Denmark

PhD Theses

1. Polyethylene Wear Analysis. Experimental and Clinical Studies in Total Hip Arthroplasty.
Maiken Stilling, June 2009
www.statsbiblioteket.dk

2. Surgical Advances in Periacetabular Osteotomy for Treatment of Hip Dysplasia in Adults
Anders Troelsen, March 2009
Acta Orthopaedica (Suppl 332) 2009;80

3. The Influence of Local Bisphosphonate Treatment on Implant Fixation
Thomas Vestergaard Jakobsen, December 2008
www.statsbiblioteket.dk

4. Adjuvant therapies of bone graft around non-cemented experimental orthopaedic implants. Stereological methods and experiments in dogs
Jørgen Baas, July 2008
Acta Orthopaedica (Suppl 330) 2008;79

5. CoCrMo alloy, *in vitro* and *in vivo* studies
Stig Storgaard Jakobsen, June 2008
www.statsbiblioteket.dk

6. Rehabilitation outcome after total hip replacement; prospective randomized studies evaluating two different postoperative regimes and two different types of implants
Mette Krintel Petersen, June 2008

www.statsbiblioteket.dk

7. Efficacy, effectiveness, and efficiency of accelerated perioperative care and rehabilitation intervention after hip and knee arthroplasty
Kristian Larsen, May 2008

www.statsbiblioteket.dk

8. Rehabilitation of patients aged over 65 years after total hip replacement - based on patients' health status
Britta Hørdam, February 2008

www.statsbiblioteket.dk

9. Evaluation of Bernese periacetabular osteotomy; Prospective studies examining projected load-bearing area, bone density, cartilage thickness and migration
Inger Mechlenburg, August 2007
Acta Orthopaedica (Suppl 329) 2008;79

10. Combination of TGF- β 1 and IGF-1 in a biodegradable coating. The effect on implant fixation and osseointegration and designing a new in vivo model for testing the osteogenic effect of micro-structures in vivo
Anders Lamberg, June 2007

www.statsbiblioteket.dk

11. On the longevity of cemented hip prosthesis and the influence on implant design
Mette Ørskov Sjøland, April 2007

www.statsbiblioteket.dk

12. Reaming procedure and migration of the uncemented acetabular component in total hip replacement
Thomas Baad-Hansen, February 2007

www.statsbiblioteket.dk

13. Studies based on the Danish Hip Arthroplasty Registry
Alma B. Pedersen, 2006

www.statsbiblioteket.dk

14. DEXA-scanning in description of bone remodeling and osteolysis around cementless acetabular cups

Mogens Berg Laursen, November 2005

www.statsbiblioteket.dk

15. Biological response to wear debris after total hip arthroplasty using different bearing materials

Marianne Nygaard, June 2005

www.bibliotek.dk

16. The influence of RGD peptide surface modification on the fixation of orthopaedic implants

Brian Elmengaard, December 2004

www.statsbiblioteket.dk

17. Stimulation and substitution of bone allograft around non-cemented implants
Thomas Bo Jensen, October 2003

www.statsbiblioteket.dk

18. Surgical technique's influence on femoral fracture risk and implant fixation.
Compaction versus conventional bone removing techniques

Søren Kold, January 2003

www.statsbiblioteket.dk

19. The influence of hydroxyapatite coating on the peri-implant migration of polyethylene particles

Ole Rahbek, October 2002

www.statsbiblioteket.dk

20. Gene delivery to articular cartilage
Michael Ulrich-Vinther, September 2002

www.statsbiblioteket.dk

21. In vivo and vitro stimulation of bone formation with local growth factors
Martin Lind, January 1996

www.statsbiblioteket.dk

Doctoral Theses

1. Gene therapy methods in bone and joint disorders. Evaluation of the adeno-associated virus vector in experimental models of articular cartilage disorders, periprosthetic osteolysis and bone healing
Michael Ulrich-Vinther, March 2007

Acta Orthopaedica (Suppl 325) 2007;78

2. Adult hip dysplasia and osteoarthritis. Studies in radiology and clinical epidemiology
Steffen Jacobsen, December 2006

Acta Orthopaedica (Suppl 324) 2006;77

3. Calcium phosphate coatings for fixation of bone implants. Evaluated mechanically and histologically by stereological methods
Søren Overgaard, 2000

Acta Orthop Scand (Suppl 297) 2000;71

4. Growth factor stimulation of bone healing. Effects on osteoblasts, osteomies, and implants fixation
Martin Lind, October 1998

Acta Orthop Scand (Suppl 283) 1998;69

5. Hydroxyapatite ceramic coating for bone implant fixation. Mechanical and histological studies in dogs
Kjeld Søballe, 1993
Acta Orthop Scand (Suppl 255) 1993;54

List of Papers

This PhD thesis is based on following papers:

I.

Quantitative mouse model of implant-associated osteomyelitis and the kinetics of microbial growth, osteolysis, and humoral immunity.

Li D*, Gromov K*, Søballe K, Puzas JE, O'Keefe RJ, Awad H, Drissi H, Schwarz EM.

*equal contribution

J Orthop Res. 2008 Jan;26(1):96-105

II.

Effects of anti-resorptive agents on the establishment of chronic osteomyelitis

Gromov K*, Li D*, Proulx S, Xie C, Xing L, Søballe K, Puzas JE, O'Keefe RJ, Awad H, Drissi H, Schwarz EM.

*equal contribution

in submission

III.

Efficacy of colistin-impregnated beads to prevent multidrug-resistant *A. baumannii* implant-associated osteomyelitis.

Crane DP*, Gromov K*, Li D, Søballe K, Wahnes C, Büchner H, Hilton MJ, O'Keefe RJ, Murray CK, Schwarz EM.

*equal contribution

J Orthop Res. 2009 Jan 27. [Epub ahead of print]

In the following these papers will be referred to by their roman numerals as Paper (I-III).

Supervisors

Main Supervisor:

Kjeld Søballe, Professor, MD, DMSc

Department of Orthopaedics

Aarhus University Hospital, Aarhus, Denmark

Co-Supervisors:

Micheal Ulrich-Vinther, Associate Professor, MD, DMSc

Department of Orthopaedics

Aarhus University Hospital, Aarhus, Denmark

Edward M Schwarz, Professor, PhD

Department of Orthopedics

University of Rochester, Rochester, NY, USA

Correspondence:

Kirill Gromov, MD

Orthopaedic Research Laboratory

Department of Orthopaedics

Aarhus University Hospital

Norrebrogade 44, Build. 1A

Dk-8000 Aarhus C

Denmark

Email: kirgromov@yahoo.dk

Preface and acknowledgements

This PhD thesis is based on scientific work conducted during my enrolment as PhD student at the faculty of Health Sciences, Aarhus University, from 2007-2009. The experimental work was performed at Orthopaedic Research Laboratory, Aarhus University Hospital, Denmark and Orthopaedic Research Laboratory, University of Rochester, Rochester, USA. The studies are a continuation of the work performed during my enrolment as research year student at the Health Sciences, Aarhus University, from September 2003 - August 2004.

Research can be challenging and frustrating but at the same time extremely rewarding.

I would like to thank my main supervisor, Prof. Kjeld Søballe for introducing me to medical research, and for providing me with an opportunity to explore this wonderful aspect of medicine. I am very grateful to my co-supervisor Dr. Michael Ulrich-Vinther, for his scientific mentoring and support during my research.

Thanks to Dr. Ebbe Stender Hansen for introducing me to my supervisors and to Dr. Edward Schwarz, who served as my mentor during my stay in Rochester, NY, for his tremendous support and guidance.

I am truly grateful to all my friends and colleagues at Rochester, NY, for making my stay in the United States an amazing experience and for introducing me to wonderful things such as country-bars and golf.

Thanks to my co-authors, for sharing their time, experience and brilliant ideas with me. I have greatly enjoyed our collaboration and hope that there is more to come.

Finally, thanks you to my family and friends. You all mean the world to me and I could not have done this without you.

Abstract in Danish

Osteomyelitis er en hyppig infektiøs sygdom, som er karakteriseret ved progressiv inflammation samt knogleresorption. På trods af de relativt mange tilfælde af osteomyelitis (112.000 årlige tilfælde i USA og 240 i Danmark), har infektionsraterne for ledproteser og eksterne frakturfixatorer været lave, således at henholdsvis 0.3-11% og 5-15% af indgrebene kompliceredes med infektion, hvilket har resulteret i lav interesse for ekstensiv klinisk prospektiv forskning. Osteomyelitis inducerer osteolyse omkring implantatet, hvilket kan medføre frakturer som komplicerer revisionskirurgi. Dette har ført til enkelte tilfælde hvor ortopædkirurger har brugt bisphosphonater for at forhindre knogleresorptionen og således bevare knogledensiteten, uden at kende til disses effekt på kronisk infektion. Endvidere har der i de senere år, været en alarmerende stigning i antal af rapporterede tilfælde af kæbeknoglenekrose (ONJ) – en patologisk proces som er associeret til brug af bisphosphonater. Disse problemstillinger kræver således en dybere forståelse for interaktionen mellem antiresorptive terapier og osteomyelitis. På trods af, at osteomyelitis er og forbliver et alvorligt problem i ortopædkirurgien, har yderligere forskningsfremgang været sparsom. Dette kan til dels skyldes at der ikke findes en eksperimentel *in vivo* dyremodel, som kan kvantificere det bakterielle load, måle bakteriernes metaboliske aktivitet over tid, samt evaluere immunresponsen og osteolysen.

For at overkomme disse hindringer, har vi udviklet en eksperimentel murin model som simulerer implantatassocieret osteomyelitis. I denne model bliver infektionen induceret via en stålnål, som er coated med varierende mængder af *S. Aureus* og indsat transkortikalt gennem tibias metafyse. Vi har analyseret dyrene ved hjælp af røntgenoptagelser, histologiske og serologiske analyser. Det bakterielle load og aktiviteten blev målt ved hjælp af Real-Time PCR og *in vivo bioluminescence* målinger. Disse forsøg demonstrerer den første kvantitative model af implantatassocieret osteomyelitis, som definerer mikrobiologisk vækst, osteolyse samt det humorale immunrespons efter infektionen (**artikel I**).

For at bedre kunne forstå den effekt som bisphosphonat behandlingen potentielt kan have på osteomyelitis, og samtidigt kaste noget lys over kæbeknoglenekrosens patogenese, undersøgte vi interaktionerne af terapi i vores dyremodel. Vi har undersøgt to forskellige typer af anti-resorptive stoffer: den hyppigst brugte bisphosphonat Alendronat og biologisk antagonist Osteoprotegrin. Begge typer stoffer førte til øgning af svære infektionstilfælde. Dette fund var ledsaget af signifikant hæmning af osteolysen samt nedsættelse af volumen i de drænerende lymfeknuder, hvilket kunne insinuere at den anti-resorptive behandling nedsætter effluxen af lymfe fra knoglemarven under etableringen af infektionen, og således fører til øget intraossøst tryk, infektion og knoglesmerter **(artikel II)**.

Til sidst, har vi evalueret den effekt som colistin polymethyl methacrylate-kugler har på behandlingen af osteomyelitis induceret af *A. Baumannii*. Dette blev undersøgt via vores tidligere beskrevne model, hvor dyr blev inficeret med kliniske isolater af multiresistente *A. Baumannii*. For at vurdere effekten af colistinprofylaksen, blev mus enten behandlet med parenteral colistin eller lokal colistin ved hjælp af colistin PMMA-kugler. Mens parenteral colistinprofylakse ingen effekt havde på infektionen sammenlignet med placebo, nedsatte lokal colistinprofylakse infektionsraten signifikant **(artikel III)**.

Abstract

Osteomyelitis is a common infectious disease characterized by progressive inflammation and bone destruction. Although the total number of osteomyelitis cases is high in that approximately 112,000 and 240 orthopedic device-related infections occur per year in the US and Denmark respectively, at an approximate hospital cost of \$15,000-70,000 per incident [1] the infection rates for joint prosthesis and fracture-fixation devices have been only 0.3-11% and 5-15% of cases respectively over the last decade, which resulted in a low interest in rigorous prospective clinical studies. Since osteomyelitis induces osteolysis around the implant, which can lead to fractures and complicate revision surgery, orthopedists have anecdotally used anti-resorptive bisphosphonates in these patients to preserve bone stock without knowledge of their effects on chronic infection. Furthermore, in the recent years there has been an alarming increase in reports of osteonecrosis of the jaw, a condition that has been associated with bisphosphonate usage. Although osteomyelitis remains a serious problem in orthopedics, progress has been limited by the absence of an *in vivo* model that can quantify the bacterial load, metabolic activity of the bacteria over time, immunity and osteolysis.

To overcome these obstacles, we developed a murine model of implant-associated osteomyelitis in which a stainless steel pin is coated with *S. aureus* and implanted transcortically through the tibial metaphysis. We analyzed the animals using radiology, histology as well as serology. Bacterial load and activity was determined by Real-time quantitative PCR (RTQ-PCR) and *in vivo* bioluminescence imaging (BLI) of *luxA-E* transformed *S. aureus* (Xen29). Collectively, these studies demonstrate the first quantitative model of implant-associated osteomyelitis that defines the kinetics of microbial growth, osteolysis and humoral immunity following infection (**paper I**).

To better understand the effects of bisphosphonates on osteomyelitis, and shed light on the mechanism of osteonecrosis of the jaw, we investigated the interaction of anti-resorptive agents in our established murine model of implant-associated osteomyelitis. We investigated two distinct classes of anti-resorptive drugs: the most widely prescribed bisphosphonate alendronate and the biologic antagonist osteoprotegerin (OPG). Both agents caused an increase in severe infections. This finding

coincided with a significant decrease in osteolysis and draining lymph node volume, suggesting that anti-resorptive agents decrease efflux of marrow lymph during the establishment of osteomyelitis that could lead to a dramatic increase in intraosseous pressure, infarction and bone pain (**paper II**).

Finally, we evaluated the use of colistin polymethyl methacrylate (PMMA) beads in treating *A. baumannii* induced osteomyelitis. This was done by using our established murine OM model and infecting animals with clinical isolates of multi-drug resistant *A. baumannii*. To demonstrate efficacy of colistin prophylaxis in this model, mice were treated with either parenteral colistin or local colistin using PMMA beads. While parenteral colistin failed to demonstrate any significant effects vs. placebo, the colistin PMMA beads significantly reduced the infection rate (**paper III**).

List of abbreviations:

Aln - Alendronate

BLI – Bioluminescence

CEC – Circulating Endothelial Cells

CFU – Colony Forming Units

CT – Computed Tomography

μCT – micro Computed Tomography

H&E - Hematoxylin and Eosin stain

MDR – Multi Drug Resistant

MRI – Magnetic Resonance Imaging

MRSA – Methicillin Resistant Staphylococcus Aureus

ONJ – Osteonecrosis of the Jaw

OPG - Osteoprotegerin

RANK - Receptor Activator of Nuclear Factor κ B

PCR – Polymerase Chain Reaction

PMMA - Polymethyl Methacrylate

RTQ-PCR – Real Time Quantitative Polymerase Chain Reaction

TNF-α - Tumor Necrosis Factor Alpha

TRAP - Tartrate-resistant Acid Phosphatase

Xen29 – Bioluminescent strain of *S. Aureus*

1 Introduction

Osteomyelitis is a common infectious disease characterized by progressive inflammation and bone destruction. Although the total number of osteomyelitis cases is high in that approximately 112,000 and 240 orthopedic device-related infections occur per year in the US and Denmark respectively, at an approximate hospital cost of \$15,000-70,000 per incident [1] the infection rates for joint prosthesis and fracture-fixation devices have been only 0.3-11% and 5-15% of cases respectively over the last decade, which resulted in a low interest in rigorous prospective clinical studies. Since OM induces osteolysis around the implant, which can lead to fractures and complicate revision surgery, orthopedists have anecdotally used anti-resorptive bisphosphonates in these patients to preserve bone stock without knowledge of their effects on chronic infection. Furthermore, in the recent years there has been an alarming increase in reports of osteonecrosis of the jaw (ONJ), a condition that has been associated with bisphosphonate usage. Although osteomyelitis remains a serious problem in orthopedics, progress has been limited by the absence of an *in vivo* model that can quantify the bacterial load, metabolic activity of the bacteria over time, immunity and osteolysis.

Also, recent years of involvement in Middle-East conflict, had us facing another challenge – an increased incidence of multidrug resistant *A. baumannii* associated osteomyelitis in combat related extremity injuries, which can be difficult to treat.

To address these problems we wanted to:

- *develop a novel quantitative murine model of implant associated osteomyelitis (paper I)*
- *use this model to investigate the effects that anti-catabolic drugs have on the chronic infection (paper II)*
- *investigate whether *A. baumannii* infection can be prevented by systemic or local antibiotic prophylaxis (paper III)*

The current study was based on the following hypotheses:

- *It is possible to develop a murine model of implant-associated osteomyelitis that gives you the possibility to evaluate bacterial growth in vivo and measure the bacterial load.*
- *Anti-catabolic drugs, such as bisphosphonates, can prevent bacterial clearance during establishment of chronic osteomyelitis.*
- *It is possible to reduce infection rate of A. baumannii associated osteomyelitis using systemic or local antibiotic prophylaxis.*

2 Osteomyelitis background: etiology, causes and treatment

Chronic osteomyelitis is a severe, difficult to treat condition, often seen after trauma or invasive surgical procedures on bone, characterized by progressive inflammation and bone destruction and is caused by an infecting organism (**Figure 1A**). The infection can be developed within weeks or even months after the initial trauma or surgical procedure, and can be limited to a single portion of a particular bone or be multifocal, involving several regions such as marrow, cortex, periosteum and the soft tissue.

In some cases osteomyelitis can be seen as a secondary infection, following vascular insufficiency. This is predominately seen in Diabetes Mellitus (DM) patients, where the disease itself contributes to the infection process with several factors, such as neuropathy, ischemia as well as the metabolic consequences of diabetes itself. In these cases the bone infection is almost always preceded by an overlaying soft-tissue infection (**Figure 1B**).

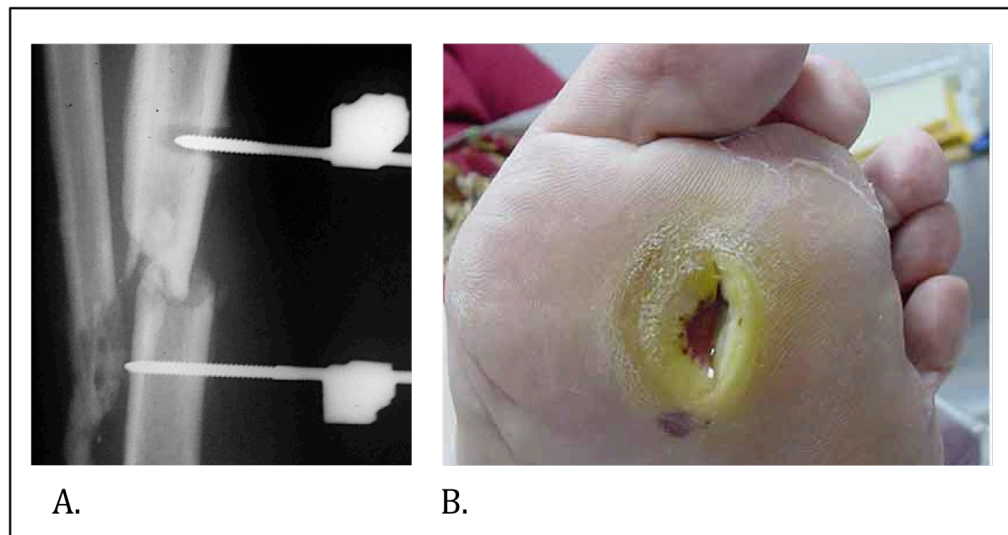


Figure 1

- A. *Infected external fracture fixator, with osteolysis around proximal screw.*
- B. *Diabetic foot, with an ulcer and underlying osteomyelitis (adapted from thefootblog.com)*

Acute osteomyelitis often occurs in children (85%), 3 times more often in boys than girls. Up to 90% of all cases are localized to metaphysis of long bones, and is often due to haematogenous spreading of bacteria from a primary infection site such as pharyngitis. Infections in neonates are often caused by Gram-negative bacteria (90%), most often *E. coli*, while *S. aureus* is the main pathogen in adult infections (78).

More than 12.000 joint replacement surgeries are performed in Denmark each year, most as a successful treatment of arthrosis or traumatic fractures [2]. The problem lies in the introduction of a foreign body, which increases the risk of possible infection. The infection can be haematogenous, but in most cases it is caused by contamination of the wound during surgery, either by airborne pathogens or by bacteria from patient's skin. Several decades ago the infection rate of such joint replacement surgeries was as high as 9% [3], but due to vigorous peroperative antibiotic treatment and other prophylactic approaches is now reduced to 1-2% [2, 4]. The highest incidence of infection is seen in shoulder and knee prosthesis implants, while hip implants are less often infected [5-7]. Every year around 240 and 112.000 orthopedic device-related infections occur in Denmark and US respectively [1, 4, 8]. These infections are associated with high morbidity, and the treatment is costly, seen from a financial as well as sociological point of view.

2.1 Pathology

The development of osteomyelitis is related to multiple microbial and host factors, such as a presence of foreign bodies in bone or an insufficient immune response in patient. As mentioned previously the wound can be contaminated during surgery with bacteria from air or patients skin (60-80%), or infection can be spread haematogenically from another infection site in the body (20-40%) [2]. *S. aureus* is by far the most common pathogen, responsible for up to 80% of cases [1], but infections with other opportunistic pathogens, primarily coagulase negative staphylococci are also seen.

S. aureus has a number of virulence factors that contribute to pathogenesis. There are factors promoting the attachment of bacteria to extracellular matrix proteins, bacterial adhesins [9, 10]; factors that promote evasion from the hosts immune response, such as

protein A and capsular polysaccharides; and factors that induce penetration and degradation of host tissue – exotoxins and hydrolases [11].

S. aureus can also form biofilm that remains a huge therapeutical challenge, because of its low penetrability to antibiotics. It is formed by a cluster of cells that attach to substratum, interface or to each other, and is embedded in a matrix of extracellular polymeric substance. These bacteria show an altered phenotype in terms of growth, gene expression and protein production [12]. The presence of an orthopedic implant induces formation of biofilm, and thus promotes the potential infection. Whether or not the biofilm is formed depends on the balance between the immune response of the patient and the virulence factors of bacterial pathogens [13].

Osteomyelitis infection is usually accompanied by bone loss at the site of infection [4, 14-16]. Bacterial infection is known to induce cascade of host proinflammatory cytokines including TNF- α and IL-1, both of which have been shown to enhance osteoclast differentiation and resorption through RANKL signaling molecules [4, 14, 15]. They also express pathogenic molecules such as LPS and teichoic acids that may have similar agonistic actions on osteoclasts [10, 17], thus promoting osteolysis **(Figure 2)**.

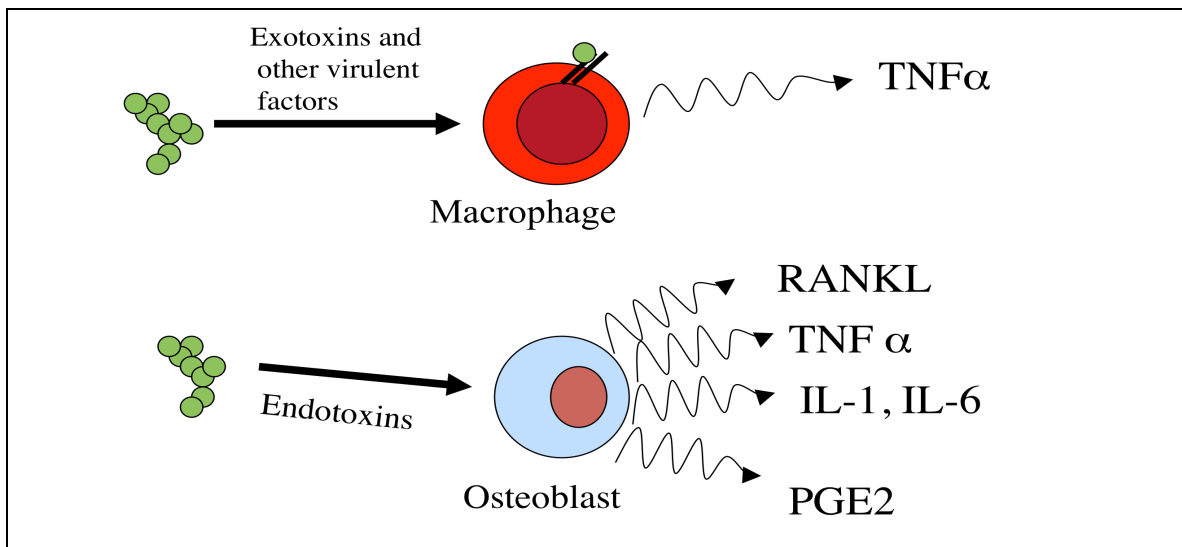


Figure 2

Bacterial exo- and endotoxins induce osteoclastic bone resorption through a cascade of host proinflammatory cytokines including IL-1 and TNF- α as well as through RANKL signaling.

2.2 Diagnosis

Diagnostics of chronic osteomyelitis infection is based on clinical, paraclinical, histopathological and radiological techniques. In some cases, the latent infection can be asymptomatic but will often present itself with pain, fever, swelling, and inflammation of the overlying soft tissue (78). Biochemical analysis of the blood shows an elevated white blood count, as well as an increased level of C-reactive protein (CRP).

The most important step in diagnosing any type of osteomyelitis is microbiological and histopathological analysis, where the offending microorganism is isolated and cultured, so that an appropriate antimicrobial therapy can be selected. Isolation of bacteria can be achieved by blood cultures (this is mostly used in haematogenous osteomyelitis) or by direct biopsy from the infected tissue [18, 19]. Samples obtained by swabs in unsterile conditions might result in contamination by bacteria from the skin and result in inaccurate microbiological diagnosis, therefore it is

recommended that the biopsies are obtained a.m. Kamme-Lindberg, where 5 samples are obtained from the same infection site using 5 separate sets of sterile instruments [20]. The samples will then be cultured and stained using H&E, Gram or Ziehl-Neelsen stains to reveal the pathogen.

Radiological analysis has also tremendous value in diagnosing the osteomyelitis infection [4, 21, 22]. The cheapest and easiest radiological method is a plain X-ray autoradiography, which shows soft tissue swelling, osteolysis and periosteal reaction. Computed Tomography (CT) and Magnetic Resonance Imaging (MRI) are more sensitive methods that provide a more detailed pattern of osteomyelitis lesion. CT is superior to plain autoradiography in visualizing bone, where cortical bone is defined with greater detail as compared to plain film and sequestrers can be identified, whilst MRI is more effective for soft tissue imaging and detection of early infection by revealing bone edema. Finally, Tc-scintigraphy can be used to reveal an increased bone turnover, but so far has a limited use because of false-positive results in cases with preceding trauma, surgery or Charcot arthropathy.

2.3 Treatment

Treatment of osteomyelitis consists of prophylaxis and medical as well as surgical treatment of an already established infection [23].

2.3.1 Prophylaxis

Prophylaxis consists of intravenous antibiotics, administered within 1 hour preoperatively and no later than 24 hours postoperatively [24] with antistaphylococcal penicillins and second-generation cephalosporins being the most common choices. Laminar airflow is also used in operating rooms to prevent infections; it increases the air exchange rate and eliminates turbulence, thus decreasing airborne bacterial contamination. Multiple studies have been published, showing that laminar airflow alone reduces risk of infection, but so far there is no conclusive evidence that it would increase the prophylactic effect of systemically administered antibiotics [2].

2.3.2 Medical

In many cases of acute osteomyelitis antimicrobial therapy would be adequate, with the choice of antimicrobial agent depending on the isolated microorganism. The antibiotic treatment should be administered intravenously for 4-6 weeks, while the clinical and paraclinical parameters are being monitored [2, 4].

2.3.3 Surgical

In cases of chronic osteomyelitis, surgical revision supplemented by antibiotic therapy is usually the only option. The goal is to remove the necrotic as well as infected bone, sequestra, and infected soft tissue, thus achieving sufficient revascularization of the infected site [25]. The infection can be classified according to Gustilo [26] that subdivides the disease into 4 categories: 1) early postoperative infection, 2) late postoperative infection, 3) acute haematogenous infection and 4) randomly diagnosed infection, with positive biopsy results after aseptic implant loosening. Depending on the type of infection one- or two-step revision surgery, with insertion of a gentamycin cement spacer, might be required [2]. In some complicated cases, where multiple revisions have been carried out and the patient condition does not allow an alternative complicated and risky procedure, Girdlestone-status can be considered, where all the implant material is removed [27].

As mentioned, antibiotic and surgical treatment can in some cases be complimented by inserting beads or cement loaded with an appropriate antibiotic. Several studies have been performed to elucidate the effect of such local antibiotic therapy [27-29] and most have found that usage of antibiotic cement has prophylactic effect against infection and decreases the number of revision surgeries.

2.4 Emergence of methicillin-resistant *S. aureus*

Methicillin-resistant *S. aureus* (MRSA) has been a problem in hospitalized patients since the 1960's, and is globally the most common nosocomial infection worldwide. Until recently the Scandinavian countries have been spared, and prior to 2002, less than 1% of all *S. aureus* grows found were MRSA strains [76]. Unfortunately

this number is rapidly increasing, and some physicians are warning of a MRSA epidemic emerging in Denmark [77]. Also, while earlier MRSA was strictly found in nosocomial infection, now it is frequently found as a community associated pathogen. The problem is much more severe and common on a global scale – where up to 50% of *S. aureus* strains found are methicillin resistant [30, 31]. MRSA infections are associated with greater lengths of hospitalization, higher mortality, increased treatment costs [32] and dramatically impact clinical management.

2.5 Multidrug resistant *Acinetobacter* in warfare

Another challenge that we are facing in treatment of osteomyelitis is multidrug resistant (MDR) *Acinetobacter* species. It has been well established from current combat-related injuries during the US military operations in Iraq and Afghanistan that the ratio of serious injuries to fatal casualties exceeds that of previous conflicts [33]. Orthopedic trauma comprises the vast majority of these war wounds, as 70 % involve musculoskeletal system [34, 35]. Thus, it is not surprising that the incidence of osteomyelitis in combat-related extremity injuries is between 2% to 15%, and is of great concern [36-38]. Most alarming is the high incidence of infections caused by multidrug-resistant *Acinetobacter* species, which can be difficult to cure in some settings [36, 39, 40]. Surprisingly this pathogen has been reported in less than 2% of nosocomial infections within the United States, but has emerged in over 30% of admitted deployed soldiers [40]. In contrast to *S. aureus*, which is responsible for > 80% of osteomyelitis infections, *Acinetobacter baumannii-calcoaceticus* complexes are Gram-negative, non-fermentive, non-spore forming, strictly aerobic, oxidase-negative coccobacillary organisms. Additionally, infections caused by *Acinetobacter* appear to be hospital-acquired and not from an initial colonization of the injury [41].

2.6 Bisphosphonates

Bisphosphonates discovered in 1960's by Fleisch et al [42] are synthetic organic analogues of pyrophosphates, that inhibit bone resorption by inducing osteoclastic inactivation and/or apoptosis of osteoclasts. When bisphosphonates are administered systemically, most of the drug that is not excreted renally is accumulated at sites of active bone turnover and binds to hydroxyapatite where it becomes metabolically inactive [43]. It is released from this inactive state in the body when the bone is resorbed through a remodeling or other bone-metabolic events, and becomes active again in its unbound state, where it again is available for either rebinding to hydroxyapatite or cellular uptake by endocytosis. Due to osteoclastic bone resorption bisphosphonates are likely to be internalized in the osteoclasts causing its release from the skeleton. The accumulation of bisphosphonate in the osteoclast leads to inhibition of its activity and/or death that results in decreasing of local bone resorption.

Early non-nitrogen-containing bisphosphonates (etidronate, clodronate, and tiludronate) are considered first-generation bisphosphonates. Because of their close structural similarity to inorganic pyrophosphates, non-nitrogen-containing bisphosphonates become incorporated into molecules of newly formed adenosine triphosphate (ATP) by the class II aminoacyl-transfer RNA synthetases after osteoclast-mediated uptake from the bone mineral surface. Intracellular accumulation of these nonhydrolyzable ATP analogues is believed to be cytotoxic to osteoclasts because they inhibit multiple ATP-dependent cellular processes, leading to osteoclast apoptosis [44]. Unlike early bisphosphonates, second- and third-generation bisphosphonates (alendronate, risedronate, ibandronate, pamidronate, and zoledronic acid) have nitrogen-containing side chains. The mechanism by which nitrogen-containing bisphosphonates promote osteoclast apoptosis is distinct from that of the non-nitrogen containing first-generation bisphosphonates. These more potent N-bisphosphonates inhibit farnesyl pyrophosphate synthase, an enzyme of the mevalonate pathway, inhibiting protein prenylation, which ultimately leads to osteoclast apoptosis [44] **(Figure 3)**

By inducing osteoclast apoptosis, bisphosphonates have become the primary therapy for treating conditions characterized by increased osteoclast-mediated bone

resorption. Such excessive and unwanted resorption has been observed in several pathologic conditions for which bisphosphonates are now used, including multiple forms of osteoporosis, Paget disease of bone, osteogenesis imperfecta, hypercalcemia and bone metastasis from malignancies [45]. These drugs have been used locally [46, 47] and systemically [48] to increase implant stability and prevent implant loosening following allograft surgery. There have also been several studies that reported the use of bisphosphonates to treat patients with osteomyelitis by inhibiting bone resorption and preservation of bone stock [49, 50].

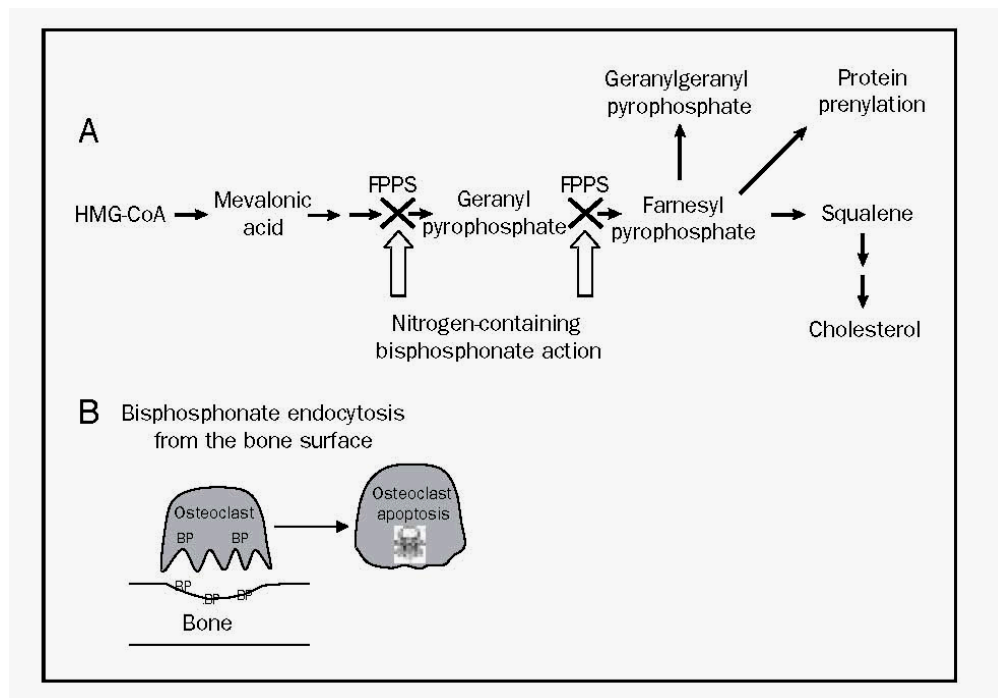


Figure 3

Bisphosphonates decrease osteoclastic bone resorption by inhibiting mevalonate pathway, which ultimately leads to osteoclast apoptosis. (adapted from Drake MT et al.)

2.7 Osteonecrosis of the jaw (ONJ)

Another clinical condition that is associated with osteomyelitis and bisphosphonate usage is osteonecrosis of the jaw (ONJ). It is a severe bone disease that affects the jaws, including the maxilla and the mandible. It is typified by exposed bone in the maxillofacial region that does not heal after 8 weeks after identification by a health care provider and may be accompanied by clinical symptoms such as swelling, pain, loosening of teeth and drainage but can also be asymptomatic [51] (**Figure 4**).

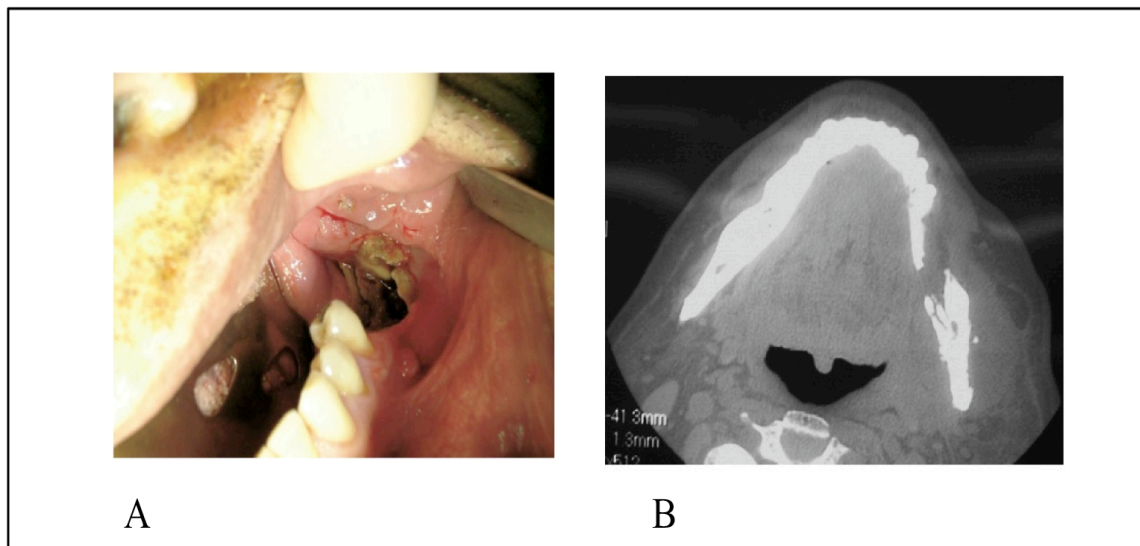


Figure 4

A. Oral view, revealing exposed bone and osteonecrosis. B. Axial CT image of bone defect in left mandible due to ONJ (adapted from Gutta et al.)

In the last decade an increasing number of ONJ cases has been reported and some medical experts even speak of an epidemic [49, 52, 53] that primarily affects cancer patients after immunosuppressive chemotherapy who also receive intravenous nitrogen-containing bisphosphonates, (pamidronate or zoledronate), for hypercalcaemia, and undergo unrelated oral surgery. However, ONJ has also been reported in healthy women taking oral alendronate for postmenopausal osteoporosis [51, 54, 55], raising serious concerns for the tens of millions of people taking these anti-resorptive agents worldwide.

The exact incidence of ONJ is unknown. However, some reports have estimated the ONJ incidence to be around 1:10.000 [56]. A single center study has reported 11% incidence of ONJ in patients with multiple myeloma treated with bisphosphonates [57]. The incidence of developing ONJ increases with the time of exposure, and this risk increases dramatically in patients treated with zoledronic acid.

Management of patients diagnosed with ONJ is currently based on staging of the disease [56]:

- Stage 1 is exposed/necrotic bone in asymptomatic patients, where no evidence of infection is present.
- Stage 2 is exposed/necrotic bone with clinical evidence of infection.
- Stage 3 is exposed/necrotic bone in patients with pain, infection and one more of the following features: pathologic fracture, extraoral fistula or osteolysis extending to the inferior border.

Briefly, current treatment of ONJ is as follows:

- Stage 1 ONJ: Conservative management with antiseptic oral rinse.
- Stage 2 ONJ: Antiseptic oral rinses combined with antibiotics.
- Stage 3 ONJ: Surgical debridement/resection in combination with antibiotic therapy.

Although the etiology of ONJ remains poorly understood, careful reviews of all the available clinical and basic science data have derived two leading theories to explain this painful condition [56, 58]. The first theory explains ONJ by inhibition of angiogenesis, which is largely derived from the precedent of steroid-induced avascular necrosis of the hip. In addition, several new studies have demonstrated bisphosphonate-inhibition of capillary tube formation, vessel sprouting and circulating endothelial cells (CEC) implying that bisphosphonates have a antiangiogenic effect and a suppressive effect on CECs of patients with ONJ [59, 60]. The second hypothesis is based on the osteoclast-inhibiting effect of anti-resorptive agents that lead to a cessation of bone

remodeling and mineralmatrix turnover [61]. This concept renders the fatigued bone susceptible to involution of blood vessels, necrosis and infection. The importance of infection in ONJ is further highlighted by the finding that essentially all cases have histopathological evidence of osteomyelitis [62, 63] although a cause and effect relationship has yet to be established.

2.8 Animal models of osteomyelitis

To date most of the information on the pathogenesis of chronic osteomyelitis gained from animal models [64]. The history of the development of animal osteomyelitis models is rather simple going back more than 100 years with a rather short list of publications stretching from 1885 to 1970, with a significant increase in number of published papers after 1970. The latter is most likely correlated to fast growing field of antibiotics and advanced orthopedic surgical procedures.

The first trials on animal models of osteomyelitis can be found in 1885, when Rodet described a novel animal model, in which staphylococci were injected intravenously to produce bone abscesses in rabbits. Many years later in 1941, Scheman et al reported a chronic osteomyelitis model using rabbits, injecting staphylococci and sodium morrhuate directly into tibia metaphysis, thus establishing the basics for modeling a chronic osteomyelitis infection in animals with the use of sclerosing agent or a foreign body, and many were to follow. By now, a large number of animal models of osteomyelitis have been created and presenting all of them would be meticulous and derivates from the framework of this thesis. Several recent reviews comprehensively cover this matter [64, 65]. Instead, I will focus on presenting the general principles in the available models, as well as presenting a few choice ones.

2.8.1 Bacterial species and inoculation

Most animal models use *S. aureus* as a bacterial strain for the establishment of the infection, because *S. aureus* is the most common pathogen in clinical cases of human osteomyelitis. Many investigators use bacterial strains isolated locally from their patients, while others used strains obtained from ATCC bank. Other bacterial strains have also

been used, such as *E. coli*, *P. aeruginosa* and *S. epidermidis*. By far, most studies use a single bacterial strain, but in a few reports two bacterial species are mixed together to mimic a complicated, mixed bacterial infection or superinfection. Inoculation numbers between 10^6 and 10^8 cfu give close to a 100% infection rate [65]. If a lower infection rate is needed for comparison studies, lower inoculation numbers can be considered, as well different implant materials or different local bone treatments.

2.8.2 Inoculation routes and infection promoters

Three main routes of inoculation have been described, namely (i) local inoculation of bacteria into bone, (ii) local inoculation through nutrient arteries and (iii) systemic intravenous inoculation. Local inoculation of bacteria into bone can be achieved by several ways: injecting bacteria into medullar cavity, injecting it through a predrilled hole or by inserting an implant already inoculated with bacteria.

Sclerosing agents are often used to promote infection. They act by causing sclerosis of vessels in the medullary canal, which subsequently leads to tissue and bone necrosis, ultimately leading to decreased host defense system, increased proliferation of bacteria and chronic osteomyelitis. The standard sclerosing agent is sodium morrhuate.

Foreign bodies and implants are also often used to increase infection rates and promote existing infection. The presence of an implant provides surface for bacterial adhesion [10] and subsequent biofilm formation. Some studies also suggest that the presence of the implant itself may result in a less effective immune response [66, 67]. This explains lower infection rates in animals that only received bacterial inoculum without any foreign body present. Most common foreign body's used are: bone cement, metal wires and intramedullary nails such as Kirschner wires.

Finally, trauma or injury to the bone, have been used to promote the infection. This can be achieved by drilling or fracturing the bone.

2.8.3 Animals

Many animals have been used in attempt to create an animal model of osteomyelitis that would allow us to study the infection *in vivo*. Here I present several choice models where different animal species have been used.

Chickens were used by Daum RS [68] in 1990, to develop an avian model of *S. aureus* infection, in which bacteria were introduced intravenously. Bacteremia, as well as survival rate was observed in this study.

Passl et al [69] developed a posttraumatic femoral osteomyelitis model in guinea pigs in 1984, in which surgically fractured femurs were infected with either *S. aureus* or *E. coli*, and some were fixed with an intramedullary pin. All animals inoculated with *S. aureus* (10^4 cfu) developed chronic osteomyelitis, while only 9 out of 12 infected with *E. coli* developed chronic infection. The introduction of intramedullary implant increased incidence of chronic osteomyelitis in *E. coli* infected animals to 100%.

A rabbit model of posttraumatic tibial osteomyelitis was introduced by Worlock et al in 1988 [70]. This model showed that inoculation of the fracture site with *Staphylococcus aureus* (10^6 cfu) caused osteomyelitis in two out of five rabbits. When the concentration of inoculum was increased to 10^7 organisms, osteomyelitis was seen in four out of five rabbits. No implant was used in this model, and the infection was detected radiologically as well as histologically.

Dogs were used by Varshney et al in 1989 [71], in which experimental osteomyelitis was evoked in 45 male dogs by inoculating hemolytic strain of *S. aureus* (10^8 cfu) into the tibial marrow cavity through a predrilled hole in metaphyseal area. Clinical, radiological and bacteriological studies were conducted to evaluate the progress of disease up to 15 weeks. Clinically localized soft tissue swelling, pain, pyrexia and lameness were observed, while autoradiography showed an extensive periosteal reaction, cortical osteolysis, new bone formation, frequent development of sequestrum. The formation of localized abscess pockets was also observed in several advanced cases. It is noteworthy that - to my knowledge - there has been no publications describing dogs for osteomyelitis models since 1995, possible due to relative high cost of animals as well as ethical aspects and public pressure.

In 1997 Kaarsemaker and co-authors [72] reported a sheep tibial osteomyelitis model. The infection was induced in adult Texas sheep by injection a sclerosing agent (tetradecylsodiumsulphate) followed by 4×10^8 cfu *S. aureus* through a drill hole in upper tibia. The animals were monitored by radiological, clinical and histological parameters for 3 months. Though the infection rate was high, so was the mortality rate (29%), whilst the extent of the infection was mostly limited to the upper part of the tibia.

A similar approach was used with a goat tibial model in 2005 [73]. The infection was induced by drilling a hole at the upper tibia and injecting sodium morrhuate, followed by 4×10^9 cfu *S. aureus* and bone wax. The rate of osteomyelitis development was estimated by autoradiography and histochemistry (96%) as well as bacteriological culture tests (82%).

Lucke M et al used rats to develop an experimental osteomyelitis in 2003 [74]. *S. aureus* was introduced into tibial medullary cavity with simulation insertion of a Kirschner wire. The animals were followed for 4 weeks with clinical, radiological and histological measurements. This model showed high infection rate (close to 100%) with as few as 10^2 cfu *S. aureus* used as infecting agent.

Finally, Yoshii et al, used a murine model of osteomyelitis in 2002 [75], that was previously described in 1974 by Ueno et al. In this model animals were infected using *S. aureus* soaked silk thread through a drilled hole in proximal tibia. The brief overview of using animal models in establishing of experimental osteomyelitis is presented in the Table 1.

Animal	Bacteria	Site	Sclerosing agent	Implant
Chicken [68]	<i>S. Aureus</i>	I.v.	÷	÷
Guinea pig [69]	<i>S. Aureus / E.coli</i>	Femur	÷	IM pin
Rabbit [70]	<i>S. Aureus</i>	Tibia	÷	÷
Dog [71]	<i>S. Aureus</i>	Tibia	÷	÷
Sheep [72]	<i>S. Aureus</i>	Tibia	+	÷
Goat [73]	<i>S. Aureus</i>	Tibia	+	Bone wax
Rat [74]	<i>S. Aureus</i>	Tibia	÷	IM K-wire
Mouse [75]	<i>S. Aureus</i>	Tibia	÷	Silk thread
Mouse (Paper I)	<i>S. Aureus</i>	Tibia	÷	Transcortical pin

Table 1 *Animal models of chronic osteomyelitis.*

3 Problems and main goals of the study

3.1 Animal models.

To date, much of our knowledge of the pathogenesis of osteomyelitis comes from animal models, which are briefly described above (see section 2.8). These models have been established to mimic infection in humans, and have been used to confirm the importance of bacterial adhaesins that have been identified from *in vitro* assays. Unfortunately, none of these models used so far contain quantitative endpoints that determine bacterial load or growth *in vivo*. Thus, they are of limited value for assessing drug effects, bacterial mutants and various host factors that may play an important role(s) in development of chronic osteomyelitis.

To overcome this obstacle we aimed to develop a novel murine model of implant associated osteomyelitis in which bacterial activity can be monitored and bacterial load quantified (**Paper I**).

3.2 Osteomyelitis and use of bisphosphonates

As described above (see section 2.8) bisphosphonates inhibit osteoclastic bone resorption and are used for treatment of millions of patients worldwide. As described in section 2.8, implant associated osteomyelitis induces osteolysis adjacent to the implant and orthopedists use bisphosphonates to preserve bone stock as well as to prevent implant loosening. However our knowledge of the effects that such treatment strategies might have on chronic infection is very limited. Additionally, bisphosphonate-associated osteonecrosis of the jaws is a significant complication in a subset of patients receiving these drugs. The emergence of osteonecrosis of the jaw epidemic calls for a further investigation of the effect that anti-catabolic therapy might have on bone infection.

To better understand the effect of bisphosphonates on osteomyelitis, and shed light on potential mechanisms of ONJ we wanted to investigate the interaction

of anti-resorptive agents in earlier established murine infection model that emulates the biology of infected orthopedic and periodontal implants (**Paper II**).

3.3 Multi-drug resistant *Acinetobacter* species

While only 2% of nosocomial infection within the United States was associated with *A. baumannii*, it has emerged in over 30% of admitted soldiers deployed in Iraq and Afghanistan. Incidence of osteomyelitis in combat-related extremity injuries is in between 2% to 15% and is of great concern, especially due to infections caused by MDR *A. baumannii*, which can be difficult to cure in some settings.

Using our murine model of implant-associated osteomyelitis, we wanted to investigate whether or not the MDR *Acinetobacter* can be effectively prevented with parenteral or local antibiotic therapy at the time of initial surgery (**Paper III**).

4 Materials and methods

4.1 strains, pathogenic challenge and surgical procedure

The UAMS-1 strain of *S. aureus* (ATCC 49230) was obtained from the American Type Culture Collection (Manassas, VA, USA). The bioluminescent strain of *S. aureus*, Xen29 (derived from ATCC 12600) was obtained from Xenogen Inc. (Cranbury, NJ, USA). Pathogenic challenge was initiated *via* a contaminated 0.25 mm diameter insect pin (Fine Science Tools, Foster City, CA) that was generated as follows. The pins were autoclaved and stored in 70% ethanol. After air-drying, the pins were incubated in 1.5 ml of an overnight luria broth culture of *S. aureus* for 20 min. Then, the pins were air dried for 5 minutes before trans-tibial implantation. The inoculating dose of bacteria was determined to be $9.5 \pm 3.7 \times 10^5$ CFU of UAMS-1 and $4.2 \pm 0.5 \times 10^5$ CFU of Xen29

per pin, by resuspending the bacteria from the pin by vigorously vortexing it in PBS and growing dilutions on agar plates.

All animal studies were performed under University Committee for Animal Resources approved protocols. C57BL/6 female 6-8 week-old mice were anesthetized with Ketamine (100 mg/kg) and Xylazine (10 mg/kg), their left tibiae were shaved and the skin was cleansed with 70% ethanol. Infection was initiated by placing the pin transcortically through the tibia. The pin was bent at both ends for stability and cut adjacent to the skin on both ends, which allowed it to be covered by the skin and to eliminate additional environmental exposure (**Figure 5**). Once the mice recovered from the anesthesia, they were returned to standard isolator cages.



Figure 5

Transcortical pin, inserted through tibia.

Considerations:

The first choice that we had to make was what animal to use for the model. We decided on mice for several reasons. First of all it is a very economic animal due to low purchase and maintenance costs. Also the small size allows relatively easy manipulation, and gave us the possibility to use bioluminescent imaging, which would not be possible with larger animals. Also specific pathogen free nature of current animals makes them very robust and sufficiently decreases risk of contamination in infection studies. Unfortunately there are several drawbacks. The small size of the animals does not facilitate testing of larger fixation devices or implants, and makes intravenous drug administration rather difficult. Also, the small size limits the possibility of performing biochemical blood analysis throughout the course of infection, due to limited blood drawing capability. We believe that the presence of a transcortical implant is essential to the infection process for two main reasons: (i) the implant provides an additional surface for bacterial adherence and (ii) the presence of the implant itself may result in a less effective immune response. These contentions are supported within context of the previous studies showing the higher infection rates observed in animal models that made use of an implant or other foreign body, compared to models that only used bacterial inoculum without an insertion of foreign body.

Unlike other models, which employ a relatively known number of bacteria injected into a predrilled tibia or marrow cavity, we chose to use the implant coated with bacteria. Our rationale was based on the assumption, that this approach would mimic the insertion of a contaminated implant, as it takes place in clinical practice, and will promote biofilm formation. However, this method does have a serious drawback - while one can accurately measure the bacterial inoculum on the implant, there is no way to determine the amount of bacteria that is actually delivered to the bone, since some of it might easily get scrapped off during the insertion. We chose to accept this flaw, and take it into account by normalizing our measurements while performing quantification analysis, and aiming to perform the surgical procedure identically every time, reducing variability in bacterial inoculum between animals.

Finally, we chose a trans-tibial implant over the intramedullary one. An intramedullary implant approach might be considered more relevant, since it reproduces a more serious clinical condition, for example mimicking an infected hip prosthesis. However, our preliminary pilot studies showed that an intramedullary model gave rise to variable spatial and temporal lesion, as well as hematologic spreading, making a reproducible, quantitative model very challenging.

4.2 Histology

After μ CT, the tibial samples were processed for decalcified histology and stained with Orange G/alcian blue (H&E), Gram-stained, or tested for tartrate-resistant acid phosphatase (TRAP).

Considerations:

Main hallmarks of chronic osteomyelitis are sequestrum and involucrum formation, which we would be able to detect using H&E staining. TRAP staining allows to visualize osteoclastic bone resorption of cortical bone and provides the possibility to evaluate osteoclast numbers, and thus to validate the effects of the anti-resorptive treatment. Finally, Gram staining would show extracellular bacteria and biofilm in the necrotic bone lesions surrounding the implant.

4.3 DNA purification and *nuc/b-actin* RTQ-PCR

Infected tibiae were disarticulated and separated from the surrounding soft tissues, and the infected segment of the bone was demineralized. DNA was extracted as described in the paper I. Real-time quantitative PCR (RTQ-PCR) for the *S. aureus*-specific *nuc* gene was performed to quantify the bacterial load. The samples were assayed in triplicate in a Rotor-Gene RG 3000 (Corbett Research, Sydney, AU). In order to control for the integrity of the DNA template between samples we performed RTQ-PCR for the mouse *β -actin* gene that detects a 260-bp product. In order to calculate the *nuc*

gene copies in a tibia sample, we first generated a standard curve with *S. aureus* genomic DNA purified directly from an overnight culture (**Figure 6**). The mean of the 3 Ct values from each tibia sample were then plotted against this curve to extrapolate the number of *nuc* genes. This number was then normalized to β -actin and the data are presented as normalized *nuc* genes per tibia.

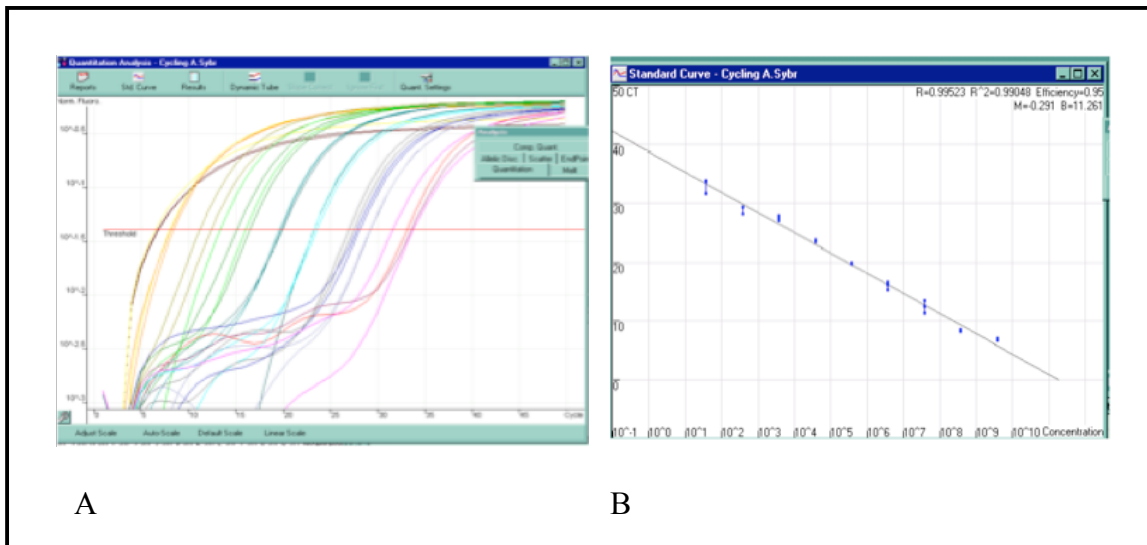


Figure 6.

A. RTQ-PCR analysis on serial dilutions of nuc gene cloned into a TOPO 2.1 plasmid B. Standard curve generated using serial dilutions of a nuc gene cloned into a TOPO 2.1 plasmid. Since the molecular weights of the nuc PCR product and TOPO plasmid are known from the DNA sequence, we can readily derive the number of nuc copies in a sample of purified pTOPO2.1-nuc plasmid based on the DNA concentration.

Considerations:

The main challenge in our study was developing a method that would allow us to quantify the bacterial load in the infected bone. The Gold Standard for quantifying bacteria in tissue is culturing bacteria from the infected tissue using serial dilution, and calculating the cfu numbers after direct plating of samples onto agar. Unfortunately, this

method is rather labour intensive and inaccurate when working with bone because bone mineralization and biofilm production makes the extraction of individual bacteria virtually impossible. To overcome this obstacle we have adapted a method that makes use of Real-Time PCR to quantify the number of a particular DNA sequence in a sample, which was successfully applied to quantify *S. aureus* levels in contaminated cheese. We quantified the number of *nuc* gene (a genetic sequence specific for *S. aureus*) in infected samples, and since each bacterium has only one copy of the *nuc* gene, the number of *nuc* copies quantified by the RTQ-PCR assay corresponds to the number of bacteria. The drawback of this method is that some amount of bacterial DNA may be damaged and destroyed during DNA purification process. By performing the DNA extraction strictly according to the protocol, we hope to extract the same “percentage” of intact DNA from bone tissue in every experiment. To further control the integrity of the DNA as well as the possible variations in initial tissue sample size, we normalized the RTQ-PCR data to *β -actin*, a household gene in mice tissue. One might argue that the severity of the infection may influence the *β -actin* levels due to necrosis, but this acellular tissue is much less than 1% of the total tibia tissue harvested for the genomic DNA preparation. It is therefore unlikely, that this variability could significantly affect our results.

4.4 *In vivo* bioluminescent imaging

Bioluminescent imaging (BLI) of mice infected with Xen29 was performed on day 0, 4, 7, 11, 14, 18 post-infection using a Xenogen IVIS camera system (Xenogen Corporation, Alameda, Calif.) (**Figure 7**). Five minute high sensitivity ventral images were taken at each time point. The BLI was quantified with the LivingImage software package 2.50.1 (Xenogen Corporation, Alameda, Calif.) by analyzing a fixed 1.5 cm diameter region of interest (ROI) centered on the pin. The photon signal was calculated as p/sec/cm²/sr.

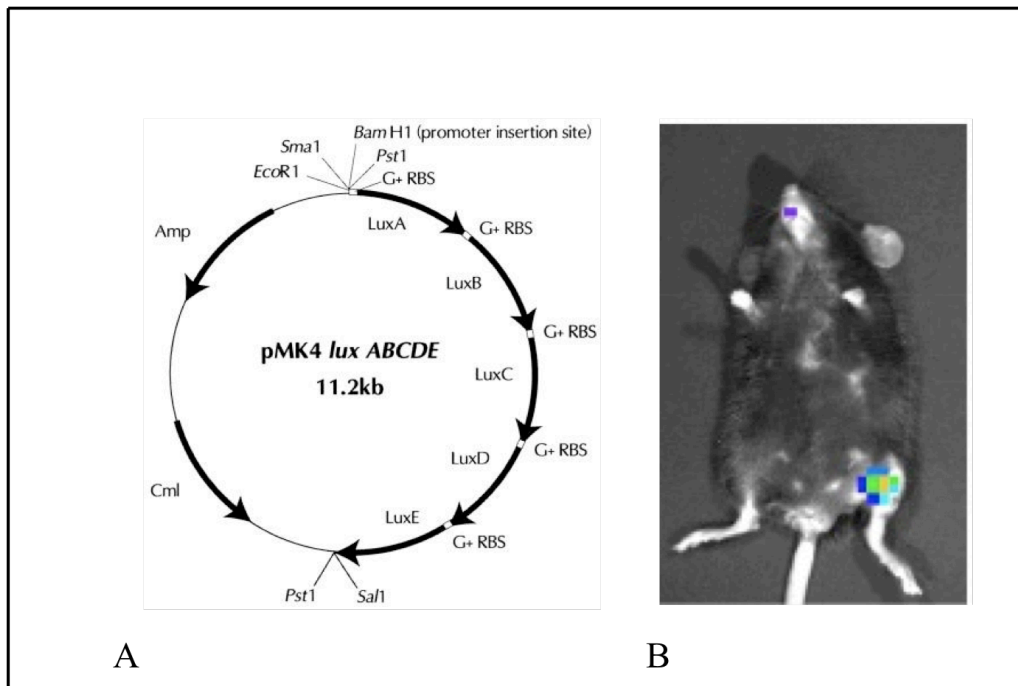


Figure 7.

A. Schematic diagram of the plasmid pMK4 luxABCDE, used to create bioluminescent *S. aureus*. B. Mouse with Xen29 infected left tibia, as seen through Xenogen IVIS camera. Bioluminescence signal around the infection site is measured with following software.

Considerations:

RTQ-PCR analysis described previously is a valuable tool in measuring bacterial load in infected tissue. Unfortunately, the RTQ-PCR approach suffers from two significant shortcomings that limit its usability. The first one is the sacrificial endpoint, which prohibits longitudinal studies. The second drawback is inability of RTQ-PCR to distinguish between metabolically active bacteria and dormant bacteria residing in biofilm. To overcome these obstacles we made use of a bioluminescent strain of *S. aureus* (Xen29) that can be quantified using longitudinal *in vivo* bioluminescent imaging - a method primarily described by Francis's group. The investigators introduced *S. aureus* that were transformed with plasmid DNA containing a *Photobacterium luminescens lux*

operon, making them highly bioluminescent and allowing detection of fewer than 100 cfu *in vitro*.

In vivo bioluminescent imaging gives us a possibility to evaluate bacterial activity *in vivo*, avoiding thereby the necessity of a sacrificial endpoint. BLI is a measure of bacterial protein synthesis and, therefore detects only metabolically active bacteria. It cannot stand alone, since it will not detect dormant bacteria that reside within biofilm but together with real-time PCR measurements, it provides a valuable tool in assessing bacterial activity and load. Unfortunately, BLI has the same shortcoming as RTQ-PCR analysis and can only give us an assessment of bacterial activity but not their actual number.

4.5 Drug treatments

Drug treatments started on the day of the surgery, except for Alendronate, which started 3 days preoperatively. Alendronate was given at 10 µg/kg i.p. once every 3 days. OPG was given at 200 µg/kg once every 3 days. TNFR:Fc was given at 200 µg/kg once every 3 days. Placebo was given as 200 µl PBS i.p. once every 3 days. Gentamycin was given daily (0.1 mg/kg i.p.).

Considerations:

Our goal was to investigate the effect that anti-catabolic drugs have on chronic osteomyelitis. We chose to investigate two distinct classes of anti-resorptive drugs: the most common prescribed bisphosphonate Alendronate, which induces osteoclast apoptosis via inhibition of mevalonate pathway (**Figure 2**), and the biologic antagonist osteoprotegerin (OPG) that inhibits osteoclast formation and induces osteoclast apoptosis by blocking receptor activator of nuclear factor kappa B (RANK) signaling pathway. TNFR:Fc was used as a control that is known to inhibit osteoclasts and exacerbate infections by inhibiting granuloma formation. We used a slightly higher dosage of bisphosphonates compared to what is used in humans (1mg/kg/week p.o. with 0.6% bioavailability) compared to 10 µg/kg i.p. once every

3 days to treat the animals. To make sure that this dosage was sufficient, we applied TRAP staining and radiology to analyze the effect the drugs had on osteoclast numbers and osteolysis. This was done for all treatments. A minor shortcoming in our strategy treatments is that we did not investigate the possible effect of zoledronic acid (the i.v. bisphosphonate that is most commonly associated with ONJ) might have on the development of the infection. However, we chose to focus on Alendronate, the most widely prescribed bisphosphonate. Also, since our main focus was inhibition of osteoclastic bone resorption, and not differences in action of bisphosphonates, it is possible to assume that treatment with zoledronic acid would have similar results to ones we achieved with Alendronate.

4.6 Antibiotic prophylaxis

For prophylactic treatment, mice (n=20) received either: (i) a control PMMA bead lacking antibiotic, (ii) a PMMA bead impregnated with 1.0 mg colistin sulphate, or (iii) intramuscular (i.m.) injection of 0.2 mg (~10mg/kg) of colistinmethate every day for 7 days as previously described in a mouse pneumonia model (reference). The 5 mm PMMA beads were implanted adjacent to the pin at the time of surgery and were secured with a suture through the skin and muscle. The parenteral colistinmethate was given at the time of the surgery and for the next 7 days with no beads. All mice were sacrificed for analysis on day 19.

Considerations:

Our first concern was to make sure that the equivalent dosage of antibiotics were delivered using both local and parenteral treatments. To address this problem we performed *in vitro* analysis of colistin release kinetics. One of the weaknesses of this approach is that we measured colistin release from PMMA beads in distilled MilliQ water, leaving a possibility that the kinetics might be altered when the bead is inserted in more solid soft tissue. Another point of potential critique is the use of PMMA beads. This approach might be questionable, since it requires a second surgery to remove the beads. Absorbable materials could have been considered instead or along with PMMA beads,

since these are readily available, and commonly used. Despite these drawbacks, we used PMMA beads because they were the most cost effective approach to assess colistin in this initial study, but the use of absorbable material should definitely be considered in future projects.

5 Results

Overview:

5.1 Study I

Aim: Creating a novel quantitative murine model of implant associated osteomyelitis.

Hypothesis: It is possible to utilize BLI imaging and RTQ-PCR to assess the bacterial load and activity during the establishment of chronic osteomyelitis.

Hypothesis confirmed: yes

Comments: We found that it is possible to measure bacterial load using RTQ-PCR in an infected bone. This method is complimented by BLI imaging that can measure bacterial metabolic activity, and thus differentiate between active and dormant bacteria. We also evaluated the immune response during the establishment of the infection and identified the dominant antigens responsible for the humoral immune response.

For detailed results please view the enclosed paper I.

5.2 Study 2

Aim: Elucidating the effect that anti-catabolic therapy has on establishment of osteomyelitis.

Hypothesis: Anti-resorptive agents alter bacterial growth during the establishment of osteomyelitis by altering lymphatic drainage without affecting angiogenesis or protective immunity.

Hypothesis confirmed: partially

Comments: Collectively, our findings indicate that while anti-resorptive agents do not exacerbate chronic osteomyelitis, because they do not interfere with protective immunity, they can increase bacterial growth during early infection by decreasing lymphatic drainage and preventing the removed of necrotic bone that harbors the bacteria.

For detailed results please view the enclosed paper II.

5.3 Study 3

Aim: To investigate whether or not the MDR *Acinetobacter* can be effectively prevented with parenteral or local antibiotic therapy at the time of initial surgery.

Hypothesis: Local antibiotic therapy at the time of the surgery can prevent establishment of MDR *Acinetobacter* osteomyelitis.

Hypothesis confirmed: yes

Comments: As predicted, the local treatment, which presumably leads to higher drug concentration levels at the site of infection, was significantly better in preventing MDR *Acinetobacter* osteomyelitis, then parenteral antibiotic treatment. We also found that the lesions created by *A. baumannii* induce blastic lesions, in contrast to the osteolytic lesions, which are mainly associated with *S. aureus* infection.

For detailed results please view the enclosed paper III.

6 Discussion

6.1 Model

Although infection rates following orthopedic surgery are considered to be low (1-2%), implant-associated osteomyelitis remains a catastrophic outcome that often require revision surgery and can ultimately lead to sepsis and death. This problem is further complicated by the emergence of multi-drug resistant strains and the absence of effective treatments for patients with methicillin-resistant *S. aureus*. We believe that progress in this area has been limited due to the absence of a quantitative animal model that can be utilized to elucidate molecular targets, evaluate novel drug interventions as well as perform potential vaccination studies. From our assessment of the literature, we surmise that a quantitative osteomyelitis model has not been developed for two reasons.

First, most research performed on this subject has been concerned with intramedullary implant models, since this represents a more serious clinical condition, with potential haematogenic spreading. Unfortunately, our preliminary studies showed that this approach gave rise to highly variable (temporal and spatial) lesions, making a quantitative model incredibly difficult if not impossible. In contrast, we have found that usage of an infected transcortical implant produced highly reproducible lesions adjacent to the pin, and never results in distal osteomyelitis, hematogenous infection or death. Whilst it could be argued that the mechanisms of infection and treatment modalities differ between intramedullary and external fixation implants, we found the transcortical pin model to be the best approach to study osteomyelitis *in vivo*. This gave us a base for developing the first quantitative model of implant-associated osteomyelitis.

The second major obstacle in developing a quantitative osteomyelitis model is extraction of individual live bacteria from the infected bone. As mentioned earlier, the Gold Standard for quantification of the bacterial load in infected tissue is bacterial culture analysis on agar plates following serial dilutions. Unfortunately it is virtually impossible to perform extraction of separate live bacteria due to calcified bone matrix and biofilm formation. Here we demonstrate two distinct methods to overcome this obstacle. The first, *nuc* RTQ-PCR, is a highly specific and sensitive method that has been successfully

used to quantify *S. aureus* levels in contaminated cheese, that allows to assess the bacterial load by quantifying the amount of bacterial DNA in infected bone. It should be noted that although we controlled for DNA integrity via β -actin RTQ-PCR, we had no way of knowing the total *nuc* yield following our rigorous extraction procedures, and therefore knowing the initial bacterial load in the bone. Thus, it is likely that the *nuc* genes per tibia that we found represent a fraction of the total number of bacteria originally present in the sample. Nevertheless, our RTQ-PCR results provide the first demonstration that: i) *in vivo* bacterial load levels can be quantified during the establishment of osteomyelitis, and ii) that the peak bacterial load is coincident with the generation of humoral immunity against the bacteria. We also found, that while the acquired humoral immune response is able to clear most bacteria (drastic decrease in *nuc* levels, when antibody formation initiates) and protect the animals from haematogenic spreading and death, it is not able to completely eradicate the infection, most likely due to the biofilm that provides bacteria with an immune-privileged environment.

As mentioned previously, real time PCR analysis cannot stand alone, because it is not able to differentiate between metabolically active bacteria, and dormant bacteria residing in biofilm. And as research on the regulators of *in vivo* biofilm formation has become a central focus in this field, developing a surrogate outcome measure of pre and post-biofilm growth is of great value. To address this issue we utilized a bioluminescent strain of *S. aureus* to study the infection longitudinally. This also bypasses the necessity of sacrificial endpoint that RTQ-PCR analysis had. We found that the bioluminescent strain of *S. aureus* (Xen29) behaves essentially the same at UAMS-1, which is the most widely used strain of *S. aureus* used in osteomyelitis research, and adopted this approach to be compatible with μ CT quantification of osteolysis and RTQ-PCR in our model of implant associated osteomyelitis. There will always be criticism when adapting results from an animal model to humans, but it is a necessary step to better understand the pathology of osteomyelitis infection and builds a base for further investigations.

We believe that the development of a quantitative model of implant-associated osteomyelitis opens the field to research that was previously unapproachable. It can be utilized to study potential drug interventions, the identification of biofilm genes through

the characterization of mutant phenotypes, identification of diagnostic and/or protective antigens and evaluating infection resistant implant coatings and treatments.

6.2 Anti-catabolic treatment

Chronic osteomyelitis infection is rather challenging to treat, and often requires complicated debridement surgery, that is further complicated by deteriorated bone stock due to osteolysis. This leaves us with an important question of whether or not, patients with implant-associated osteomyelitis would benefit from anti-catabolic treatment such as bisphosphonates to preserve bone stock and prevent implant loosening. Others have already considered this option, and there have been successful case reports of such treatments in the literature.

However, our studies indicate that this practice may be contraindicated since anti-catabolic therapy such as Alendronate and Osteoprotegrin i) increase the amount of necrotic cortical bone around the implant that serves as a nidus for infection, ii) significantly increases the incidence of high-grade infections in mice during the establishment of osteomyelitis, and iii) reduce the cortical hole through which the opsonized bacteria and lymph must drain out of the wound.

We further looked into the specific mechanism of action by which these drugs exacerbate establishment of the infection, and our findings contradict previous claims regarding the anti-angiogenic and immunosuppressive effects of anti-resorptive therapies. It has been proposed that bisphosphonates inhibit capillary tube formation, vessel sprouting and circulating endothelial cells. In contrast, our vascular micro-CT analyses failed to demonstrate any drug effects on perfusable vessels. Similarly, the findings that RANK signaling is required for lymph node development and immunoregulatory co-stimulation have led to a suspicion that RANKL-inhibition is immunosuppressive. However, our studies corroborate the prior findings of Stolina et al, who demonstrated that OPG treatment does not affect cell-mediated immune responses and granuloma formation. Therefore, we conclude that RANKL inhibition has insignificant immunoregulatory effects in establishment of osteomyelitis infection, and its ability to

increases the incidence of high-grade infection is solely due to its effects on osteoclastic bone resorption.

Our studies showed a significant decrease in popliteal lymph-node volume in treated animals, suggesting that mechanic blockage that inhibits lymph drainage and clearance of bacteria from the infection site, might be responsible for higher incidence of high-grade infections in animals subjected to anti-catabolic therapy. This is however somewhat speculative, and warrants further investigation, such as flowcytometry and immunohistological evaluation of the lymph nodes, to further elucidate the mechanism of action. Further on, quantitative analysis of the antibody production can be extremely difficult due to interspecimen variability. To achieve this, a much larger number of animals would be needed, and possibly a quantitative analysis of the western blot data can be performed.

6.3 Prophylactic antibiotic treatment

Infections caused by MDR pathogens have long been recognized to be a very serious problem in medicine, requiring vigilance when prescribing antibiotic therapy. This has been especially highlighted in recent years, since methicillin-resistant *Staphylococcus aureus* has surpassed HIV as the most deadly pathogen in the United States. Therefore, the emergence of *MDR Acinetobacter osteomyelitis* in orthopedic trauma patients is a situation that requires urgent attention. However, more recent clinical experiences in dealing with this problem suggest that *MDR Acinetobacter osteomyelitis* can be managed effectively, but may be the predecessor to more serious super-infections including MRSA. While studying combat related injuries during military conflict in the Middle East, we found that Gram-negative pathogens predominate early, and are replaced with *S. aureus* after treatment, despite use of anti-Gram-positive therapy. These findings underscore the importance of effective early treatment of *A. baumannii* infection to prevent complications.

To address these issues, we investigated the nature of *MDR A.baumannii* osteomyelitis infection versus that of *S. aureus*, and evaluated the efficacy of local high

dose colistin to prevent infection from a contaminated tibial implant in our murine model of osteomyelitis. Although, we found *MDR Acinetobacter* to be highly infectious as expected, we were surprised by several features of *A. baumannii* osteomyelitis that are remarkably distinct from *S. aureus* infection. Amongst these, were the osteoblastic lesions produced by *A. baumannii* in contrast to osteolytic lesions mostly associated with *S. aureus*. The other major difference that we found was the absence of biofilm and any histological evidence of colonized necrotic bone in mice infected with *A. baumannii*, which is always present in chronic *S. aureus* infection.

As mentioned earlier, there has been speculation that *S. aureus* infections are opportunistic, and in some cases may depend on an initial colonization by Gram-negative bacteria such as *Acinetobacter*. This further stresses the importance of early eradication of peri-implant infection following orthopedic surgery. Given that most *MDR Acinetobacter* strains are sensitive to colistin, and that PMMA beads can be readily impregnated with colistin and steadily release the drug over time, we evaluated this model of local prophylaxis versus standard parenteral colistinmethane. As predicted, the local treatment, which presumably leads to higher drug concentration levels at the site of infection, was significantly better in preventing *MDR Acinetobacter* osteomyelitis. Even though our model does not simulate soft tissue injury, often seen in these combat related injuries, we believe that our results support future evaluation of colistin impregnated PMMA beads, or absorbable materials that do not require removal, in a clinical trial to evaluate their efficacy in clearing *MDR Acinetobacter* osteomyelitis and reoccurring infections.

7 Concluding remarks and future perspectives

Our research provides future investigators with a novel model of implant associated osteomyelitis, which allows quantification of the bacterial load and *in vivo* evaluation of bacterial activity during establishment of chronic osteomyelitis. This opens the field for future investigations of potential bacterial mutants, drug interactions and evaluation of novel anti-microbial therapies. We have also characterized the immunodominant antigens, which can be utilized for developing novel rapid diagnostic methods, and possible vaccination studies.

Our finding, that anti-catabolic therapy increases incidence of high-grade infection during the establishment of chronic osteomyelitis, provides new insight in the mechanisms responsible for ONJ. Although our proposal that bisphosphonates and OPG inhibit lymph drainage from the infection site is somewhat speculative, we still believe that it provides new valuable knowledge about underlying mechanisms of ONJ and is extremely relevant for millions of people taking these drugs worldwide. However more studies are needed to further investigate the effect that anti-catabolic treatment has on the immune system.

Finally we have shown that local antibiotic prophylaxis with colistin loaded PMMA beads inserted at the time of the surgery, decreases incidence of posttraumatic implant associated osteomyelitis. This finding opens up for experimental studies in larger animals using absorbable materials, and potential clinical trials.

References

1. Darouiche, R.O., *Treatment of infections associated with surgical implants*. N Engl J Med, 2004. **350**(14): p. 1422-9.
2. Jørgensen, P.H., K. Gromov, and K. Søballe, [*Prevention of prosthesis infections*]. Ugeskr Laeg, 2007. **169**(48): p. 4159-63.
3. Charnley, J., *Postoperative infection after total hip replacement with special reference to air contamination in the operating room*. Clin Orthop Relat Res, 1972. **87**: p. 167-87.
4. Lew, D.P. and F.A. Waldvogel, *Osteomyelitis*. Lancet, 2004. **364**(9431): p. 369-79.
5. Fitzgerald, R.H., *Infected Total Hip Arthroplasty: Diagnosis and Treatment*. The Journal of the American Academy of Orthopaedic Surgeons, 1995. **3**(5): p. 249-262.
6. David, T.S. and M.S. Vrahas, *Perioperative lower urinary tract infections and deep sepsis in patients undergoing total joint arthroplasty*. The Journal of the American Academy of Orthopaedic Surgeons, 2000. **8**(1): p. 66-74.
7. Rupp, M.E. and G.L. Archer, *Coagulase-negative staphylococci: pathogens associated with medical progress*. Clin Infect Dis, 1994. **19**(2): p. 231-43; quiz 244-5.
8. Toms, A.D., et al., *The management of peri-prosthetic infection in total joint arthroplasty*. The Journal of bone and joint surgery British volume, 2006. **88**(2): p. 149-55.
9. Clarke, S.R. and S.J. Foster, *Surface adhesins of Staphylococcus aureus*. Adv Microb Physiol, 2006. **51**: p. 187-224.
10. Elasri, M.O., et al., *Staphylococcus aureus collagen adhesin contributes to the pathogenesis of osteomyelitis*. Bone, 2002. **30**(1): p. 275-80.
11. Foster, T.J., *Immune evasion by staphylococci*. Nat Rev Microbiol, 2005. **3**(12): p. 948-58.
12. Stewart, P.S., *Mechanisms of antibiotic resistance in bacterial biofilms*. Int J Med Microbiol, 2002. **292**(2): p. 107-13.
13. Gristina, A.G. and J.W. Costerton, *Bacterial adherence to biomaterials and tissue. The significance of its role in clinical sepsis*. The Journal of bone and joint surgery American volume, 1985. **67**(2): p. 264-73.
14. Arron, J.R. and Y. Choi, *Bone versus immune system*. Nature, 2000. **408**(6812): p. 535-6.
15. Nair, S.P., et al., *Bacterially induced bone destruction: mechanisms and misconceptions*. Infect Immun, 1996. **64**(7): p. 2371-80.
16. Puzas, J.E., et al., *Regulation of osteoclastic activity in infection*. Meth Enzymol, 1994. **236**: p. 47-58.
17. Leitner, G., et al., *Staphylococcus aureus strains isolated from bovine mastitis: virulence, antibody production and protection from challenge in a mouse model*. FEMS Immunol Med Microbiol, 2003. **35**(2): p. 99-106.
18. Howard, C.B., et al., *Fine-needle bone biopsy to diagnose osteomyelitis*. The Journal of bone and joint surgery British volume, 1994. **76**(2): p. 311-4.

19. Jacobson, I.V. and W.L. Sieling, *Microbiology of secondary osteomyelitis. Value of bone biopsy*. S Afr Med J, 1987. **72**(7): p. 476-7.
20. Kamme, C. and L. Lindberg, *Aerobic and anaerobic bacteria in deep infections after total hip arthroplasty: differential diagnosis between infectious and non-infectious loosening*. Clin Orthop Relat Res, 1981(154): p. 201-7.
21. Gold, R.H., R.A. Hawkins, and R.D. Katz, *Bacterial osteomyelitis: findings on plain radiography, CT, MR, and scintigraphy*. AJR American journal of roentgenology, 1991. **157**(2): p. 365-70.
22. Kaim, A.H., T. Gross, and G.K. von Schulthess, *Imaging of chronic posttraumatic osteomyelitis*. European radiology, 2002. **12**(5): p. 1193-202.
23. Gahrn-Hansen, B., et al., [*Staphylococcus aureus infections--the clinical picture and treatment*]. Ugeskr Laeg, 2002. **164**(32): p. 3759-63.
24. Classen, D.C., et al., *The timing of prophylactic administration of antibiotics and the risk of surgical-wound infection*. N Engl J Med, 1992. **326**(5): p. 281-6.
25. Eckardt, J.J., P.Z. Wirganowicz, and T. Mar, *An aggressive surgical approach to the management of chronic osteomyelitis*. Clin Orthop Relat Res, 1994(298): p. 229-39.
26. Tsukayama, D.T., R. Estrada, and R.B. Gustilo, *Infection after total hip arthroplasty. A study of the treatment of one hundred and six infections*. The Journal of bone and joint surgery American volume, 1996. **78**(4): p. 512-23.
27. Griffiths, H.J., et al., *Total hip replacement and other orthopedic hip procedures*. Radiol Clin North Am, 1995. **33**(2): p. 267-87.
28. Block, J.E. and H.A. Stubbs, *Reducing the risk of deep wound infection in primary joint arthroplasty with antibiotic bone cement*. Orthopedics, 2005. **28**(11): p. 1334-45.
29. Engesaeter, L.B., et al., *Antibiotic prophylaxis in total hip arthroplasty: effects of antibiotic prophylaxis systemically and in bone cement on the revision rate of 22,170 primary hip replacements followed 0-14 years in the Norwegian Arthroplasty Register*. Acta orthopaedica Scandinavica, 2003. **74**(6): p. 644-51.
30. Klevens, R.M., et al., *Invasive methicillin-resistant Staphylococcus aureus infections in the United States*. JAMA, 2007. **298**(15): p. 1763-71.
31. Muto, C.A., et al., *SHEA guideline for preventing nosocomial transmission of multidrug-resistant strains of Staphylococcus aureus and enterococcus*. Infection control and hospital epidemiology : the official journal of the Society of Hospital Epidemiologists of America, 2003. **24**(5): p. 362-86.
32. Cosgrove, S.E., et al., *Comparison of mortality associated with methicillin-resistant and methicillin-susceptible Staphylococcus aureus bacteremia: a meta-analysis*. Clin Infect Dis, 2003. **36**(1): p. 53-9.
33. Covey, D.C., *Iraq war injuries*. Orthopedics, 2006. **29**(10): p. 884-6.
34. Covey, D.C., *Combat orthopaedics: a view from the trenches*. The Journal of the American Academy of Orthopaedic Surgeons, 2006. **14**(10 Spec No.): p. S10-7.
35. Owens, B.D., et al., *Characterization of extremity wounds in Operation Iraqi Freedom and Operation Enduring Freedom*. Journal of orthopaedic trauma, 2007. **21**(4): p. 254-7.

36. Murray, C.K. and D.R. Hospenthal, *Treatment of multidrug resistant Acinetobacter*. *Curr Opin Infect Dis*, 2005. **18**(6): p. 502-6.
37. Yun, H.C., J.G. Branstetter, and C.K. Murray, *Osteomyelitis in military personnel wounded in Iraq and Afghanistan*. *The Journal of trauma*, 2008. **64**(2 Suppl): p. S163-8; discussion S168.
38. Murray, C.K., et al., *Prevention and management of infections associated with combat-related extremity injuries*. *The Journal of trauma*, 2008. **64**(3 Suppl): p. S239-51.
39. Abbo, A., et al., *Multidrug-resistant Acinetobacter baumannii*. *Emerging Infect Dis*, 2005. **11**(1): p. 22-9.
40. Davis, K.A., et al., *Multidrug-resistant Acinetobacter extremity infections in soldiers*. *Emerging Infect Dis*, 2005. **11**(8): p. 1218-24.
41. Scott, P., et al., *An outbreak of multidrug-resistant Acinetobacter baumannii-calcoaceticus complex infection in the US military health care system associated with military operations in Iraq*. *Clin Infect Dis*, 2007. **44**(12): p. 1577-84.
42. Fleisch, H., et al., *The influence of pyrophosphate analogues (diphosphonates) on the precipitation and dissolution*. *Calcified tissue research*, 1968: p. Suppl:10-10a.
43. Roelofs, A.J., et al., *Molecular mechanisms of action of bisphosphonates: current status*. *Clin Cancer Res*, 2006. **12**(20 Pt 2): p. 6222s-6230s.
44. Drake, M.T., B.L. Clarke, and S. Khosla, *Bisphosphonates: mechanism of action and role in clinical practice*. *Mayo Clin Proc*, 2008. **83**(9): p. 1032-45.
45. Ross, J.R., et al., *A systematic review of the role of bisphosphonates in metastatic disease*. *Health technology assessment (Winchester, England)*, 2004. **8**(4): p. 1-176.
46. Jakobsen, T., et al., *Local bisphosphonate treatment increases fixation of hydroxyapatite-coated implants inserted with bone compaction*. *J Orthop Res*, 2009. **27**(2): p. 189-94.
47. Jakobsen, T., et al., *Local alendronate increases fixation of implants inserted with bone compaction: 12-week canine study*. *J Orthop Res*, 2007. **25**(4): p. 432-41.
48. Jensen, T.B., et al., *Systemic alendronate treatment improves fixation of press-fit implants: a canine study using nonloaded implants*. *J Orthop Res*, 2007. **25**(6): p. 772-8.
49. Soubrier, M., et al., *Pamidronate in the treatment of diffuse sclerosing osteomyelitis of the mandible*. *Oral surgery, oral medicine, oral pathology, oral radiology, and endodontics*, 2001. **92**(6): p. 637-40.
50. Wright, S.A., et al., *Chronic diffuse sclerosing osteomyelitis treated with risedronate*. *J Rheumatol*, 2005. **32**(7): p. 1376-8.
51. Khosla, S., et al., *Bisphosphonate-associated osteonecrosis of the jaw: report of a task force of the American Society for Bone and Mineral Research*. *J Bone Miner Res*, 2007. **22**(10): p. 1479-91.
52. Estefanía Fresco, R., R. Ponte Fernández, and J.M. Aguirre Urizar, *Bisphosphonates and oral pathology II. Osteonecrosis of the jaws: review of the*

- literature before 2005. Medicina oral, patología oral y cirugía bucal, 2006. 11(6): p. E456-61.*
53. Hellstein, J.W. and C.L. Marek, *Bisphosphonate osteochemonecrosis (bis-phossy jaw): is this phossy jaw of the 21st century?* J Oral Maxillofac Surg, 2005. **63(5)**: p. 682-9.
 54. Shane, E., et al., *Osteonecrosis of the jaw: more research needed.* J Bone Miner Res, 2006. **21(10)**: p. 1503-5.
 55. Woo, S.B., J.W. Hellstein, and J.R. Kalmar, *Narrative [corrected] review: bisphosphonates and osteonecrosis of the jaws.* Ann Intern Med, 2006. **144(10)**: p. 753-61.
 56. Gutta, R. and P.J. Louis, *Bisphosphonates and osteonecrosis of the jaws: science and rationale.* Oral surgery, oral medicine, oral pathology, oral radiology, and endodontics, 2007. **104(2)**: p. 186-93.
 57. Zervas, K., et al., *Incidence, risk factors and management of osteonecrosis of the jaw in patients with multiple myeloma: a single-centre experience in 303 patients.* Br J Haematol, 2006. **134(6)**: p. 620-3.
 58. Hewitt, C. and C.S. Farah, *Bisphosphonate-related osteonecrosis of the jaws: a comprehensive review.* J Oral Pathol Med, 2007. **36(6)**: p. 319-28.
 59. Allegra, A., et al., *Patients with bisphosphonates-associated osteonecrosis of the jaw have reduced circulating endothelial cells.* Hematological oncology, 2007. **25(4)**: p. 164-9.
 60. Marx, R.E., et al., *Bisphosphonate-induced exposed bone (osteonecrosis/osteopetrosis) of the jaws: risk factors, recognition, prevention, and treatment.* J Oral Maxillofac Surg, 2005. **63(11)**: p. 1567-75.
 61. Marx, R.E., *Pamidronate (Aredia) and zoledronate (Zometa) induced avascular necrosis of the jaws: a growing epidemic.* J Oral Maxillofac Surg, 2003. **61(9)**: p. 1115-7.
 62. Bagan, J.V., et al., *Avascular jaw osteonecrosis in association with cancer chemotherapy: series of 10 cases.* J Oral Pathol Med, 2005. **34(2)**: p. 120-3.
 63. Hansen, T., et al., *Osteonecrosis of the jaws in patients treated with bisphosphonates - histomorphologic analysis in comparison with infected osteoradionecrosis.* J Oral Pathol Med, 2006. **35(3)**: p. 155-60.
 64. Norden, C.W., *Lessons learned from animal models of osteomyelitis.* Rev Infect Dis, 1988. **10(1)**: p. 103-10.
 65. An, Y.H., Q.K. Kang, and C.R. Arciola, *Animal models of osteomyelitis.* The International journal of artificial organs, 2006. **29(4)**: p. 407-20.
 66. Zimmerli, W., P.D. Lew, and F.A. Waldvogel, *Pathogenesis of foreign body infection. Evidence for a local granulocyte defect.* Journal of Clinical Investigation, 1984. **73(4)**: p. 1191-200.
 67. Zimmerli, W., et al., *Pathogenesis of foreign body infection: description and characteristics of an animal model.* J Infect Dis, 1982. **146(4)**: p. 487-97.
 68. Daum, R.S., et al., *A model of Staphylococcus aureus bacteremia, septic arthritis, and osteomyelitis in chickens.* J Orthop Res, 1990. **8(6)**: p. 804-13.
 69. Passl, R., et al., *A model of experimental post-traumatic osteomyelitis in guinea pigs.* The Journal of trauma, 1984. **24(4)**: p. 323-6.

70. Worlock, P., et al., *An experimental model of post-traumatic osteomyelitis in rabbits*. British journal of experimental pathology, 1988. **69**(2): p. 235-44.
71. Varshney, A.C., et al., *Experimental model of staphylococcal osteomyelitis in dogs*. Indian J Exp Biol, 1989. **27**(9): p. 816-9.
72. Kaarsemaker, S., G.H. Walenkamp, and A.E. vd Bogaard, *New model for chronic osteomyelitis with Staphylococcus aureus in sheep*. Clin Orthop Relat Res, 1997(339): p. 246-52.
73. Salgado, C.J., et al., *A model for chronic osteomyelitis using Staphylococcus aureus in goats*. Clin Orthop Relat Res, 2005(436): p. 246-50.
74. Lucke, M., et al., *A new model of implant-related osteomyelitis in rats*. J Biomed Mater Res Part B Appl Biomater, 2003. **67**(1): p. 593-602.
75. Yoshii, T., et al., *Inhibitory effect of roxithromycin on the local levels of bone-resorbing cytokines in an experimental model of murine osteomyelitis*. J Antimicrob Chemother, 2002. **50**(2): p. 289-92.
76. Jarlov, J.O. and J.K. Moller, [*Methicillin resistant Staphylococcus aureus--a problem i Denmark?*]. Ugeskr Laeger, 2006. **168**(7): p. 665.
77. Westh, H., et al., [*Epidemic increase in methicillin-resistant Staphylococcus aureus in Copenhagen*]. Ugeskr Laeger, 2006. **168**(7): p. 671-3.
78. Sneppen, O. et al. *Orthopædisk kirurgi*. 6. udgave. 2006

Appendix I

Quantitative Mouse Model of Implant-Associated Osteomyelitis and the Kinetics of Microbial Growth, Osteolysis, and Humoral Immunity

Dan Li,¹ Kirill Gromov,^{1,2} Kjeld Søballe,² J. Edward Puzas,¹ Regis J. O'Keefe,¹ Hani Awad,¹ Hicham Drissi,¹ Edward M. Schwarz¹

¹The Center for Musculoskeletal Research, University of Rochester Medical Center, 601 Elmwood Avenue, Box 665, Rochester, New York 14642

²The Department of Orthopedics, Aarhus University Hospital, Aarhus, Denmark

Received 19 January 2007; accepted 24 April 2007

Published online 3 August 2007 in Wiley InterScience (www.interscience.wiley.com). DOI 10.1002/jor.20452

ABSTRACT: Although osteomyelitis (OM) remains a serious problem in orthopedics, progress has been limited by the absence of an in vivo model that can quantify the bacterial load, metabolic activity of the bacteria over time, immunity, and osteolysis. To overcome these obstacles, we developed a murine model of implant-associated OM in which a stainless steel pin is coated with *Staphylococcus aureus* and implanted transcortically through the tibial metaphysis. X-ray and micro-CT demonstrated concomitant osteolysis and reactive bone formation, which was evident by day 7. Histology confirmed all the hallmarks of implant-associated OM, namely: osteolysis, sequestrum formation, and involucrum of Gram-positive bacteria inside a biofilm within necrotic bone. Serology revealed that mice mount a protective humoral response that commences with an IgM response after 1 week, and converts to a specific IgG2b response against specific *S. aureus* proteins by day 11 postinfection. Real-time quantitative PCR (RTQ-PCR) for the *S. aureus* specific *nuc* gene determined that the peak bacterial load occurs 11 days postinfection. This coincidence of decreasing bacterial load with the generation of specific antibodies is suggestive of protective humoral immunity. Longitudinal in vivo bioluminescent imaging (BLI) of *luxA-E* transformed *S. aureus* (Xen29) combined with *nuc* RTQ-PCR demonstrated the exponential growth phase of the bacteria immediately following infection that peaks on day 4, and is followed by the biofilm growth phase at a significantly lower metabolic rate ($p < 0.05$). Collectively, these studies demonstrate the first quantitative model of implant-associated OM that defines the kinetics of microbial growth, osteolysis, and humoral immunity following infection. © 2007 Orthopaedic Research Society. Published by Wiley Periodicals, Inc. J Orthop Res 26:96–105, 2008

Keywords: osteomyelitis; *Staphylococcus aureus*; osteolysis; humoral immunity; bioluminescent imaging

INTRODUCTION

Osteomyelitis (OM) is a common infectious disease characterized by progressive inflammation and bone destruction.^{1–3} This condition may be caused by a variety of microorganism, however, *Staphylococcus aureus* is responsible for >80% of these infections.¹ Although the total number of osteomyelitis cases is high in that approximately 112,000 orthopedic device-related infections occur per year in the US at an approximate hospital

cost of \$15,000–70,000 per incident, the infection rates for joint prosthesis and fracture-fixation devices have been only 0.3%–11% and 5%–15% of cases, respectively, over the last decade,^{2,3} which resulted in a low interest in rigorous prospective clinical studies. Another challenging issue hampering the progress in the OM research field is the absence of a quantitative animal model. It is well known that in vitro cultures rapidly select for growth of organisms that do not elaborate an extracellular capsule. As such, biofilm biology, which plays a critical role in resistance of chronic OM to antibiotic therapy by serving as a dominant protective barrier from the action of antibiotics, can only be studied with in vivo models.⁴ To date, much of our knowledge of the pathogenesis of OM comes from animal models,⁵ which have existed in chicken,⁶ rat,^{7,8} guinea pig,⁹ rabbit,¹⁰ dog,¹¹ sheep,¹² goat,¹³ and most recently

The first two authors contributed equally to this work.

This article includes Supplementary Material available via the Internet at <http://www.interscience.wiley.com/jpages/0736-0266/suppmat>.

Correspondence to: Edward M. Schwarz (Telephone: 585-275-3063, Fax: 585-756-4727; E-mail: Edward_Schwarz@URMC.Rochester.edu)

© 2007 Orthopaedic Research Society. Published by Wiley Periodicals, Inc.

mouse.¹⁴ While these models have been used to confirm the importance of bacterial adhesions identified from in vitro assays,^{15–17} none of them contain quantitative endpoints that can determine bacterial load or growth in vivo. Thus, they are of limited value for assessing drug effects, bacterial mutants, and the role of host factors during the establishment of chronic OM.

In this study, we developed a novel murine model of implant-associated osteomyelitis in which a stainless steel pin is coated with *S. aureus* and implanted transcortically through the tibial metaphysis. The resulting infection closely resembles clinical OM. This generates a reproducible abscess without hematogenous spreading or death in >90% of mice. By adapting real-time quantitative PCR (RTQ-PCR) to detect the *S. aureus* specific *nuc* gene that is used to assess contaminated food,¹⁸ and a bioluminescent strain (Xen29) that can be quantified using longitudinal in vivo bioluminescent imaging (BLI),¹⁹ we have elucidated the pattern of pathogenic growth during the establishment of implant-associated OM. We also performed serology and micro-CT analyses to assess the host response to infection. Our findings demonstrate the establishment of a quantitative small animal surrogate that can be used to evaluate the efficacy of novel interventions for OM.

MATERIALS AND METHODS

S. aureus Strains and Pathogenic Challenge

The UAMS-1 strain of *S. aureus* (ATCC 49230) was obtained from the American Type Culture Collection (Manassas, VA). The bioluminescent strain of *S. aureus*, Xen29 (derived from ATCC 12600), was obtained from Xenogen Inc. (Cranbury, NJ). Pathogenic challenge was initiated via a contaminated 0.25-mm diameter insect pin (Fine Science Tools, Foster City, CA) that was generated as follows. The pins were autoclaved and stored in 70% ethanol. After air-drying, the pins were incubated in 1.5 ml of an overnight luria broth culture of *S. aureus* for 20 min. Then, the pins were air dried for 5 min before trans-tibial implantation. The inoculating dose of bacteria was determined to be $9.5 \pm 3.7 \times 10^5$ CFU of UAMS-1 and $4.2 \pm 0.5 \times 10^5$ CFU of Xen29 per pin, by vigorously vortexing the pin in PBS to resuspend the bacteria and growing dilutions on agar plates.

Animal Surgery

All animal studies were performed under University Committee for Animal Resources approved protocols. C57BL/6 female 6–8-week-old mice were anesthetized with Ketamine (100 mg/kg) and Xylazine (10 mg/kg), their left tibiae were shaved, and the skin was cleansed with 70% ethanol. Infection was initiated by placing the pin transcortically through the tibia via medial to lateral

implantation. The pin was bent at both ends for stability and cut adjacent to the skin on both ends, which allowed it to be covered by the skin and to eliminate additional environmental exposure. Once the mice recovered from the anesthesia, they were returned to standard isolator cages without additional treatment until sacrifice, except for the gentamycin treatment group that received 0.1 mg/kg/day i.p.

In Vivo Radiology and Bioluminescent Imaging

Longitudinal osteolysis was assessed radiographically using a Faxitron Cabinet x-ray system (Faxitron, Wheeling, IL) as we have previously described.²⁰ Bioluminescent imaging (BLI) of mice infected with Xen29 was performed on days 0, 4, 7, 11, 14, and 18 post-infection using a Xenogen IVIS camera system (Xenogen Corporation, Alameda, CA). Five-minute high sensitivity ventral images were taken at each time point. The BLI was quantified with the LivingImage software package 2.50.1 (Xenogen Corporation) by analyzing a fixed 1.5-cm diameter region of interest (ROI) centered on the pin. The photon signal was calculated as p/sec/cm²/sr.

Micro-CT Analyses

After sacrifice, the pin was removed and the disarticulated tibiae were analyzed by high-resolution (10.5 μm) micro-computed tomography (μCT) (VivaCT 40; Scanco Medical AG, Basserdorf, Switzerland) to render three-dimensional images of the diaphysis as we have previously described.²¹ Images from each tibia were binarized individually at identical thresholds to allow for unbiased identification of the cortical pinholes and the extent of the osteolytic lesion in the cortices. The three-dimensional binary image was then rendered from the threshold slices, and sagittal sections through the tibia were digitally obtained so that the rendered images could be rotated to visualize the pinholes and osteolytic lesions on the lateral and medial cortical surfaces of the specimens. Since the infected pin was introduced through the medial side, and we observed more consistent and reproducible osteolysis on the medial side, we chose to only quantify the area of osteolysis on the medial side. The maximal osteolytic area was computed for each specimen using a semi-automated filter in Adobe Photoshop[®] CS (Adobe Systems, Inc., San Jose, CA) which thresholds the pinhole area, sums the number of pixels in the thresholded region, and then computes the area in mm² after calibrating against 1-mm scale bar (9,216 pixels/mm²). This area measurement was then used to quantitatively describe the maximum size of the osteolytic cortical lesions for the group as mean ± SEM (Fig. 1).

Histologic Evaluation of OM

After μCT, the tibial samples were processed for decalcified histology and stained with Orange G/alcian blue (H&E), Gram-stained, or tested for tartrate-

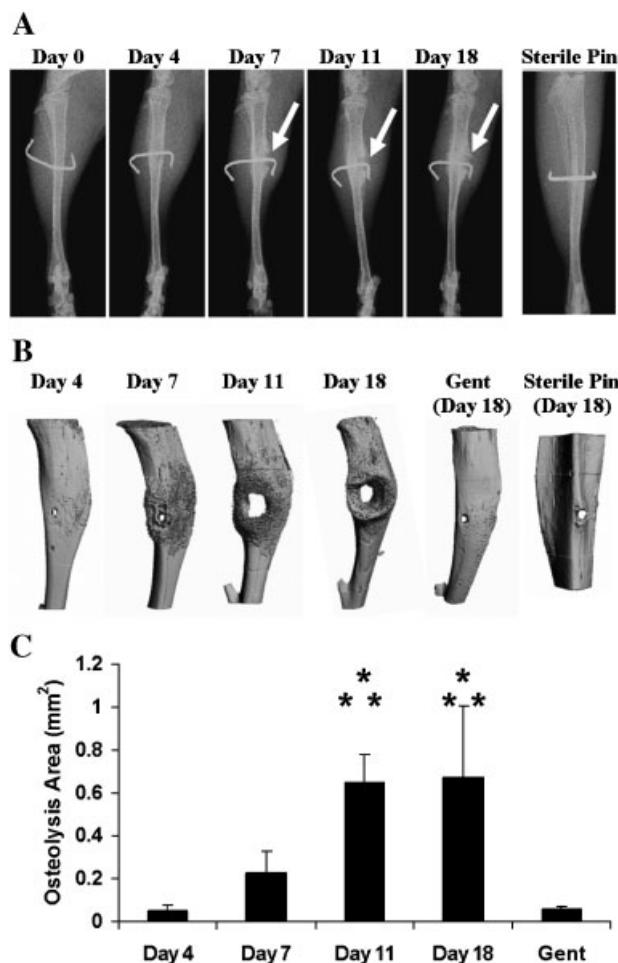


Figure 1. Radiographic progression of trans-tibial implant-associated osteomyelitis. (A) Longitudinal x-rays of a representative mouse that received a trans-tibial pin coated with Xen29 *S. aureus*. Gentamycin and sterile pin controls at Day 18 are also shown. X-rays were taken on the indicated day after surgery. Arrows indicate the osteolysis around the pin, which was evident at 7 days and thereafter. Also of note is the absence of any lesions distal to the pin. (B) Medial views of reconstructed μ CT images of representative tibiae from mice ($N=5$) that received a trans-tibial pin coated with Xen29 *S. aureus* and were sacrificed on the indicated day. Also shown are control mice that received a trans-tibial pin coated with Xen29 *S. aureus* and were treated with parenteral gentamycin (Gent), or received a sterile pin. (C) The osteolytic area around the pin was quantified as described in Materials and Methods, and the data are presented as the mean \pm SD (* $p < 0.05$ vs. Day 4; ** $p < 0.05$ vs. Gent Day 18). There was no difference in the osteolysis area between the gentamycin and sterile pin controls (data not shown).

resistant acid phosphatase (TRAP) activity as we have described previously.²²

DNA Purification and *nuc*/ β -Actin Real-Time Quantitative PCR (RTQ-PCR)

Infected tibiae were disarticulated and separated from the surrounding soft tissues. Then the tibia was cut into

small pieces with scissors, and demineralized individually with 0.5 M EDTA (pH 7.5) in 1.5 ml polypropylene tubes. The tubes were agitated on a shaker at 4°C for 24 h, centrifuged at 5,500 rpm for 20 min, and the precipitate was resuspended in fresh EDTA. This process was repeated three to five times until the bone fragments were completely decalcified. The samples were then washed three times with ddH₂O and the pellet was resuspended in 360 ml buffer ATL (Qiagen, Valencia, CA) with 40 μ l proteinase K (Qiagen), and incubated at 55°C until the bone tissues were fully digested and the solution was clear. Then 400 μ l buffer AL (Qiagen) with 5 μ l proteinase K was added, and the samples were placed on ice and sonicated five times, at level 15, for 10 s with 1-min resting intervals between the sonications (Microson Ultrasonic Cell Disruptor, Misonix Inc., Farmingdale, NY). After sonication, DNA was purified using DNeasy Tissue kit (Qiagen) according to the manufacturer's protocol. The final sample of DNA was eluted in 100 μ l of ddH₂O, and stored at -20°C.

RTQ-PCR for the *S. aureus*-specific *nuc* gene was performed to quantify the bacterial load with primers 5'-GCGATTGATGGTGATACGGTT-3' and 5'-AGCCAA-GCCTTGACGAACTAA-3' that amplify a 269-bp product, as previously described.¹⁸ The reactions were carried out in a final volume of 20 μ l consisting of 0.3 μ M primers, 1 \times Sybr Green PCR Super Mix (BioRad, Hercules, CA), and 2 μ l of the purified tibia DNA template. The samples were assayed in triplicate in a Rotor-Gene RG 3000 (Corbett Research, Sydney, Australia). In order to control for the integrity of the DNA template between samples, we performed RTQ-PCR for the mouse β -actin gene that detects a 124-bp product using primers 5'-AGA TGT GAA TCA GCA AGC AG-3' and 5'-GCG CAA GTT AGG TTT TGT CA-3'. In order to calculate the *nuc* gene copies in a tibia sample, we first generated a standard curve with *S. aureus* genomic DNA purified directly from an overnight culture. The mean of the three CT values from each tibia sample were then plotted against this curve to extrapolate the number of *nuc* genes. This number was then normalized to β -actin and the data are presented as normalized *nuc* gene copies per sample.

Serology

In order to determine total immunoglobulin isotype (Ig) levels, blood samples were collected from the animals on days 0, 4, 7, 11, and 14 using retro-orbital bleeding, and an ELISA on the sera was performed using the Mouse Typer Sub-Isotyping Kit (BioRad) as we have previously described.²³ Specific antibodies against *S. aureus* proteins were detected by Western blotting. The protein was obtained from a 100 ml culture of bacteria in log phase, in which the protein extract was prepared using the Complete Bacterial Proteome Extraction Kit (Calbiochem, San Diego, CA) according to the manufacturer's instructions. Twenty micrograms of total *S. aureus* protein per well was boiled in Laemmli loading buffer and separated in NuPAGETM10% Bis-Tris SDS

Gels (Invitrogen, Carlsbad, CA) by electrophoresis. The proteins were transferred to a PVDF membrane (Millipore, Billerica, MA) and stained with Ponceau Red (Sigma, St. Louis, MO) to control for protein loading and transfer efficiency. The membrane was then cut into single lanes and blocked with PBS, 0.1% Tween 20 (PBST) and 5% non-fat dry milk for 1 h at room temperature. Afterwards, each lane was incubated with a unique serum (10 μ l serum in 5 ml of PBST) as the primary antibody for 1 h at room temperature. The strips were then washed three times in 0.1% PBST, 15 min each at room temperature. The strips were then pooled and incubated with 1.5 μ l HRP-conjugated goat anti-mouse IgG antibody (BioRad) in 30 ml blocking buffer for 1 h at RT. The strips were then washed three times in PBST, 15 min each at room temperature. Finally, the strips were reassembled with the molecular weight marker strip and imaged with ECL+ (Amersham) chemiluminescence autoradiograph.

RESULTS

Murine Trans-Tibial Model of Implant-Associated Osteomyelitis

In our initial attempt to develop a quantitative model of implant-associated OM, we chose an intramedullary implant approach, since this represents the serious infections in patients with total joint replacements. However, repeated attempts failed to provide evidence that a reproducible abscess could be generated (data not shown). This led us to conclude that it is challenging to consistently achieve a quantitative model of intramedullary implant-associated OM, although others have recently succeeded.²⁴

Next, we investigated a trans-tibial implant approach that mimics OM of external fixation pins. In our initial experiments, an insect pin coated with Xen29 was surgically implanted into the left tibia of mice. Longitudinal x-rays demonstrated osteolysis adjacent to the pin within 7 days (Fig. 1A). Moreover, this mode of infection led to a highly reproducible localized abscess in >90% of the mice, and never resulted in detectable hematogenous spreading, sepsis, or death. In order to quantify the osteolysis, we performed a time-course study in which the infected tibiae were analyzed by μ CT (Fig. 1B and C). These results are consistent with sequestrum formation in which osteoclastic bone resorption of cortical bone around the infected implant occurs with concomitant reactive periosteal bone formation.

The presence of OM in the mice was confirmed by histological analyses on tibiae that received infected or sterile pins. Figure 2 demonstrates

that the tibial transcortical pin model contains all of the salient features of chronic OM including: sequestrum and involucrum formation, osteoclastic resorption of the cortical bone, and Gram stained extracellular bacteria and biofilm that reside in the necrotic bone surrounding the implant. None of the negative controls, including heat killed *S. aureus* and non-pathogenic *E. coli* (data not shown), demonstrated these features.

Kinetics of Infection and the Host Immunity during the Establishment of OM

Since it is impossible to effectively extract live bacteria from infected bone to quantify the in vivo bacterial load due to the calcified matrix and biofilm, we adapted an RTQ-PCR method to determine the number of *nuc* gene per tibia as a surrogate outcome measure. Using PCR primers specific for murine β -actin and *S. aureus nuc*, we first validated the sensitivity and specificity of the assay (detection of <10 copies per sample with a single peak; Supplemental Fig. A). Then, we used this assay to complete a time-course study on infected tibiae samples to assess the in vivo bacterial load during the establishment of OM. Figure 3A and B shows that the bacterial load peaked on day 11 postsurgery and dropped sharply thereafter. The sharp drop suggests that the host has generated an effective immune response that clears the bacteria.

Since effective clearance of *S. aureus* is partially dependent on humoral immunity, we evaluated antisera from infected mice over the course of infections. In order to determine when mice produce specific high affinity antibodies against *S. aureus* proteins after infections, we performed Western blots on whole-cell bacterial extracts using sera from the challenged animals as the primary antibody. The results demonstrated the generation of specific anti-*S. aureus* IgG antibodies by day 11, which increase thereafter (Fig. 3C). An assessment of total Ig levels in the sera of these challenged mice demonstrated an initial increase in IgM levels after 1 week, which was converted to IgG2b at 2 weeks (Fig. 3D). Taken together, these results indicate that establishment of implant-associated OM is consistent with classical microbial pathogenesis and immunity in which the bacteria enjoy an initial growth period in the naive host that is terminated by an acquired humoral response. The finding that mice are unable to completely eradicate *S. aureus* infection after generating a functional humoral response is consistent with the fact that antibodies cannot penetrate biofilm.

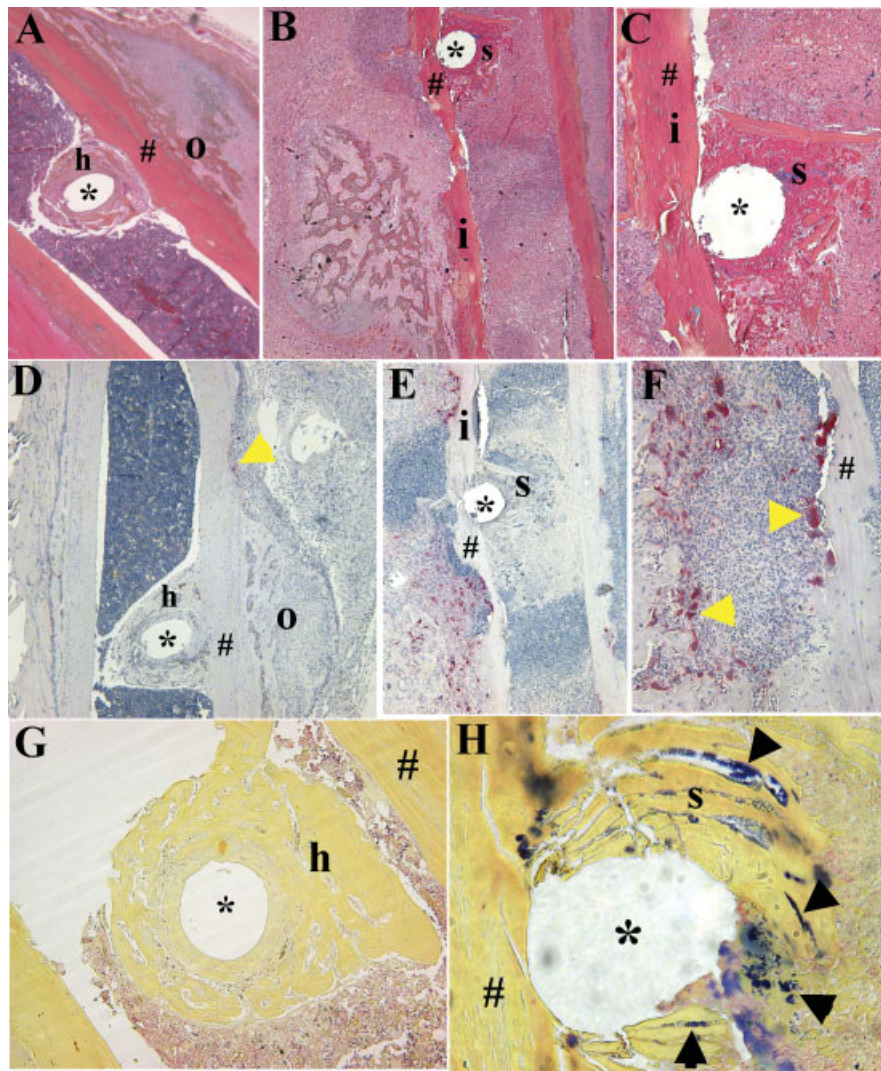


Figure 2. Histological evaluation of the trans-tibial implant-associated model of osteomyelitis. H&E (A–C), TRAP (D–F) and Gram stained (G, H) sections of histology sections at the pin site (*) adjacent to the tibial cortex (#), 9 days after implantation of a sterile pin (A, D, G), or a pin coated with UAMS-1 *S. aureus* (B, C, E, F, H). Of note is the new bone (h) that forms around the sterile pin (A, D, G) vs. the necrotic sequestrum (s) and involucrum (i) adjacent to the infected pin. While very few TRAP+ osteoclasts (yellow arrowheads) were present in the uninfected samples (D), numerous osteoclasts appear to be actively resorbing the cortex adjacent to the infected pin, and remodeling the new woven bone that is encasing the involucrum (E, F). Gram staining confirmed the absence of bacteria in the specimens with the sterile pin (G) and their presence (black arrowheads) within the necrotic bone around the infected pins (H).

Bioluminescent Imaging (BLI) Quantification of Bacterial Metabolism during the Establishment of OM

While the results of our RTQ-PCR studies demonstrate its ability to quantify bacterial load in vivo, the assay has two fundamental shortcomings that limit its utility. The first is the sacrificial endpoint, which prohibits longitudinal studies. The second is that RTQ-PCR cannot distinguish between metabolically active bacteria and dormant microbes within biofilm. Since this resolution is critical for

the investigation of pathogenic mechanisms and evaluation of novel interventions, we examined the utility of BLI in our trans-tibial implant model. In our time-course studies with Xen29, only background signal was detected in mice that receive a sterile pin (Fig. 4) or infected mice treated with parenteral gentamycin (data not shown). In contrast, the BLI of infected, untreated tibiae demonstrated a sharp fourfold increase from baseline on day 4, which subsequently dropped to background levels by day 11.

Based on the finding that BLI peaks on day 4 and *nuc* levels peak on day 11 along with the facts that bioluminescent of *S. aureus* Xen 29 results from the reaction of enzymes and protein substrates synthesized by the *lux* operon and that *nuc* is a single copy gene in the *S. aureus* chromosome, we hypothesized that BLI is a measure of *S. aureus* metabolic activity (protein synthesis), while *nuc* levels are indicative of bacteria number. This

theory also predicts that the BLI:*nuc* ratio is greater early on in infections compared to dormancy in latent infection. To test this, we performed linear regression analyses of BLI versus *nuc* gene copy number before the presence of biofilm on day 2 and on day 18 when humoral immunity limits the bacteria to biofilm growth. These analyses demonstrated that there is no relationship between BLI and *nuc* gene copy number on day 2 (Fig. 5A), while there is a highly significant correlation between these outcome measures on day 18 (Fig. 5B). Moreover, the finding that the BLI:*nuc* ratio is 15 times greater on day 2 versus day 18 (Fig. 5C) further substantiates BLI as an outcome measure of metabolic activity and *nuc* levels as a measure of bacterial load.

DISCUSSION

Although infection rates following orthopedic surgery are considered to be low,^{2,3} implant-associated OM remains a catastrophic outcome that often requires revision surgery and can lead to sepsis and death.¹ This problem is compounded by the emergence of multi-drug resistant strains and the absence of effective treatments for patients with methicillin-resistant *S. aureus* (MRSA).^{1,3} Progress in this area has been limited due to the absence of a quantitative animal model that can be utilized to elucidate molecular targets and evaluate novel interventions. From our assessment of the literature, we surmise that a quantitative OM model has not been developed for two reasons. First, the field has been overly concerned with intramedullary implant models, since this represents the more serious clinical condition.⁸⁻¹³ Unfortunately, we found that this

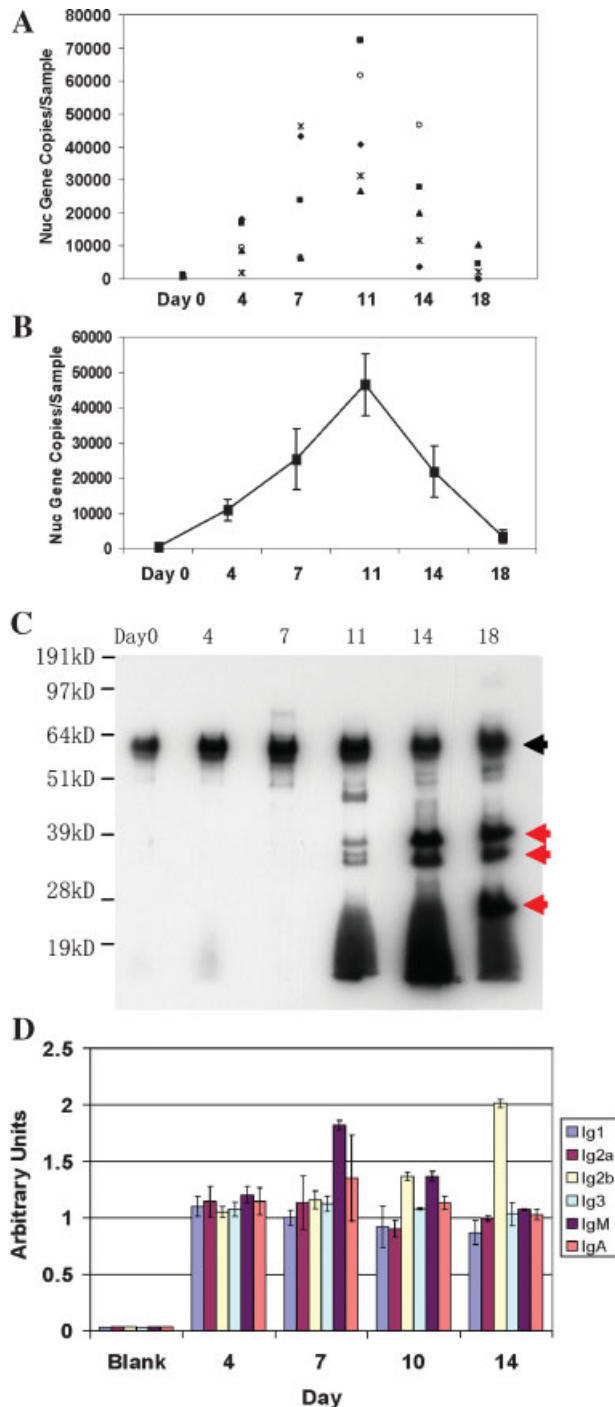


Figure 3. Kinetics of infection and host immunity during the establishment of OM. A time-course experiment was performed in which mice (N=5) received a trans-tibial pin coated with UAMS-1 *S. aureus* and were sacrificed at the indicated time after surgery. Genomic DNA was purified from the infected tibiae and used as the template for *nuc* and β -actin RTQ-PCR as described in Materials and Methods. (A) Data for each individual mouse, or (B) the mean for each group are presented with the standard deviation. (C) Sera were collected from mice (N=5) before (Day 0) and on Days 4, 7, 11, and 14 days after receiving a trans-tibial pin coated with *S. aureus* UAMS-1, and used as the primary antibody in Western blots of total *S. aureus* UAMS-1 protein extract. In the data shown from a representative animal, the black arrowhead indicates a pre-immune reactive band, and red arrowheads indicate the *S. aureus* specific reactive bands. (D) Total Ig levels in sera of mice (N=5) obtained on the indicated day following surgery were determined by ELISA as described in Materials and Methods. The data from a representative mouse are presented as the mean \pm SD of quadruplicates. Of note is the dominance of IgM on Day 7 and IgG2b on Day 14.

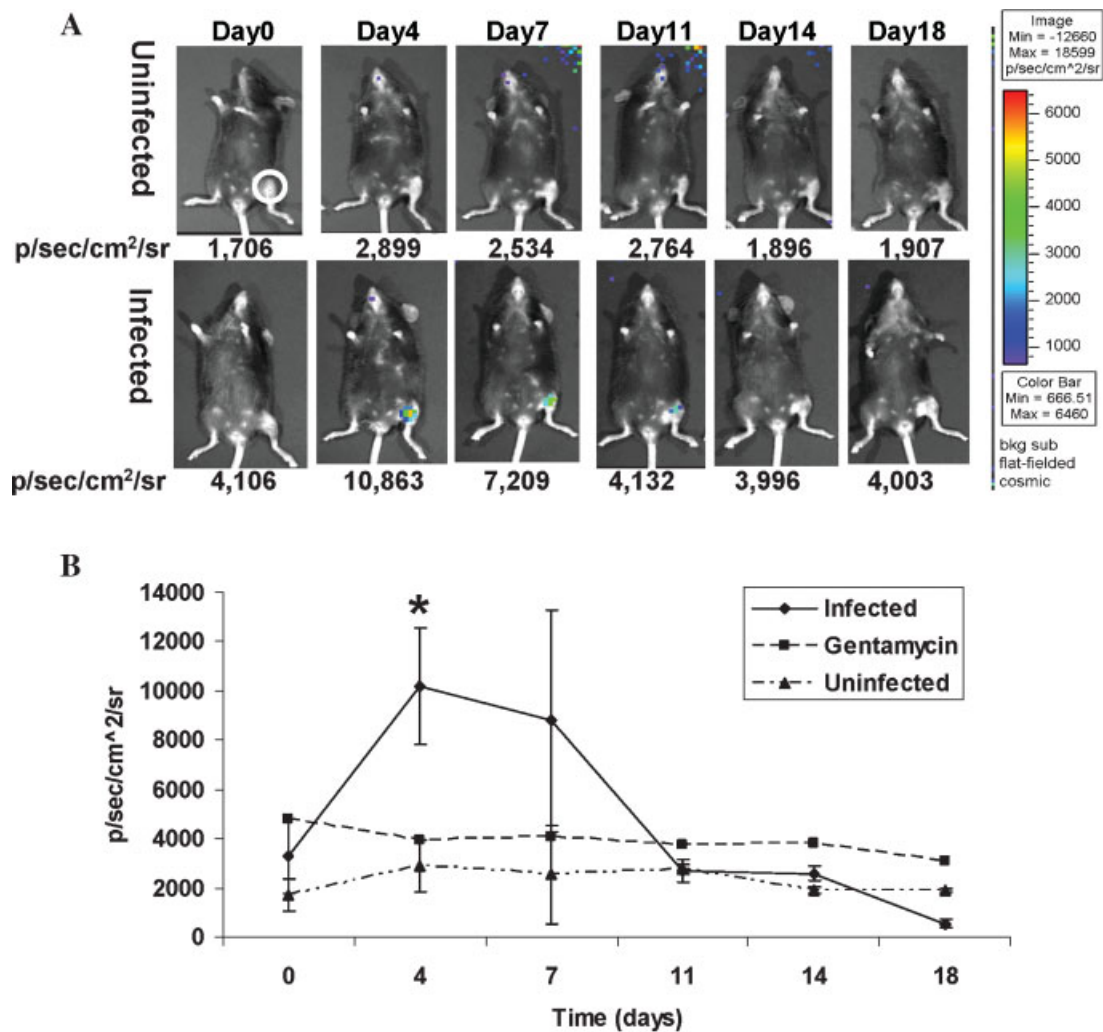


Figure 4. Bioluminescent Imaging (BLI) quantification of bacterial growth during the establishment of chronic osteomyelitis. (A) BLI levels at the site of infection were assessed longitudinally in mice that received a sterile trans-tibial pin (Uninfected), or a pin coated with Xen 29 *S. aureus* (Infected), that were imaged on the indicated day. The circle in the top left image highlights the 1.5-cm diameter region of interest (ROI) that was assessed for BLI in each mouse at each time point. (B) The data from mice ($N=5$) that were Uninfected, Infected, or infected and treated with parenteral antibiotics (Gentamycin) were assessed for BLI longitudinally at the indicated time following surgery. The data are presented as the mean \pm SD (*significantly greater vs. Day 0; $p < 0.05$).

model gave rise to highly variable (temporal and spatial) lesions, making a reproducible, quantitative model very challenging, although others have recently succeeded.²⁴ In contrast, we have found that implantation of an infected transcortical pin always produces lesions adjacent to the pin, and never results in distal OM, hematogenous infection, or death (Fig. 1). Thus, while it could be argued that the mechanisms of infection and treatment modalities differ between intramedullary and external fixation implants, we find the transcortical pin model to be the best approach to study OM in vivo.

The second roadblock towards the development of a quantitative OM model is the difficulty in extracting individual live bacteria, classically known as colony forming units (CFU), from infected bone. Here we demonstrate two independent methods to overcome this obstacle. The first, *nuc* RTQ-PCR, is a highly specific and sensitive method that has been successfully used to quantify *S. aureus* levels in contaminated cheese.¹⁸ It should be noted that although we control for DNA integrity via β -actin RTQ-PCR, we have no way of knowing the total *nuc* yield following our rigorous extraction procedures. Thus, it is likely that the *nuc* genes per

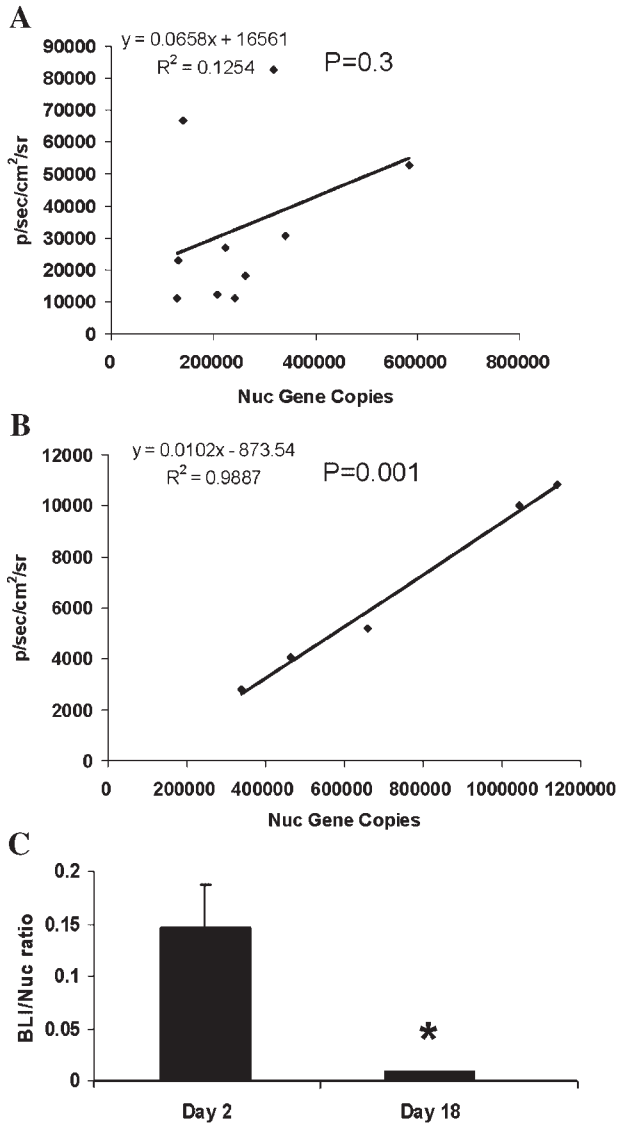


Figure 5. BLI is a function of bacterial metabolism. Mice received a trans-tibial pin coated with Xen29, and the BLI and *nuc* levels were determined on Day 2 (A), or Day 18 (B). A linear regression analysis was performed and the line of best fit is displayed with its equation, correlation coefficient (R^2), and significance (p). (C) These data were also used to determine the mean BLI:*nuc* ratio \pm SD (* $p < 0.05$ vs. Day 2).

tibia that we present represent a fraction of the total number of bacteria originally present in the sample. Furthermore, it is likely that our ability to extract *nuc* genes from infected tibiae becomes less efficient when the bacteria are residing in dense biofilm. Thus, the rather low *nuc* gene levels observed in latent infections (day 18), may be an underrepresentation of the actual bacterial load. This may also explain the remarkable effects of the anti-*S. aureus* antibodies on *nuc* gene levels (Fig. 3), as it is known that biofilm provide bacteria

with an immune-privileged environment. Nevertheless, our RTQ-PCR results provide the first demonstration that: i) in vivo bacterial load levels can be quantified during the establishment of OM; and ii) that the peak bacterial load is coincident with the generation of humoral immunity against the bacteria.

As mentioned above, two critical aspects of OM research that cannot be addressed by our RTQ-PCR approach are longitudinal studies and assessment of microbial metabolic activity. As research on the regulators of in vivo biofilm formation has become a central focus in this field, developing a surrogate outcome measure of pre- and post-biofilm growth is of great value. To this end, we have investigated the utility of BLI, which has emerged as a research technique with enormous potential.²⁵ Contag and colleagues were the first to utilize bioluminescent strains of pathogens to study infection longitudinally in mice.²⁶ Subsequent studies have proven the value of BLI over conventional methods in studying disease and therapeutic interventions in animals.²⁵ More recently, this group generated bioluminescent *S. aureus* Xen29 for this purpose.¹⁹ In our hands, Xen29 behaves essentially the same at UAMS-1, which is the most widely used strain of *S. aureus* used in OM research.⁹⁻¹³ Thus, we adopted this approach to be compatible with μ CT quantification of osteolysis and RTQ-PCR in our model of OM.

The first interesting result we obtained with BLI was that it peaked on day 4 (Fig. 4), well before the peak of bacterial load and the appearance of adaptive immunity (Fig. 3). Since BLI is a function of metabolic activity (protein synthesis), not bacterial load, our interpretation of these results is that there is a brief exponential bacterial growth phase that peaks on day 4, and is followed by the initiation of the biofilm growth phase that occurs at a low metabolic rate. Once this biofilm growth phase is initiated, perhaps due to the exhaustion of nutrients in the necrotic tissue, the bacterial load continues to increase. Microbes are shed from the biofilm until protective immunity is acquired on day 11. Afterwards, bacterial persistence is restricted to the biofilm in necrotic tissue indefinitely. To test this theory, we postulated that at a given time during infection, *nuc* copy number (1 *nuc* gene per bacterium) only correlates with BLI (mean rate of *luxA-E* protein synthesis for all of the bacteria) during periods of homogenous growth. In support of this theory, we found that no correlation exists during concomitant planktonic (high metabolic rate) and colonized (lower metabolic rate) bacterial growth, which is known to occur 48 h after

infection, and when the inter-animal variability between the proportion of planktonic to colonized bacteria is expected to be great (Fig. 5A). In contrast, when the bacteria are restricted to biofilm growth (low metabolic rate), due to acquired immunity at day 18, and there is no inter-animal variability between the proportions of planktonic to colonized bacteria, a significant correlation exists between *nuc* and BLI (Fig. 5B). Furthermore, we found that the BLI:*nuc* ratio early on in infection (day 2) is 15-fold greater versus chronic infection (day 18). While further studies are needed to formally demonstrate the kinetics of biofilm formation *in vivo*, our findings clearly distinguish these two phases of bacterial growth.

In summary, the development of a quantitative model of implant-associated OM opens the field to research that was previously unapproachable. New avenues include: the identification of biofilm genes through the characterization of mutant phenotypes, identification of diagnostic and/or protective antigens, and facile evaluation of infection-resistant implants such as the Selfprotective “smart” devices,²⁷ and novel drug efficacy. Although there are some fundamental limitations of this model with regard to its ability to accurately represent the true clinical problems associated with infected intramedullary implants and prostheses, we find that this trans-tibial mouse model, which displays all of the salient features of infected external fixation pins, to be a quantitative model suitable for most of these needs.

ACKNOWLEDGMENTS

The authors thank Laura Yanoso for technical assistance with the micro-CT, and Krista Scorsone for technical assistance with the histology. This work was supported by research grants from the US Army Medical Research Acquisition Activity (USAMRAA), Orthopaedic Trauma Research Program (OTRP) W81XWH-07-1-0124, and the National Institutes of Health PHS awards AR48681, DE17096, AR52674, AR51469, AR46545, AR54041, and AR53459.

REFERENCES

1. Darouiche RO. 2004. Treatment of infections associated with surgical implants. *N Engl J Med* 350:1422–1429.
2. Lew DP, Waldvogel FA. 2004. Osteomyelitis. *Lancet* 364:369–379.
3. Toms AD, Davidson D, Masri BA, et al. 2006. The management of peri-prosthetic infection in total joint arthroplasty. *J Bone Joint Surg [Br]* 88:149–155.

4. Costerton JW, Stewart PS, Greenberg EP. 1999. Bacterial biofilms: a common cause of persistent infections. *Science* 284:1318–1322.
5. Norden CW. 1988. Lessons learned from animal models of osteomyelitis. *Rev Infect Dis* 10:103–110.
6. Daum RS, Davis WH, Farris KB, et al. 1990. A model of *Staphylococcus aureus* bacteremia, septic arthritis, and osteomyelitis in chickens. *J Orthop Res* 8:804–813.
7. Rissing JP, Buxton TB, Weinstein RS, et al. 1985. Model of experimental chronic osteomyelitis in rats. *Infect Immun* 47:581–586.
8. Lucke M, Schmidmaier G, Sadoni S, et al. 2003. A new model of implant-related osteomyelitis in rats. *J Biomed Mater Res B Appl Biomater* 67:593–602.
9. Passl R, Muller C, Zielinski CC, et al. 1984. A model of experimental post-traumatic osteomyelitis in guinea pigs. *J Trauma* 24:323–326.
10. Worlock P, Slack R, Harvey L, et al. 1988. An experimental model of post-traumatic osteomyelitis in rabbits. *Br J Exp Pathol* 69:235–244.
11. Varshney AC, Singh H, Gupta RS, et al. 1989. Experimental model of staphylococcal osteomyelitis in dogs. *Indian J Exp Biol* 27:816–819.
12. Kaarsemaker S, Walenkamp GH, vd Bogaard AE. 1997. New model for chronic osteomyelitis with *Staphylococcus aureus* in sheep. *Clin Orthop* 339:246–252.
13. Salgado CJ, Jamali AA, Mardini S, et al. 2005. A model for chronic osteomyelitis using *Staphylococcus aureus* in goats. *Clin Orthop Relat Res* 436:246–250.
14. Marriott I, Gray DL, Tranguch SL, et al. 2004. Osteoblasts express the inflammatory cytokine interleukin-6 in a murine model of *Staphylococcus aureus* osteomyelitis and infected human bone tissue. *Am J Pathol* 164:1399–1406.
15. Patti JM, Jonsson H, Guss B, et al. 1992. Molecular characterization and expression of a gene encoding a *Staphylococcus aureus* collagen adhesin. *J Biol Chem* 267:4766–4772.
16. Johansson A, Flock JI, Svensson O. 2001. Collagen and fibronectin binding in experimental staphylococcal osteomyelitis. *Clin Orthop Relat Res* 382:241–246.
17. Elasri MO, Thomas JR, Skinner RA, et al. 2002. *Staphylococcus aureus* collagen adhesion contributes to the pathogenesis of osteomyelitis. *Bone* 30:275–280.
18. Hein I, Lehner A, Rieck P, et al. 2001. Comparison of different approaches to quantify *Staphylococcus aureus* cells by real-time quantitative PCR and application of this technique for examination of cheese. *Appl Environ Microbiol* 67:3122–3126.
19. Francis KP, Joh D, Bellinger-Kawahara C, et al. 2000. Monitoring bioluminescent *Staphylococcus aureus* infections in living mice using a novel luxABCDE construct. *Infect Immun* 68:3594–3600.
20. Zhang X, Schwarz EM, Young DA, et al. 2002. Cyclooxygenase-2 regulates mesenchymal cell differentiation into the osteoblast lineage and is critically involved in bone repair. *J Clin Invest* 109:1405–1415.
21. Koefoed M, Ito H, Gromov K, et al. 2005. Biological effects of rAAV-caAlk2 coating on structural allograft healing. *Mol Ther* 12:212–218.
22. Ito H, Koefoed M, Tiyyapanaputi P, et al. 2005. Remodeling of cortical bone allografts mediated by adherent rAAV-RANKL and VEGF gene therapy. *Nat Med* 11:291–297.
23. Schwarz EM, Krimpenfort P, Berns A, et al. 1997. Immunological defects in mice with a targeted disruption in Bcl-3. *Genes Dev* 11:187–197.

24. Antoci V Jr, King SB, Jose B, et al. 2007. Vancomycin covalently bonded to titanium alloy prevents bacterial colonization. *J Orthop Res* 25:858–866.
25. Contag CH, Bachmann MH. 2002. Advances in in vivo bioluminescence imaging of gene expression. *Annu Rev Biomed Eng* 4:235–260.
26. Contag CH, Contag PR, Mullins JI, et al. 1995. Photonic detection of bacterial pathogens in living hosts. *Mol Microbiol* 18:593–603.
27. Parvizi J, Antoci V Jr, Hickok NJ, et al. 2007. Self-protective smart orthopedic implants. *Expert Rev Med Devices* 4:55–64.

Appendix II

Effects of anti-resorptive agents on osteomyelitis

*Kirill Gromov^{1,2}, kig@studmed.au.dk *Dan Li¹, dan_li@urmc.rochester.edu

Steven T. Proulx¹, proulx@seas.rochester.edu Chao Xie¹, chao_xie@urmc.rochester.edu

Kjeld Søballe², kjeld.soballe@mail1.stofanet.dk

Regis J. O'Keefe¹, regis_okeefe@urmc.rochester.edu

Hani A. Awad^{1,3}, hani_awad@urmc.rochester.edu

Lianping Xing¹, lianping_xing@urmc.rochester.edu

and Edward M. Schwarz^{1,4}, edward_schwarz@urmc.rochester.edu

¹ The Center for Musculoskeletal Research, University of Rochester, Rochester, New York

² The Department of Orthopedics, Aarhus University Hospital, Aarhus, Denmark

³ Department of Biomedical Engineering, University of Rochester, Rochester, New York

⁴To whom correspondence should be addressed:

Dr. Edward M. Schwarz

The Center for Musculoskeletal Research

University of Rochester Medical Center

601 Elmwood Avenue, Box 665, Rochester, NY 14642

Phone 585-275-3063, FAX 585-756-4727

E-mail: EdwardSchwarz@URMC.Rochester.edu.

*These authors contributed equally to this work.

This work was supported by research grants for the US Dept. of Defense (ERMS No.06136016 and UID No. 99853) and the National Institutes of Health PHS awards AR48681, DE17096, AR52674, AR51469, AR46545, AR54041 and AR53459.

Conflict of Interest

Dan Li, Kirill Gromov, Steven T. Proulx, Chao Xie, Kjeld Søballe, Regis J. O'Keefe,

Hani A. Awad, and Lianping Xing have nothing to disclose.

Edward M. Schwarz is a paid consultant and owns stock of Amgen Inc.

ABSTRACT: The effects of anti-resorptive agents on osteomyelitis (OM) are unknown. Our studies demonstrate that these drugs can increase in the incidence of high-grade infections during the establishment of OM by decreasing lymphatic drainage and preventing the removal of necrotic bone that harbors the bacteria.

Introduction: Although bisphosphonates have been used to prevent osteolysis around septic implants, their effects on infection are unknown. Additionally, the mechanisms responsible for the interactions between bisphosphonates and bone infection in ONJ are controversial. Thus, we examined this in a murine model of implant-associated OM.

Materials and Methods: Mice received a transtibial implant contaminated with bioluminescent *S. aureus* (Xen29) and treated with alendronate (Aln) and osteoprotegerin (OPG), or PBS (placebo), gentamycin and etanercept (TNFR:Fc) controls. Infection, immunity, osteolysis, vascularity, and popliteal lymph node (PLN) size were assessed by BLI, RTQ-PCR, ELISA, x-ray, micro-CT, histology and MRI.

Results: None of the drugs affected humoral immunity, angiogenesis, or chronic infection. However, the significant ($p < 0.05$ vs. PBS) inhibition of cortical osteolysis and decreased draining lymph node size in Aln and OPG treated mice was associated with a significant ($p < 0.05$) increase in the incidence of high-grade infections during the establishment of OM. In contrast, the high-grade infections in TNFR:Fc treated mice were associated with immunosuppression, as evidenced by the absence of granulomas and presence of Gram⁺ biofilm in the bone marrow. Interestingly, micro-CT analysis of Aln and OPG treated mice demonstrated that the bone void around infected implants is due to both osteoclastic resorption of cortical bone and inhibition of periosteal reactive bone formation.

Conclusions: These findings indicate that while anti-resorptive agents do not exacerbate chronic OM, they can increase bacterial growth during early infection by decreasing lymphatic drainage and preventing the removed of necrotic bone that harbors the bacteria.

INTRODUCTION

Although the incidence of orthopaedic bone infection, known as osteomyelitis (OM), for joint prostheses and fracture-fixation devices have remained at 0.3-11% and 5-15% respectively over the last decade^(1,2), the emergence of methicillin-resistant *Staphylococcus aureus* (MRSA) has dramatically impacted clinical management^(3,4). Since OM induces osteolysis around the implant, which can lead to fractures and complicate revision surgery, orthopedists have anecdotally used anti-resorptive bisphosphonates in these patients to preserve bone stock without knowledge of their effects on chronic infection^(5,6).

Another clinical condition that is associated with OM and bisphosphonate use is the recent osteonecrosis of the jaw (ONJ) epidemic^(7,8), which primarily affects cancer patients on immunosuppressive chemotherapy that also receive intravenous pamidronate or zoledronate for hypercalcaemia, and undergo unrelated oral surgery. However, ONJ has also been reported in healthy women taking oral alendronate for postmenopausal osteoporosis^(9,10), raising serious concerns for the tens of millions of people taking these anti-resorptive agents^(11,12). Although the etiology of ONJ remains unknown, careful reviews of all the available clinical and basic science data have derived two leading theories to explain this painful condition⁽¹³⁻¹⁵⁾. The first is inhibition of angiogenesis, which is largely derived from the precedent of steroid-induced avascular necrosis of the hip, and new studies that have demonstrated bisphosphonate-inhibition of capillary tube formation, vessel sprouting and circulating endothelial cells⁽¹⁶⁻¹⁸⁾. The other is the osteoclast-inhibiting effect of anti-resorptive agents that lead to a cessation of bone remodeling and mineral:matrix turnover⁽¹⁶⁾. This renders the fatigued bone susceptible to

involution of blood vessels, necrosis and infection. The impact of infection in ONJ is further highlighted by the finding that essentially all cases have histopathological evidence of OM^(19,20), however, a cause and effect relationship has yet to be established.

To better understand the effects of bisphosphonates on OM, and shed light on potential mechanisms of ONJ, we investigated the interaction of anti-resorptive agents in an established murine trans-tibial infected pin model that emulates the biology of infected orthopaedic and periodontal implants⁽²¹⁾. This model takes advantage of a gentamycin sensitive, *luxA-E* transformed strain of *S. aureus* (Xen29)⁽²²⁾, whose metabolic activity and bacterial load can be quantified *in vivo* using longitudinal bioluminescence imaging (BLI) and *nuc* quantitative real-time PCR (QRT-PCR) respectively⁽²¹⁾. This model also has micro-CT outcome measures of osteolysis and vascularity, serological analyses of the protective IgG2b humoral response that appears by day 11, and traditional histology of osteoclasts and Gram-stained biofilm⁽²¹⁾. Here we investigated two distinct classes of anti-resorptive drugs: the most widely prescribed bisphosphonate alendronate (Aln)⁽⁸⁾, which induces osteoclast apoptosis via inhibition of the mevalonate pathway of isoprenoid biosynthesis⁽²³⁾; and the biologic antagonists osteoprotegerin (OPG) that inhibits osteoclast formation and induces osteoclast apoptosis by blocking receptor activator of nuclear factor kappa B (RANK) signaling pathway⁽²⁴⁾. While these studies demonstrated that neither Aln nor OPG could induce or exacerbate chronic OM, likely because they do not affect the protective humoral response nor inhibit angiogenesis in our model, both agents caused an increase in high-grade infections as defined by significant increases in the number of mice with BLI and *nuc* gene levels above maximum placebo levels. This finding coincided with a significant decrease in osteolysis and draining

lymph node size, suggesting that anti-resorptive agents decrease efflux of marrow lymph during the establishment of OM. Thus, these effects could lead to a dramatic increase in intraosseous pressure, infarction and bone pain, which are the hallmarks of OM and ONJ.

MATERIALS AND METHODS

Murine OM model and drug treatments

All animal studies were performed under University of Rochester Committee for Animal Resources approved protocols. Pathogenic challenges were performed as previously described⁽²¹⁾. Briefly, OM was initiated by surgically implanting a contaminated 0.25 mm diameter insect pin (Fine Science Tools, Foster City, CA) containing $\sim 5 \times 10^5$ CFU of Xen29 (Cranbury, NJ) medial to lateral through the left tibia of C57BL/6 female 6-8 week-old mice anesthetized with ketamine (100 mg/kg) and xylazine (10 mg/kg). Drug treatments started on the day of surgery, except for Aln, which started 3 days before surgery. Aln (Calbiochem, San Diego, CA) was given at 10 μ g/kg i.p. once every 3 days. OPG (R&D Systems, Minneapolis, MN) was given at 200 μ g i.p. once every 3 days. TNFR:Fc (Amgen, Thousand Oaks, CA) was given at 200 μ g i.p. once every 3 days. Placebo was given as 200 μ l PBS i.p. once every 3 days. Gentamycin (Calbiochem, San Diego, CA) was given daily (0.1 mg/kg i.p.).

Radiology and bioluminescent imaging

Longitudinal osteolysis was assessed radiographically using a Faxitron Cabinet x-ray system (Faxitron, Wheeling, IL, USA) as we have previously described⁽²¹⁾. Bioluminescent imaging (BLI) of mice infected with Xen29 was performed on day 0, 4,

7, 11, 14, 18 post-infection using a Xenogen IVIS camera system (Xenogen Corporation, Alameda, Calif.) as we have previously described⁽²¹⁾. Five minute high sensitivity ventral images were taken at each time point. The BLI was quantified with the LivingImage software package 2.50.1 (Xenogen Corporation, Alameda, Calif.) by analyzing a fixed 1.5 cm diameter region of interest (ROI) centered on the pin. The photon signal was calculated as p/sec/cm²/sr.

Micro-CT analyses were performed on tibiae after removing the pin and surrounding musculature by high-resolution (10.5 μm) micro-computed tomography (μCT) (VivaCT 40; Scanco Medical AG, Basserdorf, Switzerland) to render 3D images of the diaphysis as we have previously described⁽²⁵⁾. For osteolysis quantitation, the maximal osteolytic area of the cortical and reactive bone voids were computed for each specimen using a semi-automated filter in Adobe Photoshop® CS (Adobe Systems, Inc., San Jose, CA) as we have previously described⁽²¹⁾. Vascular micro-CT analyses around the pin were performed on tibiae that were perfused with Microfil MV-122 (Flowtech, South Windsor, CT) lead chromate-based contrast agent as we have previously described⁽²⁶⁾. After the initial micro-CT scan, the samples were decalcified in a 10% EDTA solution, and rescanned to image the perfused contrast. By registering the 2D slices before and after decalcification, contour lines were drawn to define a region of interest that only included 0.5mm infected bone with the pin site in the middle. The tomograms were globally thresholded based on X-ray attenuation and used to render 3D images of the vasculature in the region of interest, excluding the vessels in the surrounding tissues. Histomorphometric analysis based on direct distance transform methods^(27,28) was subsequently performed on the 3D images to quantify parameters of

vascular network morphology, including vasculature volume (Vasc. Vol.), vessel thickness (Vess.Th), vessel density (Vess. Den.: defined as an average number of vessels intersected by test lines passing through the 3D image normalized by test line length), vessel spacing (Vess. Sp.), and degree of anisotropy^(28,29).

MR scans were performed on a 3 Tesla Siemens Trio MRI (Siemens Medical Solutions, Erlangen, Germany) with a custom surface coil and fat-suppressed, T1-weighted pulse sequences as we have previously described^(30,31). Quantification of PLN volume was performed with Amira 3.1 (TGS, Mercury Computer Systems, Inc, San Diego, CA) as we have previously described^(30,31).

Histologic evaluation of OM

After μ CT, the tibial samples were processed for decalcified histology and stained with Orange G/alcian blue (H&E), Gram-stained, or stained for tartrate-resistant acid phosphatase (TRAP) activity as we have described previously⁽³²⁾.

Immunohistochemistry to identify T-cells, B-cells, macrophages and neutrophils was performed as described previously⁽³³⁾, using primary antibodies specific for CD3 (diluted 1:100; Novocastra, Newcastle, UK), CD45R/B220 (diluted 1:300; BD Biosciences Pharmingen, San Jose, CA, USA), F4/80 (diluted 1:80; AbD Serotec, Raleigh, NC, USA), and Neu7/4 (clone# MCA771G, diluted 1:2000, AbD Serotec, Raleigh, NC) respectively. Osteoclasts were quantified as the mean \pm SD number of TRAP+ multinucleated cells in the 10x field centered on the pin tract from three contiguous 3 μ m sections 500 μ m apart, as previously described⁽³⁴⁾.

DNA purification and nuc/β-actin RTQ-PCR

Total DNA was extracted from infected tibiae and analyzed by RTQ-PCR for the *S. aureus*-specific *nuc* gene standardized to mouse *β-actin* as previously described⁽²¹⁾. The *nuc* gene was amplified with DNA primers 5'GCGATTGATGGTGATACGGTT 3' and 5'AGCCAAGCCTTGACGAACTAA 3' that produce a 269-bp product⁽³⁵⁾. The *β-actin* gene was amplified with DNA primers 5'-AGA TGT GAA TCA GCA AGC AG-3' and 5'-GCG CAA GTT AGG TTT TGT CA-3' that produce a 124-bp product⁽²¹⁾. The reactions were carried out in a final volume of 20 μl consisting of 0.3 μM primers, 1x Sybr Green PCR Super Mix (BioRad, Hercules, CA), and 2 μl of the purified tibia DNA template. The samples were assayed in triplicate in a Rotor-Gene RG 3000 (Corbett Research, Sydney, AU). In order to calculate the *nuc* gene copies in a tibia sample, we first generated a standard curve with *S. aureus* genomic DNA purified directly from an overnight culture. The mean of the 3 Ct values from each tibia sample were then plotted against this curve to extrapolate the number of *nuc* genes. This number was then normalized to *β-actin* and the data are presented as normalized *nuc* gene copies per sample.

Serology

In order to determine total immunoglobulin isotype (Ig) levels, blood samples were collected from the animals on days 0, 4, 7, 11 and 14 using retro-orbital bleeding, and an ELISA on the sera was performed using the Mouse Typer Sub-Isotyping Kit (BioRad, Hercules, CA) as we have previously described⁽²¹⁾.

Statistical analysis

All values are presented as means \pm SD. Significant differences between groups in the histology, micro-CT, serology, MRI and PLN weight analyses were determined by ANOVA with Bonferroni correction. A Fisher's exact test was performed to determine significant differences in the incidence of infection and high-grade infection. The correlation between BLI vs. *nuc* was estimated using Pearson's correlation coefficient and tested for significance using a two-sided *t*-test. In all cases, $p < 0.05$ was considered significant.

RESULTS

Anti-resorptive drug effects on osteoclast numbers, necrotic bone and biofilm in chronic OM

In order to assess the effects of anti-resorptive agents on the establishment of implant-associated OM, we investigated five experimental groups in the Xen29-infected trans-tibial pin model⁽²¹⁾: Group 1 received effective gentamycin prophylaxis that prevents infection (Gent), Group 2 received placebo (PBS), Group 3 received OPG, Group 4 received Aln, and Group 5 received the tumor necrosis factor (TNF) antagonist etanercept (TNFR:Fc) as a control that is known to inhibit osteoclasts⁽³⁶⁾ and exacerbate infections by inhibiting granuloma formation⁽³⁷⁾. Upon initial inspection of the x-rays taken on day 18, effects of all three anti-resorptive treatments displayed remarkable large soft-tissue abscesses compared to the Gent and PBS controls (Fig. 1a-e). Histological analyses of these tibiae also confirmed the significant effects of these drugs on the reduction of osteoclasts numbers at the bone-implant interface (Fig. 1f-o). Although, TNF blockade also reduced osteoclast numbers to a certain extent, it is noteworthy that

the effects of TNFR:Fc on bone histology were significantly different from all of the other groups, indicating a different mechanism of action. Consistent with the osteoclast results, we found that OPG and Aln treated mice had large amounts of unresorbed necrotic cortical bone adjacent to the pin tract (Fig. 1h-i, m-n), which served as a nidus for infection as evidenced by the presence of Gram⁺ biofilm in parallel sections (Fig. 1r-s). In contrast, the extensive osteolysis in the PBS and TNFR:Fc treated mice appeared to have removed all of the necrotic bone around the pin hole (Fig. 1g, j), and there was no evidence of bacteria at these sites in parallel sections (Fig. 1l, o). However, infection in these animals was evident from Gram⁺ biofilm within necrotic bone fragments that were likely generated during implantation of the pin (Fig. 1q,t). As expected from effective prophylaxis, Gent treated mice had no evidence of osteolysis or infection (Fig. 1a,f,k,p).

Anti-resorptive drugs increase the incidence of high-grade infections during the establishment of chronic OM

In order to assess the effects of Aln, OPG and TNFR:Fc on Xen29 metabolism and bacterial load during the establishment of implant-associated OM, we performed longitudinal BLI before, during and after the establishment of protective humoral immunity (Days 7, 11, 18, respectively) in our model(21) (Fig. 2a-c). While these experiments failed to demonstrate any significant differences between the averages of the groups ($p>0.05$), indicating that the drugs cannot exacerbate infection by themselves, we did observe a few mice in the OPG, Aln and TNFR:Fc groups that had remarkably high BLI values, suggestive of “high-grade” infection. To test this we performed Fisher’s exact tests comparing the number of uninfected, infected and high-grade infected mice in

each group (Fig. 2a-c). These results demonstrated that while Aln and OPG did not increase the incidence of infection at any time they caused a significant increase in the number of mice with high-grade infections early on (Day 7 and 11). Interestingly, the effects of TNFR:Fc were similar with the exception that TNF inhibition caused a 100% infection rate on Day 7.

In order to confirm our observation that anti-resorptive drugs induce high-grade infections during the establishment of OM, we quantified the bacterial load on day 7 and day 18 (Figs. 2d-e). Interestingly, while no differences were observed early on, the OPG, Aln and TNFR:Fc groups all had significantly more high-grade chronic infections on day 18. In order to demonstrate that the high-grade infections determined by BLI and RTQ-PCR were in the same animals, we performed a linear regression analysis of all the day 18 data (Fig. 2f). This significant correlation ($R^2=0.64$, $p<0.05$) validates our findings that anti-resorptive agents can increase the incidence of high-grade OM.

Anti-resorptive drug effects on osteolysis, angiogenesis and immunity during the establishment of chronic OM

In order to better understand the mechanism by which anti-resorptive drugs increase the incidence of high-grade OM, we investigated their effects on bone volume, vasculature and host immune responses during the infection. First, we performed micro-CT analyses on the infected tibiae to assess bone and vasculature around the pin on day 18. While the micro-CT images of the bone corroborated the x-ray and histology findings (Fig. 1), the most striking result was the zone of inhibited reactive bone formation around the infected pins of Aln and OPG treated mice (Fig. 3a). This zone appeared as an almost

perfect ring ~2mm in diameter, and is the first formal demonstration that OM-induced osteolysis observed in radiographs is largely due to inhibition of bone formation rather than pure osteoclastic bone resorption. Independent quantification of the osteolytic area in the cortical and reactive bone demonstrated that Aln and OPG completely inhibit cortical resorption, but have no effects on reactive bone formation (Fig. 3b). In contrast, despite its ability to decrease osteoclast numbers and promote high-grade OM, TNFR:Fc did not significantly inhibit cortical osteolysis compared to PBS controls.

Given that avascular necrosis is often associated with OM, we also quantified vascularity in the infected tibiae via 3D-microCT of lead chromate perfused vessels. These studies failed to detect any significant differences between any of the five groups in terms of vasculature volume, vessel thickness, vessel density, vessel spacing, and degree of anisotropy (Fig. 4). Thus, none of the drug effects in our model can be explained by changes in angiogenesis.

To test if drug induced immunosuppression of humoral immunity was responsible for the high-grade infections, we examined total Ig levels in sera from the animals over the course of infection (Fig. 5a). These data confirmed the induction of the previously characterized IgG2b response in all of the mice, and demonstrate that none of the drugs inhibited humoral immunity against Xen29. This finding is consistent with the 100% survival rate from a bacterial challenge that would cause lethal sepsis in immunodeficient mice. We also reanalyzed the histology to assess drug effects on granuloma formation (Fig. 5b-i). Although Aln and OPG could not prevent infection of necrotic bone adjacent to the implant, we found no evidence of biofilm formation anywhere else (Fig. 5b,c). In fact, we could readily identify active granulomas in immediate proximity to the pin that

were completely Gram negative (Fig. 5d,e), indicating that anti-resorptive drugs do not interfere with innate immunity. In contrast, mice treated with TNFR:Fc had Gram positive biofilm in both necrotic bone and soft tissue adjacent to the pin (Fig. 5f-i). Furthermore, there was no evidence of an organized cellular immune response around the infected soft tissue (Fig. 5i). These results are consistent with the critical role for TNF in innate immunity and granuloma formation.

While considering alternative mechanisms responsible for the high-grade OM, we reflected on an explanation as to why the host chooses to mount such a vigorous osteolytic response to infection in which a much greater bone void is generated than what would be expected based on the margins of the biofilm (e.g. $>2\text{mm}^3$ vs. $<0.2\text{mm}^3$). The simplest explanation for this is that efficient drainage of the infection requires a large cavity for efflux of pus out of the medullary canal, which is under enormous intraosseous pressure from the recruitment and proliferation of immune cells and fluid. Thus, we reasoned that inhibition of cortical resorption would compromise this process as evidenced by a significant decrease in draining lymph node volume. To test this hypothesis we performed *in vivo* MRI to quantify the popliteal lymph node (PLN) volume on day 9 (Fig. 6a), which demonstrated that both OPG, Aln and TNFR:Fc significantly decrease PLN volume during the peak of infection. We also analyzed the tibiae and PLN of these mice *ex vivo*, which demonstrated two remarkable observations. First, there was no macroscopic evidence of pus draining from the pin tract of the OPG and Aln treated mice (Fig. 6b). This was to be expected based on the micro-CT data, which demonstrated the cortical whole is approximately the same size as the implant (Fig. 3). Secondly, OPG and Aln significantly inhibited the expansion of the draining PLN, but had no effects on

the contralateral PLN, as determined by weight (Fig. 6c). Immunohistochemical analysis of these PLN with antibodies specific for B-cells (B220), T-cells (CD3), neutrophils (Neu7/4) and macrophages (F4/40) failed to generate any remarkable findings (data not shown), as the PBS samples simply appeared larger. Thus, future studies are required to formally demonstrate the relationship between lymphatic egress from the infected medullary canal and PLN expansion during the establishment of OM.

DISCUSSION

Although infection rates following bone-implant surgery remain fairly low, the total number of OM cases is high⁽³⁾, and the recent surge in MRSA further underscores the significance of this clinical problem⁽⁴⁾. At best, this catastrophic outcome requires a challenging revision surgery that is further complicated by deteriorated bone stock due to osteolysis. Thus, an important unanswered question regarding the treatment of patients with implant-associated OM is whether or not they would benefit from anti-resorptive therapy. Despite the successful case reports in the literature^(5,6), our study indicates that this practice may be contraindicated since Aln and OPG: i) increase the amount of necrotic cortical bone around the implant that serves as a nidus for infection (Fig. 1), ii) significantly increases the incidence of high-grade infections in mice during the establishment of OM (Fig. 2), and iii) reduce the cortical hole (Fig. 3) through which the opsonized bacteria and lymph must drain out of the wound (Fig. 6).

Equally important to our positive findings are results that refute claims regarding the anti-angiogenic and immunosuppressive effects of anti-resorptive therapies. In search of the etiology of ONJ, others have reported that bisphosphonates inhibit capillary tube

formation, vessel sprouting and circulating endothelial cells⁽¹⁶⁻¹⁸⁾, and cited this as a mechanistic factor in the condition. In contrast, our vascular micro-CT analyses failed to demonstrate any drug effects on perfusable vessels >10 μ m (Fig. 4). Thus, our findings are more consistent with reports from others who have argued against this theory based on the fact that drugs such as thalidomide, with far greater anti-angiogenic capacity, do not result in ONJ⁽¹⁶⁾. Similarly, the findings that RANK signaling is required for lymph node development^(38,39) and immunoregulatory co-stimulation^(40,41) have led to a suspicion that RANK-ligand inhibition is immunosuppressive. However, our studies corroborate the prior findings of Stolina et al, who demonstrated that OPG treatment does not affect cell-mediated immune responses and granuloma formation⁽⁴²⁾, and the recent finding that humans genetically deficient in RANKL have severe osteopetrosis without immunodeficiency⁽⁴³⁾. Therefore, we conclude that RANKL inhibition has insignificant immunoregulatory effects in the setting of *in vivo* pathogenic challenge, and that its ability to increase the incidence of high-grade OM can be entirely attributed to its effects on osteoclastic bone resorption, as these effects could be replicated with Aln (Figs. 1-3). To further abate concerns regarding the clinical use of a biologic RANK antagonist (i.e. denosumab⁽⁴⁴⁾), we demonstrated that OPG and TNFR:Fc mediate similar effects on OM via different mechanisms, as evidenced by their differential effects on osteolysis, granuloma formation, and lymphatics. Given the remarkable clinical success of anti-TNF therapy over the last decade, and its much greater effects on the immune system compared to OPG, it is becoming more apparent that immunosuppression is unlikely to be a major limitation of biologic anti-resorptive therapy.

The most surprising results of our study was the observation that the massive bone

void around the transtibial implant was largely due to inhibition of reactive bone formation rather than osteoclastic bone resorption, as evidenced by the micro-CT images of the Aln and OPG treated samples (Fig. 3a). Most interestingly is that this inhibition of bone formation appears as a perfectly symmetrical ring that extend >1mm from the biofilm adjacent to the pin. Thus, it is clear that this is mediated by an indirect mechanism that likely involves a secreted factor (i.e. noggin, DKK1, SOST) that has a gradient expression pattern originating from the infected bone. Elucidation of this factor(s) is now the subject of ongoing investigation, as it could also prove to be important for preventing inflammation mediated bone loss in aseptic conditions such as erosive arthritis and periprosthetic osteolysis.

While we do not want to overstate the implications of our findings as they relate to the emerging ONJ epidemic, we feel that there are several parallels that warrant discussion. The first and most frustrating is the absence of etiologic factors that are necessary and sufficient to faithfully reproduce OM and ONJ in similar individuals. Even though a correlation between ONJ and bisphosphonate use in cancer patients following oral surgery has been established^(7,8), its overall incidence in this population is >10%⁽¹³⁻¹⁵⁾. Similarly, despite our best efforts in a controlled experiment model, we have been unable to establish conditions that lead to equivalent OM in genetically identical littermates, in which many of the mice that receive a Xen29 coated pin remain uninfected (Fig. 2). This indicates that stochastic epigenetic factors, such as the amount of necrotic bone available for bacterial adhesion, and the temporally restricted period for this event to occur, may be critical to the establishment of both OM and ONJ.

The other parallel that deserves mention is the potential association between

inhibited lymphatics during the establishment of bone infection and bone pain.

Clinically, OM and ONJ are primarily discovered as a result of symptomatic bone pain, whose nature is largely unknown. Our novel finding that OPG and Aln drug inhibition of resorption is associated with significant decreased lymphatics during the establishment of bone infection implies that there must be a marked increase in intraosseous pressure at this time, which would be expected to induce bone pain characteristic of that seen in OM and ONJ. Interestingly, recent clinical studies have demonstrated that surgery-induced lymphedema is a major cause of local pain, and improvement of lymphatic drainage is an effective therapy in these patients(45). Thus, the association of decreased lymph node size and drainage in our model of OM warrants further investigation.

ACKNOWLEDGMENTS

The authors would like to thank Dr. Christopher Beck of the Department of Biostatistics, for his assistance with the statistical analyses. We also thank Laura Yanoso for technical assistance with the micro-CT and Krista Scorsone for technical assistance with the histology. This work was supported by research grants for the US Dept. of Defense (ERMS No.06136016 and UID No. 99853) and the National Institutes of Health PHS awards AR48681, DE17096, AR52674, AR51469, AR46545, AR54041 and AR53459.

REFERENCES

1. Lew DP, Waldvogel FA 2004 Osteomyelitis. *Lancet* **364**(9431):369-79.
2. Toms AD, Davidson D, Masri BA, Duncan CP 2006 The management of peri-prosthetic infection in total joint arthroplasty. *J Bone Joint Surg Br* **88**(2):149-55.
3. Darouiche RO 2004 Treatment of infections associated with surgical implants. *N Engl J Med* **350**(14):1422-9.
4. Klevens RM, Morrison MA, Nadle J, Petit S, Gershman K, Ray S, Harrison LH, Lynfield R, Dumyati G, Townes JM, Craig AS, Zell ER, Fosheim GE, McDougal LK, Carey RB, Fridkin SK 2007 Invasive methicillin-resistant *Staphylococcus aureus* infections in the United States. *Jama* **298**(15):1763-71.
5. Wright SA, Millar AM, Coward SM, Finch MB 2005 Chronic diffuse sclerosing osteomyelitis treated with risedronate. *J Rheumatol* **32**(7):1376-8.
6. Soubrier M, Dubost JJ, Ristori JM, Sauvezie B, Bussiere JL 2001 Pamidronate in the treatment of diffuse sclerosing osteomyelitis of the mandible. *Oral Surg Oral Med Oral Pathol Oral Radiol Endod* **92**(6):637-40.
7. Marx RE 2003 Pamidronate (Aredia) and zoledronate (Zometa) induced avascular necrosis of the jaws: a growing epidemic. *J Oral Maxillofac Surg* **61**(9):1115-7.
8. Hellstein JW, Marek CL 2005 Bisphosphonate osteochemonecrosis (bis-phossy jaw): is this phossy jaw of the 21st century? *J Oral Maxillofac Surg* **63**(5):682-9.
9. Woo SB, Hellstein JW, Kalmar JR 2006 Systematic review: bisphosphonates and osteonecrosis of the jaws. *Ann Intern Med* **144**(10):753-61.
10. Shane E, Goldring S, Christakos S, Drezner M, Eisman J, Silverman S, Pendrys D 2006 Osteonecrosis of the Jaw: More Research Needed. *J Bone Miner Res* **21**(10):1503-1505.
11. Koka S, Clarke BL, Amin S, Gertz M, Ruggiero SL 2007 Oral bisphosphonate therapy and osteonecrosis of the jaw: what to tell the concerned patient. *Int J Prosthodont* **20**(2):115-22.
12. Khosla S, Burr D, Cauley J, Dempster DW, Ebeling PR, Felsenberg D, Gagel RF, Gilsanz V, Guise T, Koka S, McCauley LK, McGowan J, McKee MD, Mohla S, Pendrys DG, Raisz LG, Ruggiero SL, Shafer DM, Shum L, Silverman SL, Van Poznak CH, Watts N, Woo SB,

- Shane E 2007 Bisphosphonate-associated osteonecrosis of the jaw: report of a task force of the American Society for Bone and Mineral Research. *J Bone Miner Res* **22**(10):1479-91.
13. Hewitt C, Farah CS 2007 Bisphosphonate-related osteonecrosis of the jaws: a comprehensive review. *J Oral Pathol Med* **36**(6):319-28.
 14. Van den Wyngaert T, Huizing MT, Vermorken JB 2007 Osteonecrosis of the jaw related to the use of bisphosphonates. *Curr Opin Oncol* **19**(4):315-22.
 15. Gutta R, Louis PJ 2007 Bisphosphonates and osteonecrosis of the jaws: Science and rationale. *Oral Surg Oral Med Oral Pathol Oral Radiol Endod.*
 16. Marx RE, Sawatari Y, Fortin M, Broumand V 2005 Bisphosphonate-induced exposed bone (osteonecrosis/osteopetrosis) of the jaws: risk factors, recognition, prevention, and treatment. *J Oral Maxillofac Surg* **63**(11):1567-75.
 17. Ruggiero SL, Mehrotra B, Rosenberg TJ, Engroff SL 2004 Osteonecrosis of the jaws associated with the use of bisphosphonates: a review of 63 cases. *J Oral Maxillofac Surg* **62**(5):527-34.
 18. Allegra A, Oteri G, Nastro E, Alonci A, Bellomo G, Del Fabro V, Quartarone E, Alati C, De Ponte F, Cicciu D, Musolino C 2007 Patients with bisphosphonates-associated osteonecrosis of the jaw have reduced circulating endothelial cells. *Hematol Oncol.*
 19. Bagan JV, Murillo J, Jimenez Y, Poveda R, Milian MA, Sanchis JM, Silvestre FJ, Scully C 2005 Avascular jaw osteonecrosis in association with cancer chemotherapy: series of 10 cases. *J Oral Pathol Med* **34**(2):120-3.
 20. Hansen T, Kunkel M, Weber A, James Kirkpatrick C 2006 Osteonecrosis of the jaws in patients treated with bisphosphonates - histomorphologic analysis in comparison with infected osteoradionecrosis. *J Oral Pathol Med* **35**(3):155-60.
 21. Li D, Gromov K, Soballe K, Puzas JE, O'Keefe RJ, Awad H, Drissi H, Schwarz EM 2008 Quantitative mouse model of implant-associated osteomyelitis and the kinetics of microbial growth, osteolysis, and humoral immunity. *J Orthop Res* **26**(1):96-105.
 22. Francis KP, Joh D, Bellinger-Kawahara C, Hawkinson MJ, Purchio TF, Contag PR 2000 Monitoring bioluminescent *Staphylococcus aureus* infections in living mice using a novel luxABCDE construct. *Infect Immun* **68**(6):3594-600.

23. Rodan GA, Martin TJ 2000 Therapeutic approaches to bone diseases. *Science* **289**(5484):1508-14.
24. Teitelbaum SL 2007 Osteoclasts: what do they do and how do they do it? *Am J Pathol* **170**(2):427-35.
25. Koefoed M, Ito H, Gromov K, Reynolds DG, Awad HA, Rubery PT, Ulrich-Vinther M, Soballe K, Guldberg RE, Lin AS, O'Keefe R J, Zhang X, Schwarz EM 2005 Biological Effects of rAAV-caAlk2 Coating on Structural Allograft healing. *Mol Ther* **12**(2):212-8.
26. Zhang X, Xie C, Lin AS, Ito H, Awad H, Lieberman JR, Rubery PT, Schwarz EM, O'Keefe R J, Guldberg RE 2005 Periosteal progenitor cell fate in segmental cortical bone graft transplantations: implications for functional tissue engineering. *J Bone Miner Res* **20**(12):2124-37.
27. Hildebrand KA, Deie M, Allen CR, Smith DW, Georgescu HI, Evans CH, Robbins PD, Woo SL 1999 Early expression of marker genes in the rabbit medial collateral and anterior cruciate ligaments: the use of different viral vectors and the effects of injury. *J Orthop Res* **17**(1):37-42.
28. Hildebrand T, Laib A, Muller R, Dequeker J, Ruegsegger P 1999 Direct three-dimensional morphometric analysis of human cancellous bone: microstructural data from spine, femur, iliac crest, and calcaneus. *J Bone Miner Res* **14**(7):1167-74.
29. Muschler GF, Midura RJ 2002 Connective tissue progenitors: practical concepts for clinical applications. *Clin Orthop* (395):66-80.
30. Proulx ST, Kwok E, You Z, Papuga MO, Beck CA, Shealy DJ, Ritchlin CT, Awad HA, Boyce BF, Xing L, Schwarz EM 2007 Longitudinal assessment of synovial, lymph node, and bone volumes in inflammatory arthritis in mice by in vivo magnetic resonance imaging and microfocal computed tomography. *Arthritis Rheum* **56**(12):4024-4037.
31. Proulx ST, Kwok E, You Z, Beck CA, Shealy DJ, Ritchlin CT, Boyce BF, Xing L, Schwarz EM 2007 MRI and Quantification of Draining Lymph Node Function in Inflammatory Arthritis. *Ann N Y Acad Sci*.
32. Ito H, Koefoed M, Tiyapatanaputi P, Gromov K, Goater JJ, Carmouche J, Zhang X, Rubery PT, Rabinowitz J, Samulski RJ, Nakamura T, Soballe K, O'Keefe R J, Boyce BF, Schwarz EM 2005 Remodeling of cortical bone allografts mediated by adherent rAAV-RANKL and VEGF gene therapy. *Nat Med* **11**(3):291-297.
33. Gortz B, Hayer S, Redlich K, Zwerina J, Tohidast-Akrad M, Tuerk B,

- Hartmann C, Kollias G, Steiner G, Smolen JS, Schett G 2004 Arthritis induces lymphocytic bone marrow inflammation and endosteal bone formation. *J Bone Miner Res* **19**(6):990-8.
34. Schwarz EM, Benz EB, Lu AL, Goater JJ, Mollano AV, Rosier RN, Puzas JE, O'Keefe RJ 2000 A Quantitative Small Animal Surrogate To Evaluate Drug Efficacy in Preventing Wear Debris-Induced Osteolysis. *J. Ortho. Res.* **18**:849-855.
35. Hein I, Lehner A, Rieck P, Klein K, Brandl E, Wagner M 2001 Comparison of different approaches to quantify *Staphylococcus aureus* cells by real-time quantitative PCR and application of this technique for examination of cheese. *Appl Environ Microbiol* **67**(7):3122-6.
36. Li P, Schwarz EM, O'Keefe RJ, Ma L, Looney RJ, Ritchlin CT, Boyce BF, Xing L 2004 Systemic tumor necrosis factor alpha mediates an increase in peripheral CD11b^{high} osteoclast precursors in tumor necrosis factor alpha-transgenic mice. *Arthritis Rheum* **50**(1):265-76.
37. Flynn JL, Goldstein MM, Chan J, Triebold KJ, Pfeffer K, Lowenstein CJ, Schreiber R, Mak TW, Bloom BR 1995 Tumor necrosis factor-alpha is required in the protective immune response against *Mycobacterium tuberculosis* in mice. *Immunity* **2**(6):561-72.
38. Dougall WC, Glaccum M, Charrier K, Rohrbach K, Brasel K, De Smedt T, Daro E, Smith J, Tometsko ME, Maliszewski CR, Armstrong A, Shen V, Bain S, Cosman D, Anderson D, Morrissey PJ, Peschon JJ, Schuh J 1999 RANK is essential for osteoclast and lymph node development. *Genes Dev* **13**(18):2412-24.
39. Kong YY, Yoshida H, Sarosi I, Tan HL, Timms E, Capparelli C, Morony S, Oliveira-dos-Santos AJ, Van G, Itie A, Khoo W, Wakeham A, Dunstan CR, Lacey DL, Mak TW, Boyle WJ, Penninger JM 1999 OPGL is a key regulator of osteoclastogenesis, lymphocyte development and lymph-node organogenesis. *Nature* **397**(6717):315-23.
40. Anderson DM, Maraskovsky E, Billingsley WL, Dougall WC, Tometsko ME, Roux ER, Teepe MC, DuBose RF, Cosman D, Galibert L 1997 A homologue of the TNF receptor and its ligand enhance T-cell growth and dendritic-cell function. *Nature* **390**(6656):175-9.
41. Bachmann MF, Wong BR, Josien R, Steinman RM, Oxenius A, Choi Y 1999 TRANCE, a tumor necrosis factor family member critical for

- CD40 ligand-independent T helper cell activation. *J Exp Med* **189**(7):1025-31.
42. Stolina M, Guo J, Faggioni R, Brown H, Senaldi G 2003 Regulatory effects of osteoprotegerin on cellular and humoral immune responses. *Clin Immunol* **109**(3):347-54.
 43. Sobacchi C, Frattini A, Guerrini MM, Abinun M, Pangrazio A, Susani L, Bredius R, Mancini G, Cant A, Bishop N, Grabowski P, Del Fattore A, Messina C, Errigo G, Coxon FP, Scott DI, Teti A, Rogers MJ, Vezzoni P, Villa A, Helfrich MH 2007 Osteoclast-poor human osteopetrosis due to mutations in the gene encoding RANKL. *Nat Genet* **39**(8):960-2.
 44. Schwarz EM, Ritchlin CT 2007 Clinical development of anti-RANKL therapy. *Arthritis Res Ther* **9 Suppl 1**:S7.
 45. Hamner JB, Fleming MD 2007 Lymphedema therapy reduces the volume of edema and pain in patients with breast cancer. *Ann Surg Oncol* **14**(6):1904-8.

FIGURE LEGENDS

Figure 1. Anti-resorptive drugs increase the amount of necrotic bone around the infected implant during the establishment of OM. Mice (n=5) received a Xen29 infected transtibial pin and were treated with Gent, PBS, OPG, Aln and TNFR:Fc as indicated. Representative x-rays of the infected tibiae on day 18 are shown (a-e). Of note are the remarkable soft tissue abscesses around the pin in the OPG, Aln and TNFR:Fc treatment groups (arrows). Representative TRAP stained histology of the medial cortex of the infected tibiae are shown at 10x magnification (f-j) to demonstrate the remark differences in the amount of necrotic bone between the Gent, PBS and TNFR:Fc groups (arrows) and the OPG and Aln groups (brackets). These sections are also presented at 20x (k-o) to better illustrate differences in osteoclast numbers, which are presented as means \pm SD (# $p < 0.05$ vs. Gent; * $p < 0.05$ vs. PBS; + $p < 0.05$ vs. OPG). Also of note is the large region of necrotic bone (void of osteocytes) adjacent to the live cortical bone in the OPG and Aln groups (m-n), while there is essentially no necrotic cortical bone adjacent to the infected pin in the other groups (k, l, o). Parallel sections were Gram stained and the necrotic bone fragments (arrows in f, g, j) or necrotic cortex (brackets in h-i) were photographed at 40x magnification (p-t) to demonstrate the absence or presence (arrows) of biofilm.

Figure 2. Anti-resorptive drugs increase the incidence of high-grade infections during the establishment of OM. Mice received a Xen29 infected transtibial pin and were treated with PBS, Gent, OPG, Aln and TNFR:Fc as indicated. The BLI signal of each mouse on day 7 (a), day 11 (b) and day 18 (c) post-infection is presented. To assess

the drug effects on the incidence of “infections” and “high-grade infections”, thresholds were defined by the greatest BLI value of the Gent group (blue region), and the greatest BLI value of the PBS group (yellow region) respectively. Thus, BLI values greater than the maximum threshold of the PBS group are regarded as high-grade infections (orange region). Mice were sacrificed on day 7 (d) or day 18 (e), and total DNA was extracted from the implanted tibia for *nuc*/ β -*actin* RTQ-PCR as described in Methods. The data for each mouse is presented as the number of *nuc* genes per tibia standardized to a mouse β -*actin* control. Data for the Gent group are not included because *nuc* levels were undetectable. To assess the drug effects on bacterial load, a threshold was defined by the greatest *nuc* gene value of the PBS group, which distinguishes infections (yellow region) from high-grade infections (orange region). A Fisher’s exact test was performed to assess the significance of the high-grade infections. A linear regression analysis was performed with all of the day 18 data to assess the relationship between BLI vs. *nuc* (f), and significance was determined using Pearson’s correlation coefficient and a two-sided *t*-test.

Figure 3. Anti-resorptive drug inhibition of cortical bone loss reveals that OM-induced osteolysis is due to osteoclastic activity and regional suppression of periosteal bone formation. Micro-CT scans of all of the tibiae described in Figure 1 were obtained before histology, and representative medial views of 3D reconstructed images from each group are shown (a). Note the massive osteolysis in the PBS and TNFR:Fc controls, contrasted by its absence in the Gent control. Remarkably, both Aln and OPG prevented cortical bone loss, but did not prevent the OM inhibition of reactive

bone formation around the infected pin, as evidence by the ~2mm diameter ring of exposed cortical bone centered on the pinhole. The maximum osteolysis area of the original cortex of the tibiae, and the area of the void of reactive bone around the implant were determined from 2D images as described in Methods (**b**). The data are presented as the mean \pm SD (* $p < 0.05$ vs. PBS).

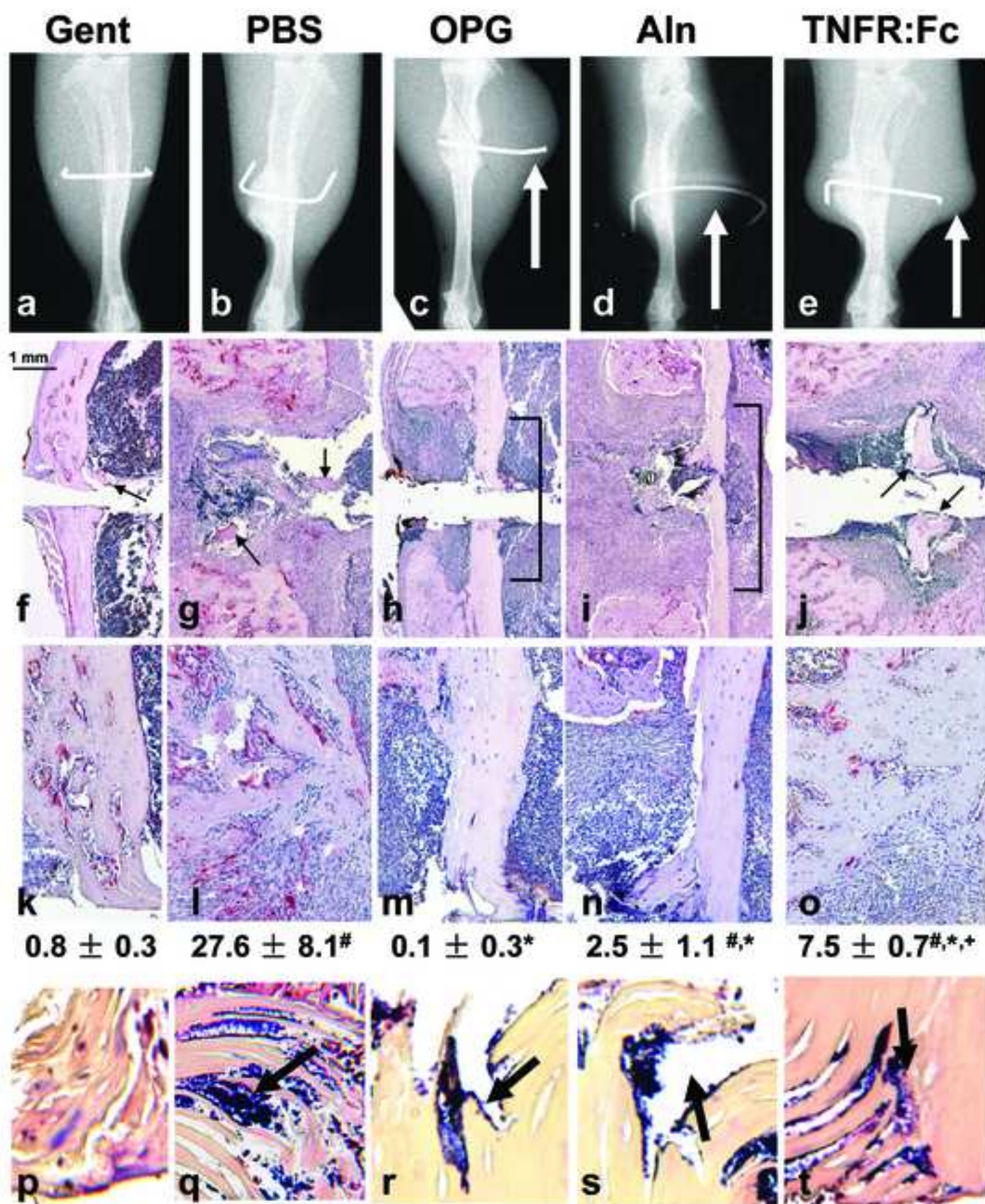
Figure 4. Anti-resorptive drugs do not affect vascularity during the establishment of implant-associated OM. Mice (n=5) received a Xen29 infected transtibial pin and were given the indicated treatments as described in Figure 1. On day 18 the mice were perfused with lead chromate and their tibiae were harvested for vascular micro-CT analyses. Representative 3D reconstructed images from each group are shown (**a**). The light gray highlighted section of undecalcified images (left) indicates the ROI, which was defined by a 2mm³ cube centered on the pin tract. The tibiae were rescanned after demineralization (center) and the vessels outside the tibiae (yellow vessels) were isolated from the vessels inside the bone (red vessels). The perfused vessels inside the bone (right) were used to quantify total vascular volume (Vasc. Vol.), number of vessels (Ves.N.), vessel thickness (Ves.Th.), vessel spacing (Ves.Sp.), and degree of anisotropy as described in Methods (**b**). No remarkable differences between groups were observed.

Figure 5. Anti-resorptive drugs are not immunosuppressive. Blood was obtained from the mice described in Figure 1 on day 18 post-surgery, and total Ig levels in the sera were determined by ELISA as described in Methods. The data from a representative mouse from each treatment group are presented as the mean of quadruplicates \pm SD (**a**).

No remarkable serologic differences between groups were observed. Photographs of Gram stained histology of an infected mouse treated with Aln taken at 10x (**b**) and 20x (**c-d**) demonstrate that biofilms are only found in necrotic bone (**c**), and that granuloma form adjacent to the pin tract (**d**) in these animals. A photograph of a parallel section of the center of the granuloma stained with H&E is shown at 20x (**e**). Photographs of Gram stained histology of an infected mouse treated with TNFR:Fc taken at 10x (**f**) and 20x (**g-h**) demonstrate that biofilms are found in both necrotic bone (**g**), and the soft tissue adjacent to the pin tract (**h**) in these animals. No granulomas were found in any of the TNFR:Fc treated mice. A photograph of a parallel section of the soft tissue containing biofilm stained with H&E is shown at 20x (**i**).

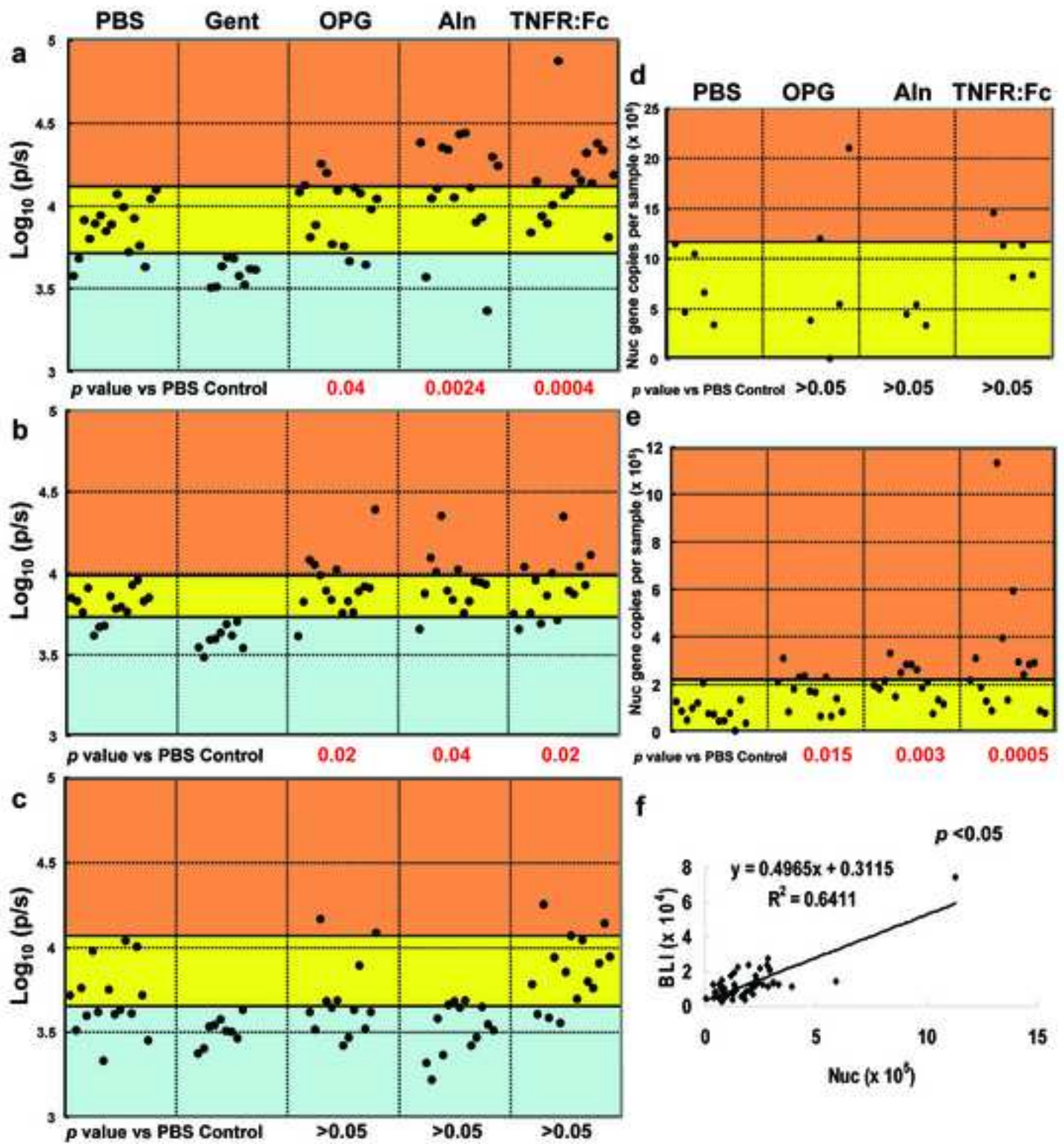
Figure 6. Anti-resorptive drugs inhibit draining lymph node expansion during the establishment of OM. Mice (n=5) received a Xen29 infected transtibial pin and were given the indicated treatments as described in Figure 1. On day 9 the mice received an *in vivo* knee MRI scan of their infected leg (**a**), and representative primary 2D (top) and reconstructed 3D images of the PLN are shown. The calculated volumes of the PLN are presented as the mean \pm SD (* $p < 0.05$ vs. PBS). Photographs of representative infected legs from these mice (**b**) demonstrate remarkable amounts of pus draining out of the tibiae of PBS and TNFR:Fc treated mice (arrows), which was not observed in the tibiae of OPG and Aln treated animals. The PLN from the infected and contralateral leg of these mice are also shown to demonstrate their remarkable differences in size. The PLN from all of the mice were weighed to quantify the differences in size, and the data are presented as the mean \pm SD (* $p < 0.05$ vs. PBS).

Figure
[Click here to download high resolution image](#)



Figure

[Click here to download high resolution image](#)



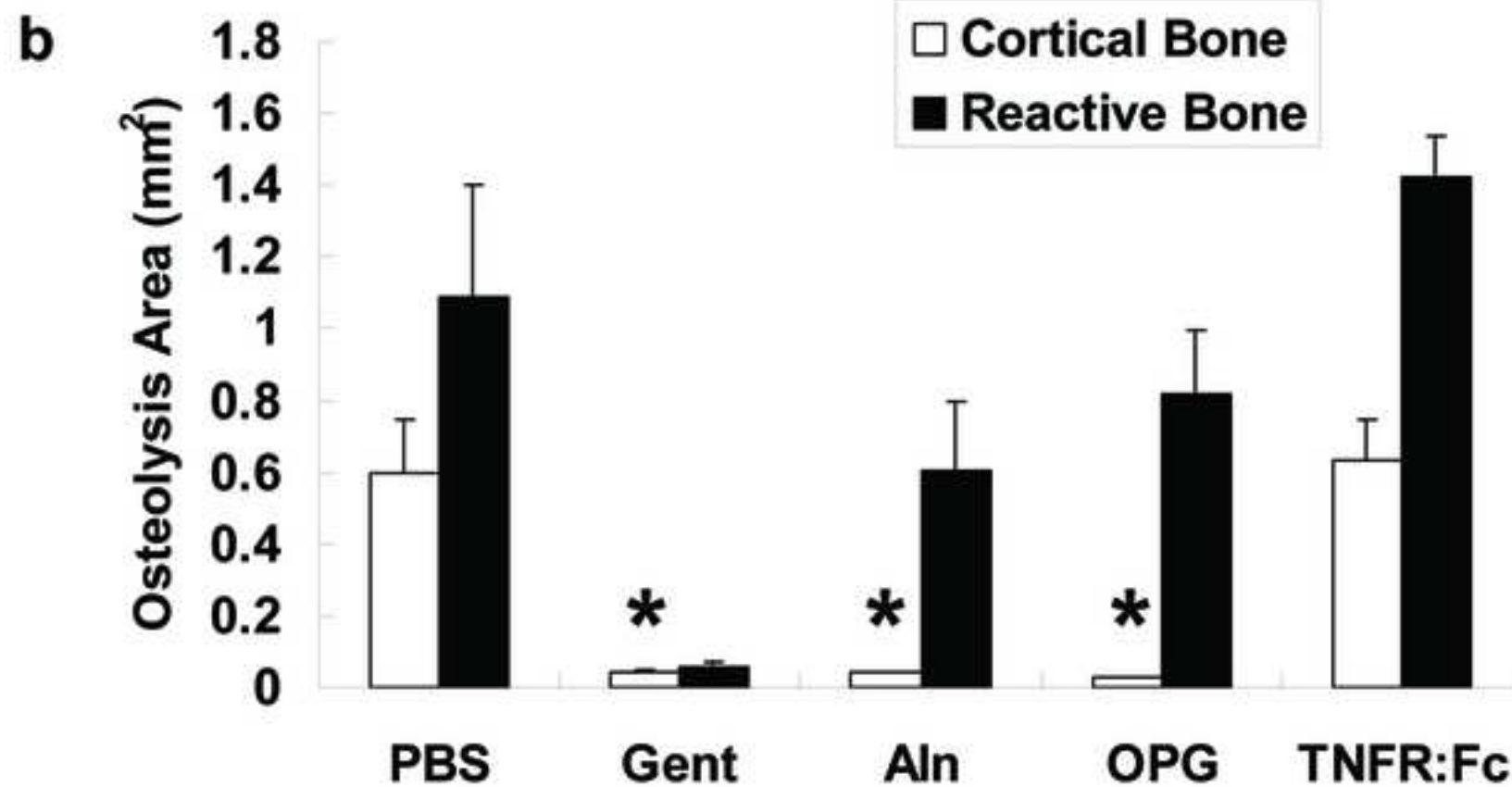
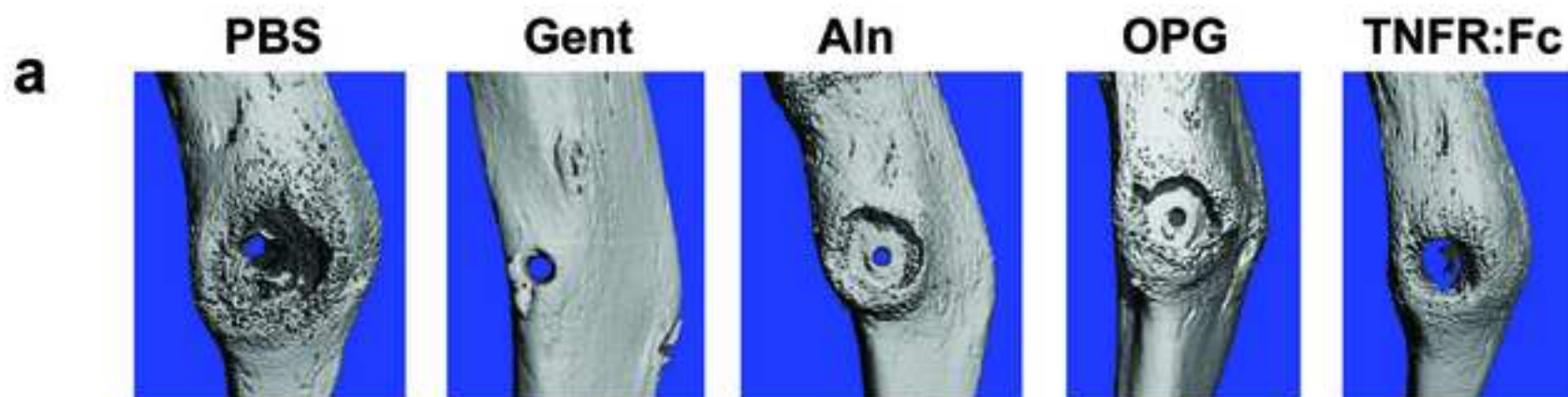


Figure
[Click here to download high resolution image](#)

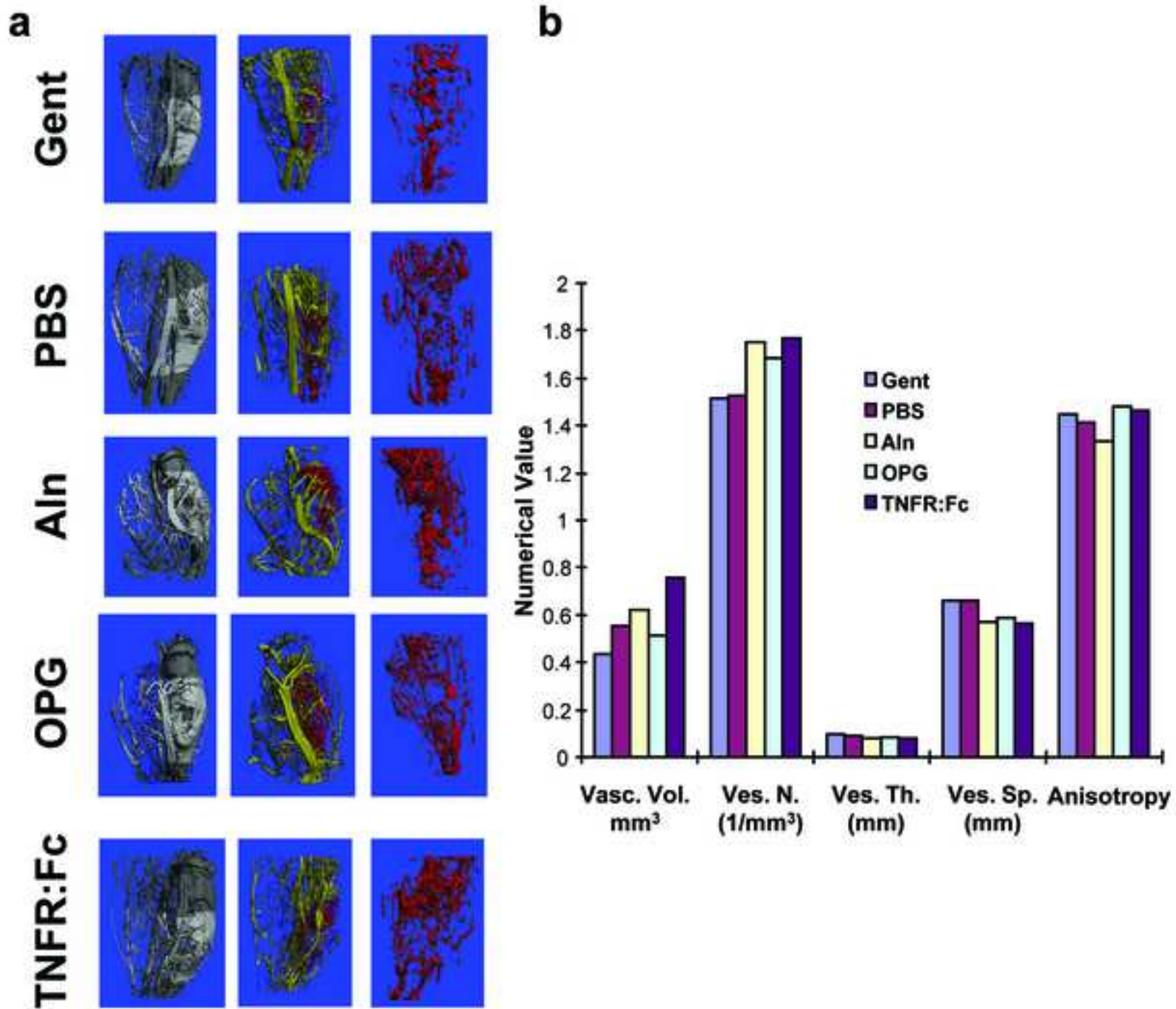
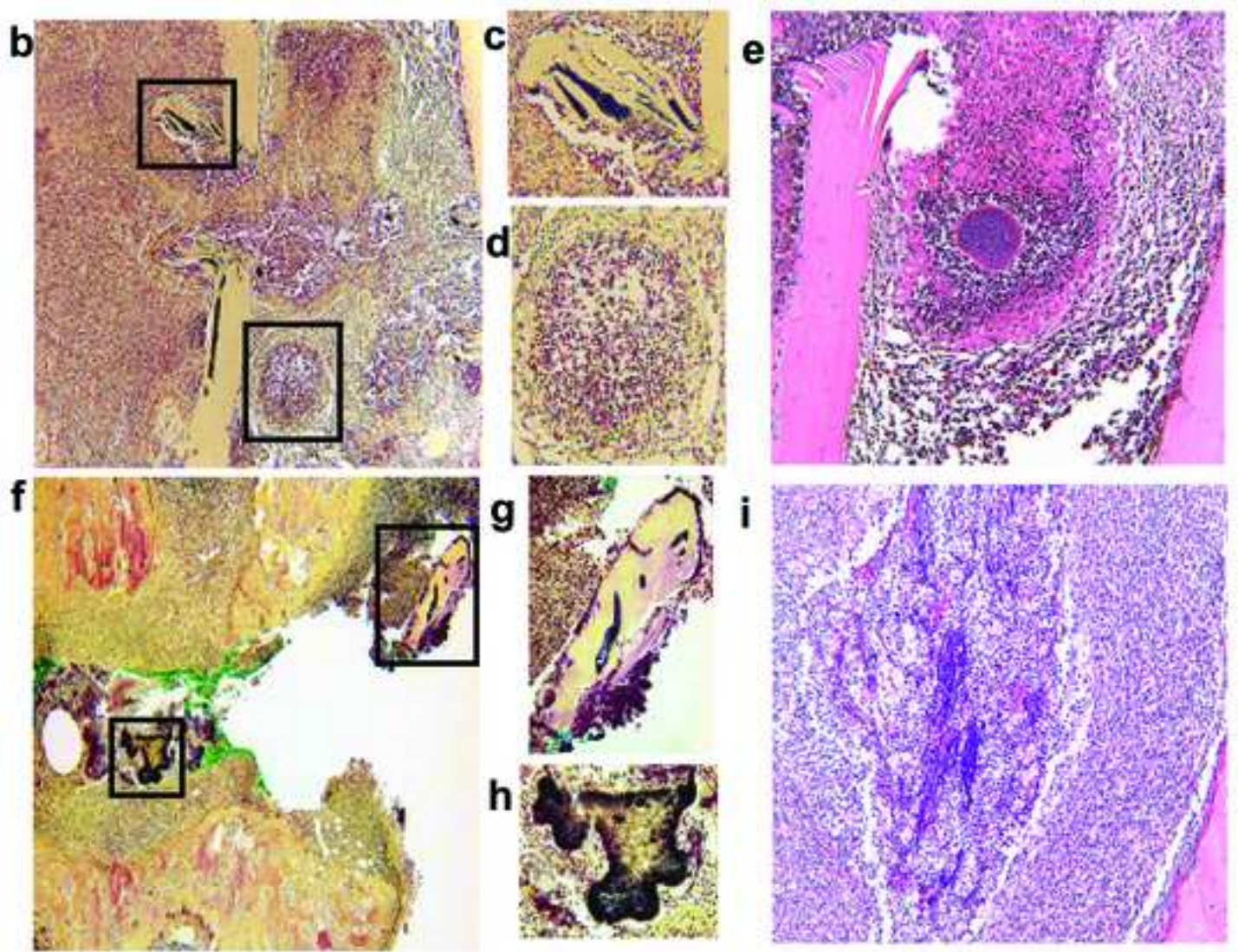
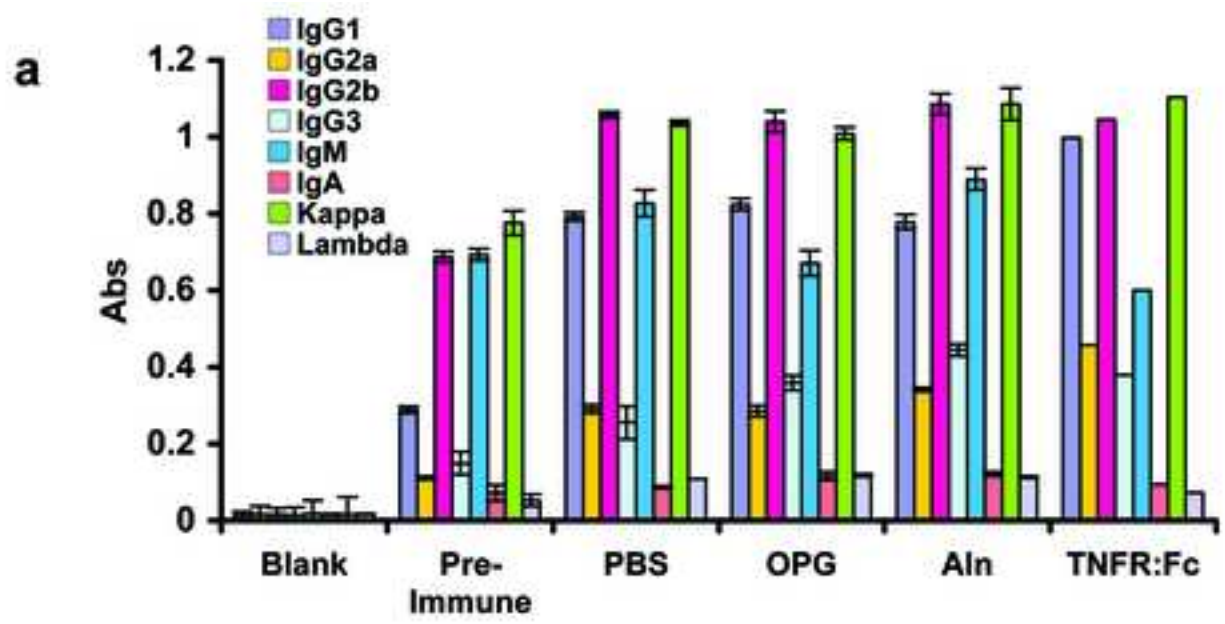
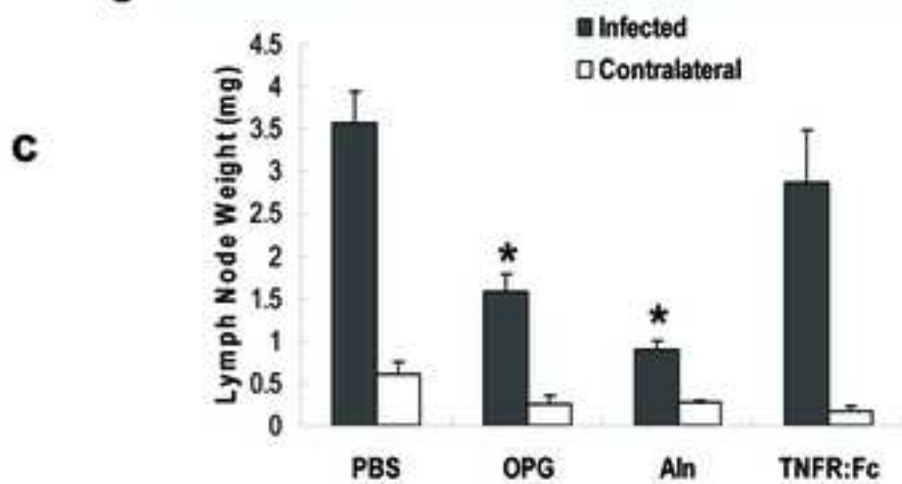
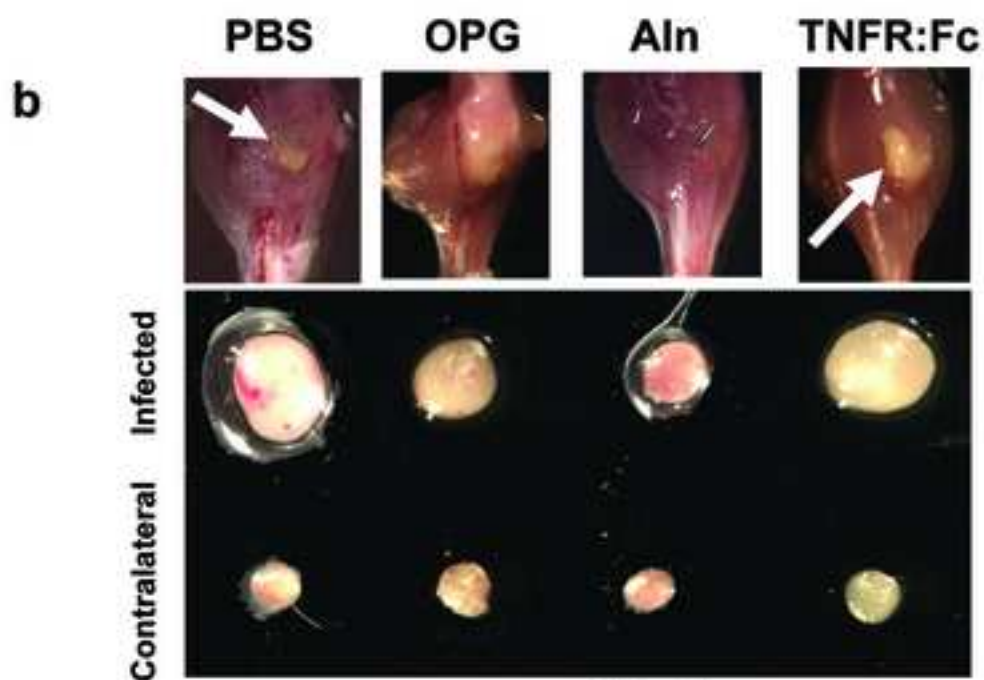
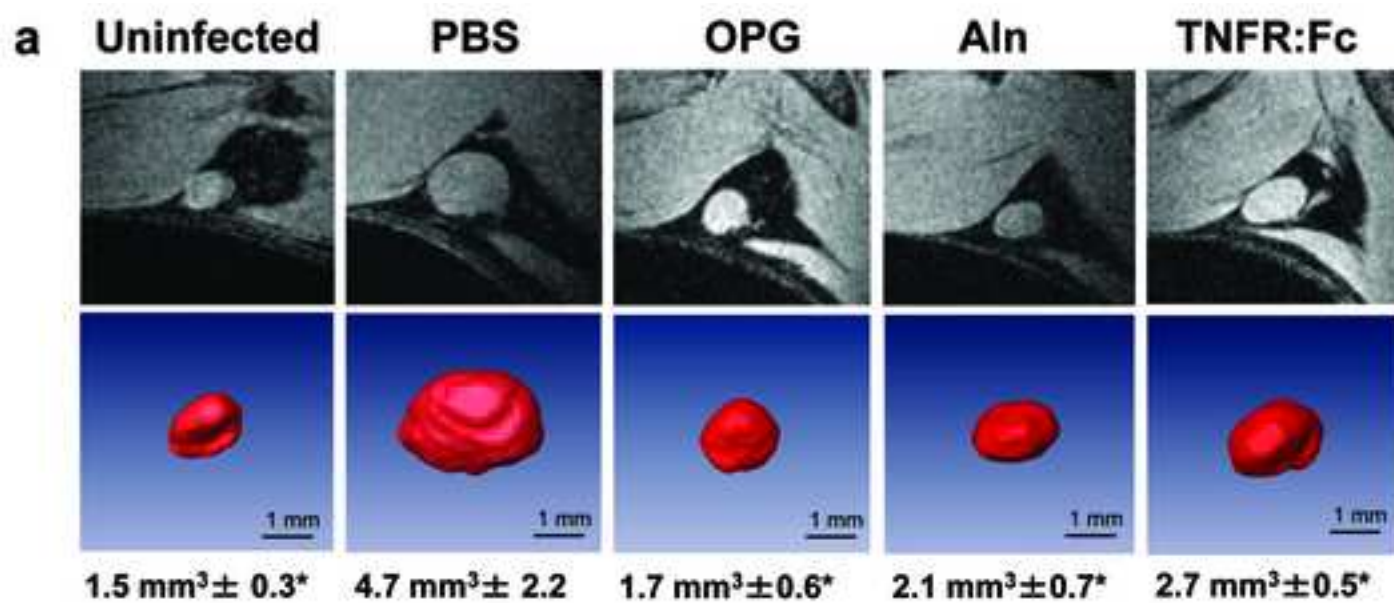


Figure
[Click here to download high resolution image](#)





Appendix III

Efficacy of Colistin-Impregnated Beads to Prevent Multidrug-Resistant *A. baumannii* Implant-Associated Osteomyelitis

Daniel P. Crane,^{1*} Kirill Gromov,^{1,2*} Dan Li,¹ Kjeld Søballe,² Christian Wahnes,³ Hubert Büchner,³ Matthew J. Hilton,¹ Regis J. O'Keefe,¹ Clinton K. Murray,⁴ Edward M. Schwarz¹

¹The Center for Musculoskeletal Research, University of Rochester Medical Center, 601 Elmwood Avenue, Box 665, Rochester, New York 14642, ²The Department of Orthopedics, Aarhus University Hospital, Aarhus, Denmark, ³Research & Development, Heraeus Medical GmbH, Wehrheim, Germany, ⁴Infectious Disease Service, Department of Medicine, Brooke Army Medical Center, Fort Sam Houston, San Antonio, Texas

Received 14 August 2008; accepted 11 December 2008

Published online in Wiley InterScience (www.interscience.wiley.com). DOI 10.1002/jor.20847

ABSTRACT: Osteomyelitis (OM) from multidrug-resistant (MDR) *Acinetobacter* has emerged in >30% of combat-related injuries in Iraq and Afghanistan. While most of these strains are sensitive to colistin, the drug is not available in bone void fillers for local high-dose delivery. To address this, we developed a mouse model with MDR strains isolated from wounded military personnel. In contrast to *S. aureus* OM, which is osteolytic and characterized by biofilm in necrotic bone, *A. baumannii* OM results in blastic lesions that do not contain apparent biofilm. We also found that mice mount a specific IgG response against three proteins (40, 47, and 56 kDa) regardless of the strain used, suggesting that these may be immuno-dominant antigens. PCR for the *A. baumannii*-specific *parC* gene confirmed a 100% infection rate with 75% of the MDR strains, and in vitro testing confirmed that all strains were sensitive to colistin. We also developed a real-time quantitative PCR (RTQ-PCR) assay that could detect as few as 10 copies of *parC* in a sample. To demonstrate the efficacy of colistin prophylaxis in this model, mice were treated with either parenteral colistin (0.2 mg colistin/methate i.m. for 7 days), local colistin (PMMA bead impregnated with 1.0 mg colistin sulfate), or an unloaded PMMA bead control. While the parenteral colistin failed to demonstrate any significant effects versus the placebo, the colistin PMMA bead significantly reduced the infection rate such that only 29.2% of the mice had detectable levels of *parC* at 19 days ($p < 0.05$ vs. i.m. colistin and placebo). © 2009 Orthopaedic Research Society. Published by Wiley Periodicals, Inc. [†]J Orthop Res

Keywords: multidrug resistant; *Acinetobacter baumannii*; osteomyelitis; colistin

It has been well established, from current combat-related injuries during US military operations in Iraq and Afghanistan, that the ratio of serious injuries to fatal casualties exceeds that of previous conflicts.¹ Orthopedic trauma comprises the vast majority of these war wounds, as 70% of casualties involve the musculoskeletal system, 26% are fractures, and 82% of the fractures are open.^{2–5} Thus, it is not surprising that the incidence of osteomyelitis (OM) in combat-related extremity injuries is between 2% to 15%, and is of great concern.^{6–8} Most alarming is the incidence of infections caused by multidrug-resistant (MDR) *Acinetobacter* species, which can be difficult to cure in some settings.^{9–11} Surprisingly, this pathogen has been reported in less than 2% of nosocomial infections within the United States, but has emerged in over 30% of admitted deployed soldiers.¹⁰

In contrast to *Staphylococcus*, which is responsible for >80% of OM infections,¹² *Acinetobacter baumannii-calcoaceticus* complex (ABC) are Gram-negative, non-fermentative, non-spore forming, strictly aerobic, oxidase-negative coccobacillary organisms. Additionally, infections caused by *Acinetobacter* appear to be hospital-acquired and not from an initial colonization of the injury.¹³ Thus, one critical question involving *Acineto-*

bacter is whether or not they can produce osteolytic OM on their own, or if they are only present in superinfections with other microorganisms. Another important question is whether or not the MDR *Acinetobacter* OM can be effectively prevented with parenteral or local antibiotic therapy at the time of initial surgery. In support of this, a clinical study has demonstrated that most MDR *Acinetobacter* strains are sensitive to colistin,¹⁰ and that colistin heteroresistance primarily occurs in patients treated with colistin.¹⁴ Thus, we aimed to test the hypotheses that: (i) pure clinical isolates of MDR *Acinetobacter* can induce implant-associated OM, and (ii) prophylactic colistin prevents these orthopedic infections. To this end, we utilized a quantitative murine model of implant-associated OM, originally developed for *S. aureus*,¹⁵ in which an insect pin is innoculated with cultured bacteria and transcortically implanted through the tibia metaphysis. Given the well-established use of antibiotic-impregnated bone cement to deliver high doses of drug locally,^{16–18} we have developed colistin sulfate-impregnated polymethylmethacrylate (PMMA) beads, since high-dose parenteral administration of colistin is limited by nephrotoxicity and neurotoxicity.¹⁹ With this system, here we provide the first evidence that *A. baumannii* can induce OM in the absence of other pathogens, however these lesions are blastic rather than osteolytic and do not contain apparent biofilms in necrotic bone. Moreover, local but not parenteral pharmacological doses of colistin are capable of preventing the establishment of MDR *Acinetobacter* implant-associated OM.

METHODS

Bacterial Strains

Four clinical isolates of *Acinetobacter baumannii* with confirmed resistance to amikacin, ampicillin, aztraeonam,

Disclaimer: The opinions or assertions contained herein are the private views of the authors and are not to be construed as official or reflecting the views of the Department of the Army, Department of Defense, or the US government. This work was prepared as part of their official duties.

*These authors contributed equally to this work.

Correspondence to: Edward M. Schwarz (T: 585-275-3063; F: 585-756-4727; E-mail: Edward_Schwarz@URMC.Rochester.edu)

© 2009 Orthopaedic Research Society. Published by Wiley Periodicals, Inc.

[†]This article is a US Government work and, as such, is in the public domain in the United States of America.

ceftriaxone, ciprofloxacin, gentamicin, imipenem, tobramycin, and vancomycin were obtained from wounded soldiers treated at the Brooke Army Medical Center at Fort Sam Houston, San Antonio, TX, under Institutional Review Board-approved protocols. Bacterial strains were grown overnight at 250 rpm and 37°C in Tryptic Soy broth (Sigma-Aldrich, St. Louis, MO). Strain sensitivity to colistin was determined by streaking overnight cultures on Tryptic Soy agar plates containing 10 µg/ml of colistinmethate (Paddock Laboratories, Inc, Minneapolis, MN).

DNA Extraction, PCR Cloning of *parC* and RTQ-PCR of *Acinetobacter* DNA

DNA was extracted from all four strains using a DNeasy Blood and Tissue Kit (Qiagen, Valencia, CA). DNA primers (forward 5'-AAAAATCAGCGGTACAGTG-3' and reverse 5'-CGA-GAGTTTGGCTTCGGTAT-3') specific for the *Acinetobacter* topoisomerase gene *parC*, were used for PCR and RTQ-PCR as previously described.²⁰ To confirm the purity of the clinical isolates, five individual colonies from each strain were isolated and the *parC* gene was amplified and sequenced using an i-cycle PCR machine (Bio-Rad, Hercules, CA). The amplification protocol was as follows: 95°C pre-melt for 15 min followed by 40 cycles of 95°C for 30 s, 54°C for 30 s, and 72°C for 30 s. To generate a standard curve for RTQ-PCR, the 196 bp *parC* fragment was cloned into the pTOPO2.1 cloning vector (Invitrogen, Carlsbad, CA), and 10-fold serial dilutions were used to perform Syber Green (Thermo Scientific VWR, Darmstadt, Germany) RTQ-PCR (Corbett Research, Sydney, Australia). A similar curve was generated using the mouse *β-actin* primers (forward 5'-AGATGTGAATCAGCAAGCAG-3' and reverse 5'-GCGCAAG-TTAGGTTTTGTCA-3'), to control for sample integrity as we have previously described.¹⁵ In order to calculate the *parC* gene copies in a tibia sample, we first generated a standard curve with *A. baumannii* genomic DNA purified directly from an overnight culture. The standard curve was generated with 10-fold dilutions of the TOPO plasmid with *parC* insert. The mean of the three Ct (cycle threshold) values from each tibia sample were then plotted against this curve to extrapolate the number of *parC* genes ($n = 24$ mice/treatment group). This number was then normalized to *β-actin* and the data are presented as normalized *parC* gene copies per sample.

Colistin In Vitro Release Kinetics

PMMA beads (Heraeus Medical GmbH, Wehrheim, Germany) were impregnated with 1.0 mg or 2.0 mg colistin sulfate (Alpharma, Copenhagen, Denmark). To assess the release kinetics of the colistin following rehydration, the beads were introduced into capped vials and totally covered with 10 mL of MilliQ water, Waltham, MA. Extraction was carried out at 37°C, and the water was exchanged every 24 h. The concentration of released colistin sulfate in the extracts was determined by conductometric measurements with a WTW platinated platinum electrode LTA 1 at 25°C. Temperature fluctuations were compensated using a WTW TFK 530 temperature electrode (WTW GmbH, Weilheim, Germany) in parallel to the conductive electrode. A calibration curve with 40 points ($R^2 = 0.999$) at concentrations between 0 and 20 g/L was recorded to calculate concentrations. All of the measured concentrations were within this range. Placebo beads were used as control, and the conductive values of the placebo beads were subtracted from detected signals before calculating colistin concentrations.

Surgery and Antibiotic Treatments

All animal studies were performed under University of Rochester Committee for Animal Resources-approved protocols. The implant-induced OM surgeries were performed on 6–8-week-old C57Bl/6 female mice as previously described.¹⁵ Briefly, mice were anesthetized with ketamine (100 mg/kg) and xylazine (10 mg/kg), shaved, and the skin was cleansed with 70% ethanol. A small incision was made in the skin on the medial side of the left leg to expose the tibial metaphysis. OM was induced via transcortical insertion of a 0.25-mm insect pin (Fine Science Tools, Foster City, CA) that was dipped into an overnight culture of *A. baumannii* or *S. aureus* (Xen29), which contaminated the pin with $\sim 2.5 \times 10^5$ colony forming units (CFU) as determined by vortexing the inoculated pins in PBS and plating out the contents on agar. For prophylactic treatment, mice ($n = 24$) received either: (1) a control PMMA bead lacking antibiotic, (2) a PMMA bead impregnated with 1.0 mg colistin sulfate, or (3) intramuscular (i.m.) injection of 0.2 mg (~ 10 mg/kg) of colistinmethate every day for 7 days, as previously described in a mouse pneumonia model.²¹ The 5-mm PMMA beads were implanted adjacent to the pin at the time of surgery and were secured with a suture through the skin and muscle. The parenteral colistinmethate was given at the time of surgery and for the next 7 days with no bead. All mice were sacrificed for analysis on day 19.

Radiology

Longitudinal plain film radiographs were obtained using a Faxitron Cabinet X-ray system (Faxitron, Wheeling, IL) as we have previously described.²² Micro-computed tomography (μ CT) was performed on tibia after sacrifice at high-resolution (10.5 µm) (VivaCT 40; Scanco Medical AG, Basserdorf, Switzerland) to render 3D images as we have previously described.²³

Histologic Evaluation of OM

After μ CT, the tibial samples were processed for decalcified histology and stained with hematoxylin and eosin (H&E), or Gram-stained as we have described previously.²⁴

Serology

The generation of specific antibodies against *A. baumannii* proteins during the establishment of chronic OM was determined by Western blotting as previously described.¹⁵ Briefly, total protein extract was obtained from a 100 mL culture of *A. baumannii*, strains BAMC 2, BAMC 3, and BAMC 4, using the Complete Bacterial Proteome Extraction Kit (Calbiochem, San Diego, CA). Twenty micrograms of total *A. baumannii* protein per well was boiled in Laemmli loading buffer and separated in NuPAGE™ 10% Bis-Tris SDS Gels (Invitrogen, Carlsbad, CA) by electrophoresis, and transferred to a PVDF membrane (Millipore, Billerica, MA). The membrane was then cut into single lanes and blocked with PBS, 0.1% Tween 20 (PBST), and 5% non-fat dry milk for 1 h at room temperature. Afterwards, each lane was incubated with a unique serum [10 µl serum in 5 ml of blocking buffer (PBST + 5% non-fat dry milk)] as the primary antibody, washed three times in 0.1% PBST, and then the strips were pooled and incubated with 1.5 µl HRP-conjugated goat anti-mouse IgG antibody (BioRad, Hercules, CA). The strips were then washed three times in PBST, 15 min each at room temperature. Finally, the strips were reas-

sembled with the molecular weight marker strip and imaged with ECL+ (GE Healthcare, Princeton, NJ) chemiluminescence autoradiograph.

RESULTS

Murine Model of Implant-Associated MDR *A. baumannii* Osteomyelitis

Having recently established a quantitative transtibial model of OM with *S. aureus*,¹⁵ we aimed to utilize this same approach to develop the first mouse model of *A. baumannii* OM. Thus, we obtained four strains of *A. baumannii* that were isolated from soldiers wounded in the Middle East and screened them for antibiotic resistance. While these isolates displayed variable resistance to the most commonly used antibiotics in orthopedic bone cement (gentamicin, tobramycin, and vancomycin), they were all sensitive to colistin (Fig. 1A). In order to assess the virulence of these strains in our mouse model, stainless steel insect pins were contaminated with an overnight culture of each strain and then surgically implanted into the tibiae of mice. The presence of infection was determined through amplification of the *A. baumannii*-specific *parC* gene. While all of the mice survived these infections, Figure 1B demonstrates the presence of chronic OM in 100% of the mice challenged with strains BAMC2, BAMC3, and BAMC4. Strain BAMC1 failed to establish infection in all of the mice tested and was therefore excluded from further experiments. Further evidence of this infection was demonstrated by the development of *A. baumannii*-specific antibodies in the sera of challenged mice, which appeared around day 11 and recognized three protein antigens 40, 47, and 56 kDa that were conserved in all four strains (Fig. 1C).

Implant-Associated MDR *A. baumannii* Osteomyelitis Is Osteoblastic

One of the salient features of OM is osteolysis around the implant and the presence of biofilm in the adjacent necrotic bone and soft tissue. Thus, we examined the effects of *A. baumannii* OM in our model compared to *S. aureus* and identified several remarkable differences between these bacterial pathogens. Most striking was that in contrast to the osteolytic response to *S. aureus*, *A. baumannii* OM induces a robust osteoblastic bone formation response around the infected pin (Fig. 2A–D). This dramatic difference in the host bone response to the bacteria was also evident in histology sections of the infected area, which confirmed the large osteolytic lesions in *S. aureus* OM filled with inflammatory tissue (Fig. 2E), contrasted by the new woven bone adjacent to the pin tract (Fig. 2F). Examination of Gram-stained sections demonstrated another interesting difference between these pathogens in that *S. aureus* OM is always associated with the presence of biofilm in necrotic bone fragments,²⁵ such as that observed in Figure 2G, whereas we were unable to identify

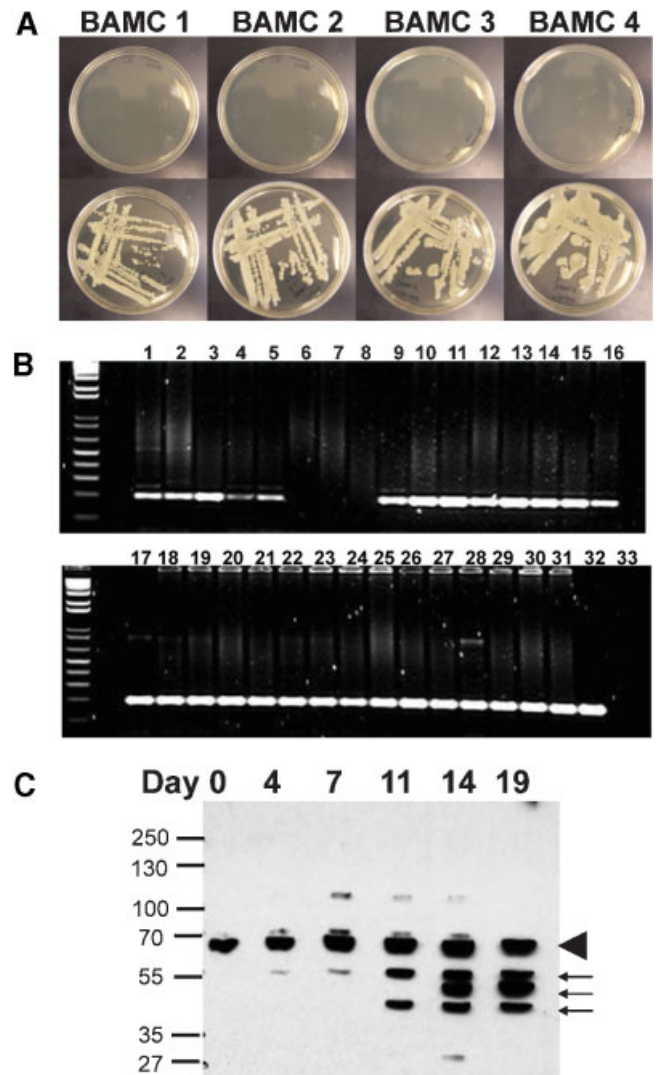


Figure 1. Characterization of MDR *A. baumannii* strains in the murine model of implant-associated osteomyelitis. (A) Four MDR *A. baumannii* clinical isolates were screened for colistin sensitivity by plating on agar medium with (top) and without (bottom) 10 µg/ml of colistinmethate. The absence of bacterial growth confirms that all strains were colistin sensitive. (B) The ability of the clinical isolates to establish chronic OM was evaluated in the murine model as described in Materials and Methods. Mice ($n = 8$) were infected with contaminated pins and their tibiae were harvested on day 19 for *parC* PCR, and the 196 bp product was resolved in a 2% agarose gel stained with ethidium bromide. Lanes 1–8 are from strain BAMC1, lanes 9–15 are from strain BAMC2, lanes 16–23 are from strain BAMC3, lanes 24–31 are from strain BAMC4, lane 32 is the pTOPO-*parC* positive control, and lane 33 is the no template negative control. (C) Mice ($n = 4$) were bled on the indicated day following infection, and their sera were used as the primary antibody in Western blots of total cell extract of the *A. baumannii* strains. A representative autoradiograph is shown demonstrating the presence of nonspecific IgG antibodies that were present in all of the sera (arrowhead) and whose titer did not increase over time, and specific IgG antibodies against *A. baumannii* proteins present in all the strains that initially appeared on day 11 and whose titer increased thereafter in all of the mice tested (arrows).

any biofilm in the necrotic tissue adjacent to the *A. baumannii*-infected pins (Fig. 2H). Although this negative finding is not conclusive, it raises the possibility that *A. baumannii* may persist as an intracellular pathogen in chronic OM.

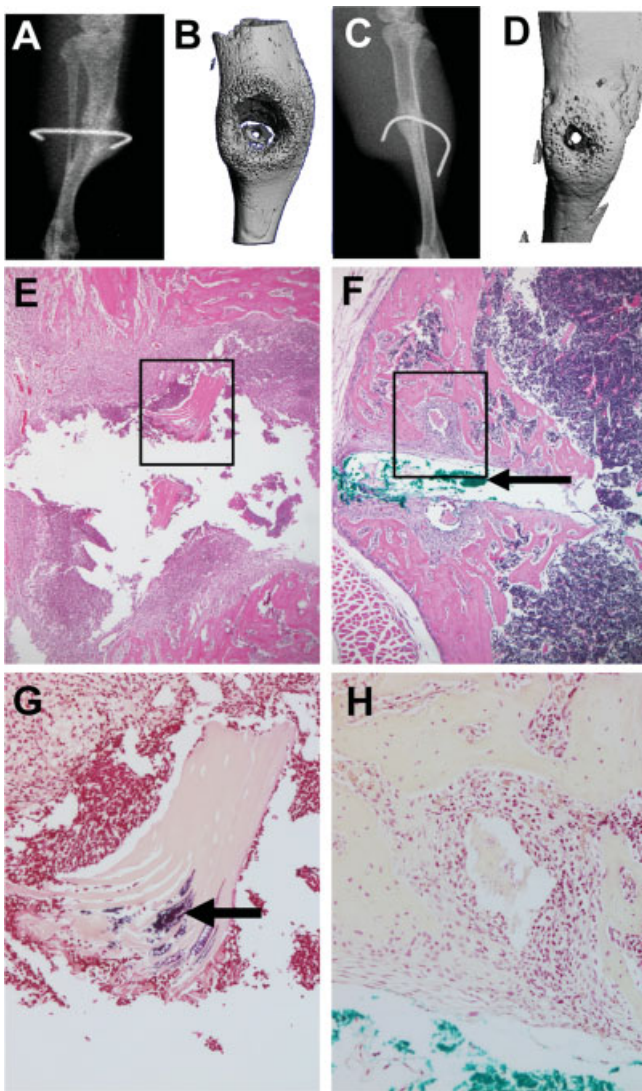


Figure 2. Differential host bone responses to *S. aureus* versus *A. baumannii* infection. Representative radiology (A–D) and histology (E–H) of *S. aureus* (A, B, E, G) and *A. baumannii* (C, D, F, H) OM in the mouse model are shown. Of note is the remarkable osteolysis that is induced by *S. aureus* as evidenced in the radiolucent X-ray (A), lytic lesion in the 3D micro-CT image (B), and the inflammatory tissue surrounding the pin tract in H&E-stained histology at 20× magnification (E). The necrotic bone fragments in these lesions (boxed region in E) were laden with biofilm that could be readily identified in parallel Gram-stained sections at 40× magnification (arrow in G). In contrast, *A. baumannii* OM was characterized by blastic lesions that were radiodense on X-ray (C), and contained copious amounts of new bone around the infected pin (D, F). This made it difficult to identify the pin tract in histology sections, which had to be confirmed by injecting pathology marking ink (Newcomer Supply Inc., Middleton, WI) into the pin hole before processing (arrow in F). Furthermore, Gram staining failed to identify any foreign material in the necrotic bone fragments adjacent to the pin tract (H).

Local Prophylactic Colistin Prevents MDR *A. baumannii* OM

In order to evaluate the efficacy of prophylactic colistin in our model, we first developed a RTQ-PCR assay to assess the in vivo bacterial load. Figure 3 demonstrates the sensitivity and specificity of this assay, which was able to reproducibly detect as few as 10 *parC* copies in infected bone. Since we were interested in assessing the

difference between parenteral and local colistin, we chose to utilize antibiotic-PMMA beads as the carrier. In pilot studies, we found that the 5-mm beads could be readily implanted adjacent to the infected pin (Fig. 4A), while 1-cm beads were too big to be used in this mouse model (Fig. 4B). We then evaluated the in vitro release kinetics of the colistin from the 5-mm beads to ensure an appropriate biodistribution of the drug over time (Fig. 4C). These studies demonstrated that 40%–50% of the loaded colistin sulfate is steadily released into solution from the beads over the first 5 days, which is when the drug would be most effective in killing bacteria initiating the chronic infection. As there were no marked differences between the 1-mg and 2-mg doses in these studies, we moved forward to in vivo challenge experiments with 1.0 mg colistin sulfate-impregnated PMMA beads. BAMC-1 was excluded from this study due to its low virulence as shown in Figure 1B. Following sacrifice on day 19, the bacterial load (Fig. 5A), incidence of infection for all strains (Fig. 5B), and the incidence of infection for each strain (Fig. 5C), was determined by RTQ-PCR. Infection rates were determined to be 75% (18/24), 71% (17/24), and 33% (8/24) for mice receiving a placebo bead, intramuscular colistinmethate injection, or colistin sulfate-impregnated PMMA bead, respectively. While the results failed to demonstrate any significant effects of parenteral colistin versus placebo control, local colistin significantly reduced the incidence of chronic OM versus both placebo and parenteral colistin. Moreover, when we analyzed the strains individually, it was clear that most of the infections in the colistin bead group were caused by BAMC-2, suggesting that this strain may have heteroresistance or may be more virulent than the other strains.

DISCUSSION

Infections caused by MDR pathogens have long been recognized to be a very serious problem in medicine, requiring vigilance when prescribing antibiotic therapy. Most recently, this subject has received tremendous attention, as epidemiology studies seem to indicate that prosthetic infections may be on the rise,^{26,27} and methicillin-resistant *Staphylococcus aureus* (MRSA) has surpassed HIV as the most deadly pathogen in the United States.²⁸ Therefore, the emergence of MDR *Acinetobacter* OM in orthopedic trauma patients was initially proposed to be a situation requiring urgent attention.^{9–11} However, more recent clinical experiences in dealing with this problem suggest that MDR *Acinetobacter* OM can be managed effectively, but may be the predecessor to more serious super-infections including MRSA.^{7,29} Of these orthopedic injuries in veterans of Operation Iraqi Freedom and Operation Enduring Freedom (OIF/OEF), we found that Gram-negative pathogens predominate early, and are replaced with staphylococci after treatment, despite nearly universal use of Gram-positive therapy. More specifically, *Acinetobacter* species were present in 70% of OM

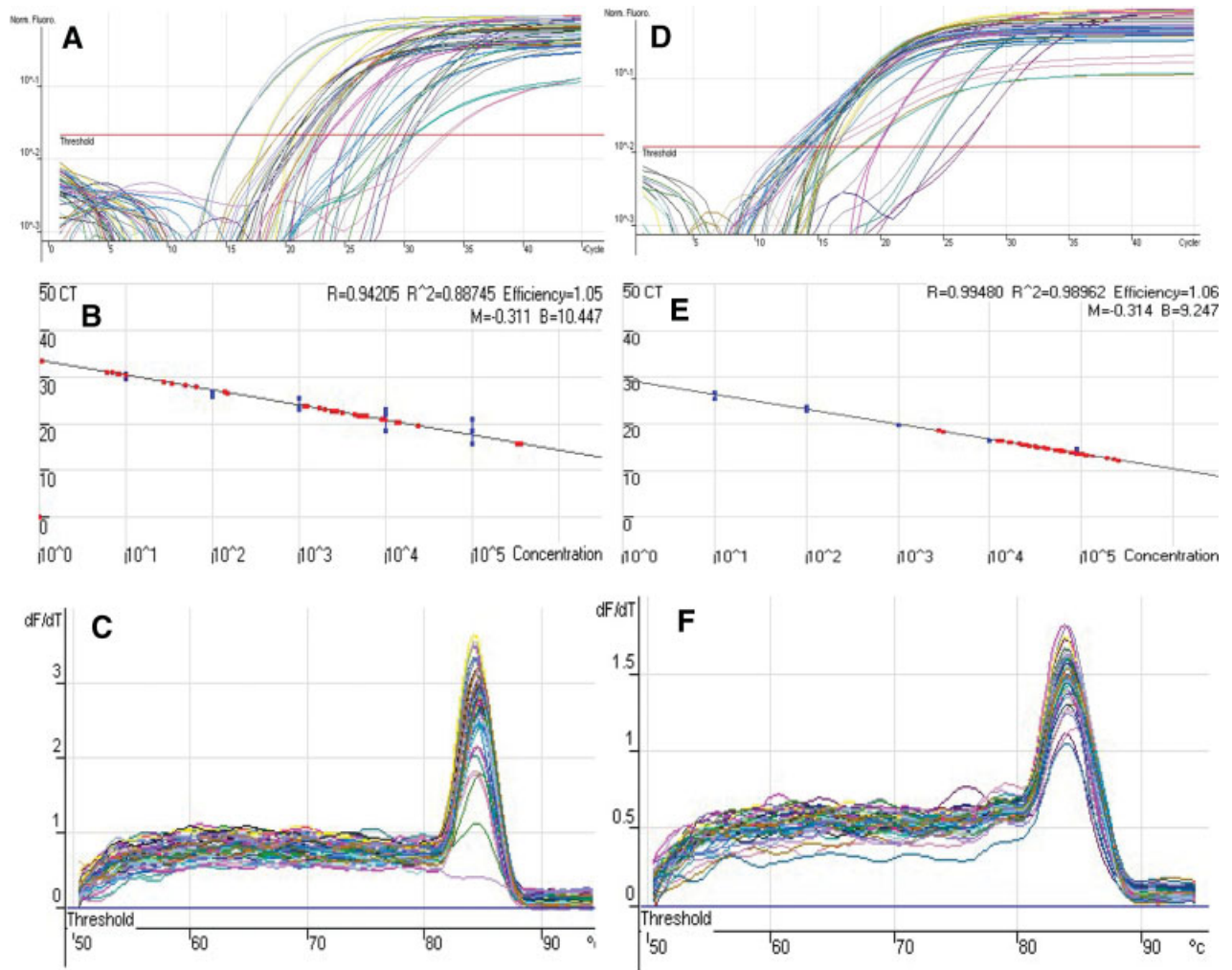


Figure 3. Sensitivity and specificity of RTQ-PCR to quantify bacterial load in *A. baumannii* OM. A real-time quantitative PCR assay to detect the *A. baumannii* bacterial load in the infected tibiae was developed by generating standard curves from 10-fold dilutions of pTOPO-*parC*, which was standardized to mouse DNA (pTOPO-*beta-actin*) as we have previously described for *S. aureus*.¹⁵ Syber green RTQ-PCR was performed with *parC* (A–C) or *beta-actin* (D–F) specific primers. The primary threshold cycle values (CT) data of the dilutions (A, D) were used to generate a standard curve for each template (blue dots in B, E). Then the DNA from the infected tibiae described in Figure 1 was extracted and amplified with the same *parC* and *beta-actin* specific primers, and extrapolated to the standard curve (red dots in B, E), allowing for an estimate of bacterial load that is presented as *parC* copies/*beta-actin* copies per sample. Given that contamination can be a problem with real-time PCR at >35 cycles, and that we could reproducibly quantify 10 copies of *parC* at 30.1 cycles, we set this value as the upper threshold limit to detect our PCR products. The purity was confirmed using a melt curve, which identified the predicted single peak for the *parC* (C) and *beta-actin* (F) PCR products, respectively.

cases at presentation, but only 5% of reoccurring OM. In contrast, *S. aureus* was only present in 13% of initial OM, while 53% of reoccurrences were infected with Staphylococcus, and 31% of the cases were MRSA. Most notable were the type III diaphyseal tibial fractures, of which 13 out of the 35 patients studied had union times of >9 months that appeared to be associated with infection, and 4 that ultimately required limb amputation due to infectious complications. These new findings underscore the importance of effective early treatment of MDR *Acinetobacter* OM, and warrant investigation of the cause and effect relationship between initial Gram-negative infections that evolve into catastrophic MRSA OM. To address these issues, here we investigated the nature of MDR *A. baumannii* OM versus that of *S. aureus*, and evaluated the efficacy of local high-dose

colistin to prevent infection from a contaminated tibial implant in a mouse model.

Although we found MDR *Acinetobacter* to be highly infectious as expected (Fig. 1), we were surprised by several features of *A. baumannii* OM that are remarkably distinct from *S. aureus* infection of bone (Fig. 2). The first is that *A. baumannii* induces blastic lesions, in contrast to the osteolytic lesions most commonly associated with OM. Although we have no information on the mechanism by which the bacteria stimulates bone formation, this may occur via induction of anabolic factors (i.e., BMPs, Wnts), and/or the down-regulation of antagonists (i.e., noggin, sost, dkk), in a similar manner as that observed in osteoblastic tumors.³⁰ The other major difference that we found was the absence of biofilm and any histological evidence of colonized necrotic bone

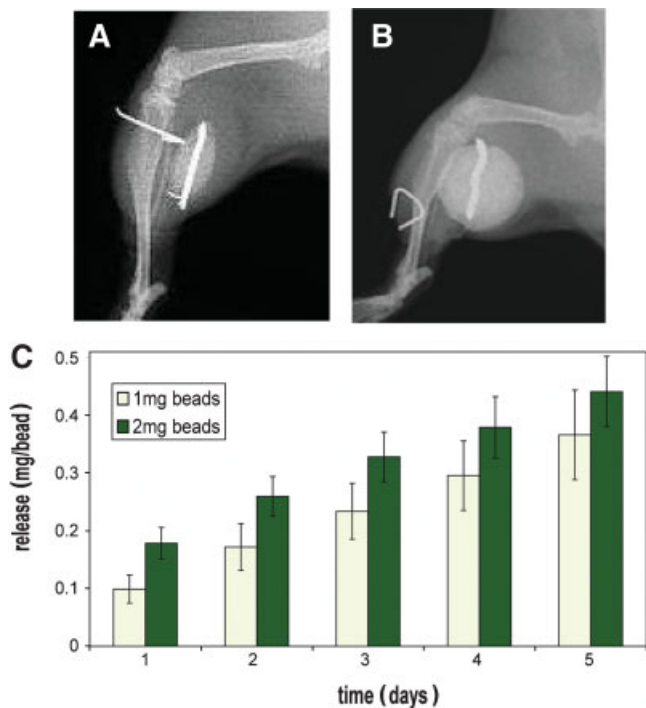


Figure 4. Colistin-impregnated PMMA beads. X-rays were taken of mice following implantation of a 5-mm (A) and 1-cm (B) PMMA bead adjacent to a transcortical pin. The in vitro colistin release kinetics of 5-mm PMMA beads impregnated with 1.0 or 2.0 mg of colistin sulfate was determined over the course of 5 days (C). The data are presented as the mean \pm SD ($n=5$) of the cumulative colistin recovered in solution at the indicated time, such that the values for each day are added to the previous values to give a cumulative total from time 0. No significant differences between the 1.0- and 2.0-mg dose were detected by *t*-test with Bonferroni correction.

in mice infected with *A. baumannii*, which is always present in chronic *S. aureus* OM. One possible explanation of these results, which needs to be explored in a focused investigation, is that *A. baumannii* persists as an obligate intracellular pathogen. In so doing, the bacteria would be immune privileged from humoral immunity (Fig. 1C), which should clear extracellular bacteria from the infection site. Additionally, the absence of extracellular bacteria and their pathogen-associated molecular patterns (PAMPs),³¹ would lead to decreased Toll-like receptor (TLR) activation of innate immunity and osteoclast activation, which causes osteolysis.³²⁻³⁵

Another interesting speculation that is brought by these data and the recent clinical studies on OM cases from OIF/OEF is the possibility that *S. aureus* infections are opportunistic, and in some cases may depend on an initial colonization by Gram-negative bacteria such as *Acinetobacter*. This scenario further stresses the importance of early eradication of peri-implant infection following orthopedic surgery, which is most effectively achieved with local drug therapy via antibiotic-impregnated bone cement,¹⁶⁻¹⁸ and potentially antibiotic-coated implants.^{36,37} Given that most MDR *Acinetobacter* strains are sensitive to colistin,¹⁰ and that PMMA beads can be readily impregnated with colistin and steadily release the drug over time (Fig. 4), we evaluated

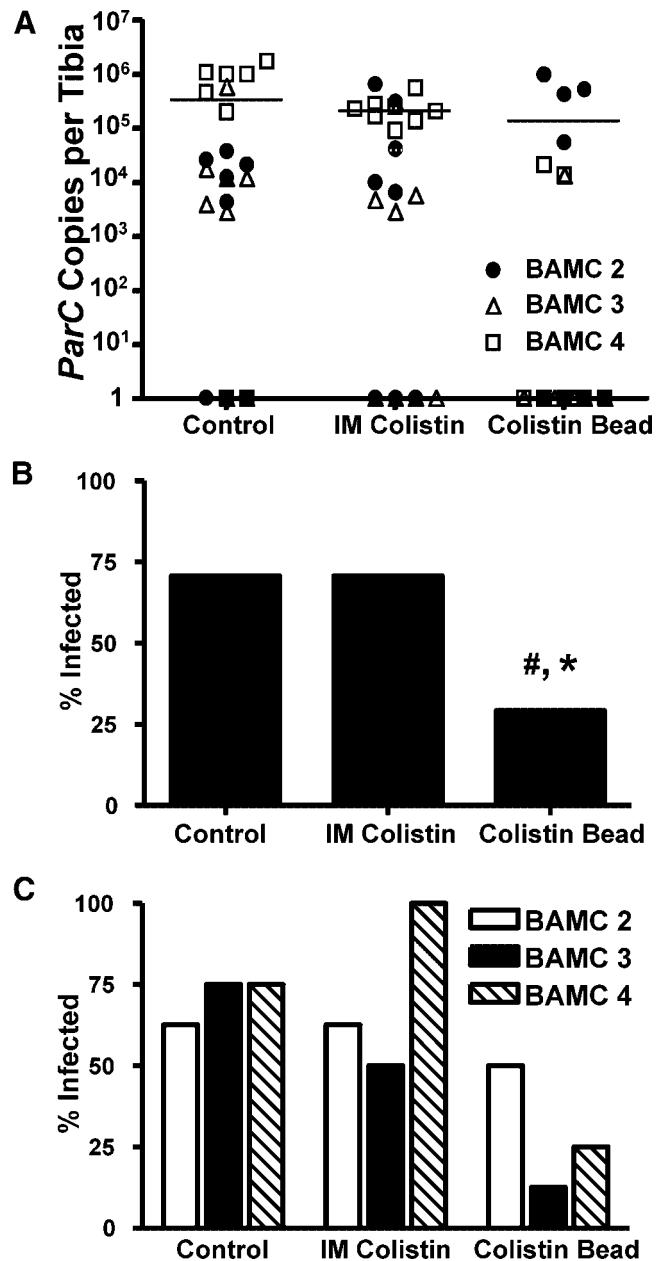


Figure 5. Local but not parenteral colistin prevents *A. baumannii* implant-associated osteomyelitis. Immediately prior to tibial implantation of a pin contaminated with the indicated strain of *A. baumannii*, mice [$n=8$] with strains BAMC-2, 3, and 4; 24 total mice per group] received either: (i) a sterile PMMA bead (placebo), (ii) daily 200 μ g intramuscular injection of colistinmethate for 7 days, or (iii) a PMMA bead impregnated with 1 mg of colistin sulfate. Following sacrifice on day 19, *par C* real-time quantitative PCR was used to measure bacterial load (A), and infection rates (B, C). Of the mice receiving the placebo, 18 out of 24 were infected; in mice receiving intramuscular colistinmethate injection, 17 out of 24 mice were infected; and in mice receiving a PMMA bead impregnated with 1 mg of colistin sulfate, 8 out of 24 mice were infected. While no significant effects of IM colistin treatment were observed versus the placebo control, the colistin-impregnated bead significantly reduced the incidence of chronic OM compared to placebo (#) and IM colistin (*, $p > 0.05$ using Fisher's exact test) (B). However, when the strains were analyzed individually (C), it was clear that BAMC2 was responsible for most of the chronic infections in the mice treated with local colistin.

this mode of local prophylaxis versus standard parenteral colistinmethate (Fig. 5). As predicted, the local treatment, which presumably leads to higher drug concentration levels at the site of infection, was significantly better in preventing MDR *Acinetobacter* OM. Considering the vast independent clinical experience with antibiotic-impregnated PMMA beads and colistin, and the absence of an accepted large animal model of OM that simulates the soft tissue injury associated with war wounds, we find that these results support the evaluation of colistin-impregnated PMMA beads, or absorbable materials that do not require removal, in a clinical trial to evaluate their efficacy in clearing MDR *Acinetobacter* OM and reoccurring infections.

ACKNOWLEDGMENTS

The authors thank Laura Yanoso for technical assistance with the micro-CT, and Krista Scorsone for technical assistance with the histology. This work was supported by research grants from the US Army Medical Research Acquisition Activity (USAMRAA), Orthopaedic Trauma Research Program (OTRP) W81XWH-07-1-0124, and the National Institutes of Health PHS awards AR48681, DE17096, AR52674, AR51469, AR46545, AR54041, and AR53459.

REFERENCES

- Covey DC. 2006. Iraq war injuries. *Orthopedics* 29:884–886.
- Owens BD, Kragh JF Jr, Macaitis J, et al. 2007. Characterization of extremity wounds in Operation Iraqi Freedom and Operation Enduring Freedom. *J Orthop Trauma* 21:254–257.
- Owens BD, Kragh JF Jr, Wenke JC, et al. 2008. Combat wounds in operation Iraqi Freedom and operation Enduring Freedom. *J Trauma* 64:295–299.
- Covey DC. 2006. Combat orthopaedics: a view from the trenches. *J Am Acad Orthop Surg* 14 (Suppl):S10–S17.
- Covey DC, Aaron RK, Born CT, et al. 2008. Orthopaedic war injuries: from combat casualty care to definitive treatment: a current review of clinical advances, basic science, and research opportunities. *Instr Course Lect* 57:65–86.
- Murray CK, Hsu JR, Solomkin JS, et al. 2008. Prevention and management of infections associated with combat-related extremity injuries. *J Trauma* 64 (Suppl):S239–S251.
- Yun HC, Branstetter JG, Murray CK. 2008. Osteomyelitis in military personnel wounded in Iraq and Afghanistan. *J Trauma* 64 (Suppl):S163–S168.
- Anonymous. 2004. *Acinetobacter baumannii* infections among patients at military medical facilities treating injured U.S. service members, 2002–2004. *MMWR* 53(45):1063–1066.
- Murray CK, Hospenthal DR. 2005. Treatment of multidrug resistant *Acinetobacter*. *Curr Opin Infect Dis* 18:502–506.
- Davis KA, Moran KA, McAllister CK, et al. 2005. Multidrug-resistant *Acinetobacter* extremity infections in soldiers. *Emerg Infect Dis* 11:1218–1224.
- Abbo A, Navon-Venezia S, Hammer-Muntz O, et al. 2005. Multidrug-resistant *Acinetobacter baumannii*. *Emerg Infect Dis* 11:22–29.
- Darouiche RO. 2004. Treatment of infections associated with surgical implants. *N Engl J Med* 350:1422–1429.
- Scott P, Deye G, Srinivasan A, et al. 2007. An outbreak of multidrug-resistant *Acinetobacter baumannii-calcoaceticus* complex infection in the US military health care system associated with military operations in Iraq. *Clin Infect Dis* 44:1577–1584.
- Hawley JS, Murray CK, Jorgensen JH. 2008. Colistin heteroresistance in *Acinetobacter* and its association with previous colistin therapy. *Antimicrob Agents Chemother* 52:351–352.
- Li D, Gromov K, Soballe K, et al. 2008. Quantitative mouse model of implant-associated osteomyelitis and the kinetics of microbial growth, osteolysis, and humoral immunity. *J Orthop Res* 26:96–105.
- Marks KE, Nelson CL Jr, Schwartz J. 1974. Antibiotic-impregnated acrylic bone cement. *Surg Forum* 25:493–494.
- Wininger DA, Fass RJ. 1996. Antibiotic-impregnated cement and beads for orthopedic infections. *Antimicrob Agents Chemother* 40:2675–2679.
- Parvizi J, Saleh KJ, Ragland PS, et al. 2008. Efficacy of antibiotic-impregnated cement in total hip replacement. *Acta Orthop* 79:335–341.
- Falagas ME, Kasiakou SK. 2005. Colistin: the revival of polymyxins for the management of multidrug-resistant gram-negative bacterial infections. *Clin Infect Dis* 40:1333–1341.
- Hamouda A, Amyes SG. 2006. Development of highly ciprofloxacin-resistant laboratory mutants of *Acinetobacter baumannii* lacking topoisomerase IV gene mutations. *J Antimicrob Chemother* 57:155–156.
- Montero A, Ariza J, Corbella X, et al. 2004. Antibiotic combinations for serious infections caused by carbapenem-resistant *Acinetobacter baumannii* in a mouse pneumonia model. *J Antimicrob Chemother* 54:1085–1091.
- Zhang X, Schwarz EM, Young DA, et al. 2002. Cyclooxygenase-2 regulates mesenchymal cell differentiation into the osteoblast lineage and is critically involved in bone repair. *J Clin Invest* 109:1405–1415.
- Koefoed M, Ito H, Gromov K, et al. 2005. Biological effects of rAAV-caAlk2 coating on structural allograft healing. *Mol Ther* 12:212–218.
- Ito H, Koefoed M, Tiyyapanaputi P, et al. 2005. Remodeling of cortical bone allografts mediated by adherent rAAV-RANKL and VEGF gene therapy. *Nat Med* 11:291–297.
- Brady RA, Leid JG, Calhoun JH, et al. 2008. Osteomyelitis and the role of biofilms in chronic infection. *FEMS Immunol Med Microbiol* 52:13–22.
- Kurtz SM, Lau E, Schmier J, et al. 2008. Infection burden for hip and knee arthroplasty in the United States. *J Arthroplasty* 23:984–991.
- Pulido L, Ghanem E, Joshi A, et al. 2008. Periprosthetic joint infection: the incidence, timing, and predisposing factors. *Clin Orthop Relat Res* 466:1710–1715.
- Klevens RM, Morrison MA, Nadle J, et al. 2007. Invasive methicillin-resistant *Staphylococcus aureus* infections in the United States. *JAMA* 298:1763–1771.
- Johnson EN, Burns TC, Hayda RA, et al. 2007. Infectious complications of open type III tibial fractures among combat casualties. *Clin Infect Dis* 45:409–415.
- Virk MS, Lieberman JR. 2007. Tumor metastasis to bone. *Arthritis Res Ther* 9 (Suppl 1):S5.
- Akira S, Takeda K, Kaisho T. 2001. Toll-like receptors: critical proteins linking innate and acquired immunity. *Nat Immunol* 2:675–680.
- Bi Y, Collier TO, Goldberg VM, et al. 2002. Adherent endotoxin mediates biological responses of titanium particles without stimulating their phagocytosis. *J Orthop Res* 20:696–703.
- Bi Y, Seabold JM, Kaar SG, et al. 2001. Adherent endotoxin on orthopedic wear particles stimulates cytokine production and osteoclast differentiation. *J Bone Miner Res* 16:2082–2091.

34. Bi Y, Van De Motter RR, Ragab AA, et al. 2001. Titanium particles stimulate bone resorption by inducing differentiation of murine osteoclasts. *J Bone Joint Surg [Am]* 83-A:501–508.
35. Nalepka JL, Lee MJ, Kraay MJ, et al. 2006. Lipopolysaccharide found in aseptic loosening of patients with inflammatory arthritis. *Clin Orthop Relat Res* 451:229–235.
36. Antoci V Jr, King SB, Jose B, et al. 2007. Vancomycin covalently bonded to titanium alloy prevents bacterial colonization. *J Orthop Res* 25:858–866.
37. Parvizi J, Antoci V Jr, Hickok NJ, et al. 2007. Selfprotective smart orthopedic implants. *Expert Rev Med Devices* 4: 55–64.